Understanding the morphological processes at Ameland Inlet

Kustgenese 2.0 synthesis of the tidal inlet research

Understanding the morphological processes at Ameland Inlet

Kustgenese 2.0 synthesis of the tidal inlet research

Author(s)

Edwin Elias
Stuart Pearson
Ad van der Spek

Deltares

Understanding the morphological processes at Ameland Inlet
Kustgenese 2.0 synthesis of the tidal inlet research

Client	Rijkswaterstaat Water, Verkeer en Leefomgeving
Contact persons	Harry de Looff and Stefan Pluis
Reference	Kustgenese 2.0, zaaknummer 31123135
Keywords	Kustgenese 2.0, tidal inlet, morphology, ebb tidal delta, sediment-bypassing, Ameland, Wadden Sea

Documentgegevens

Version	1.0
Date	04-03-2020
Project number	1220339-008
Document ID	1220339-008-ZKS-0008
Pages	82
Status	final

Authors

	Edwin Elias	
	Stuart Pearson	
	Ad van der Spek	

Doc. version	Authors	Review	Approve	Publish
1.0	Edwin Elias	Arno Nolte	Toon Segeren	
	Stuart Pearson			
	Ad van der Spek			

Deltares

Summary

The objective of this Coastal Genesis 2.0 report is to synthesize the current understanding of the role of the Ameland ebb-tidal delta in the coastal system, and the processes underlying meso-scale ebb-tidal delta dynamics. Such knowledge is not only essential for future sustainable coastal management of Ameland Inlet, but also provides valuable lessons for the other inlets of the Wadden Sea and the (closed off) inlets in the Voordelta.

This report serves as technical background document for the technical advice on the possibilities for ebb-tidal delta nourishments and their potential added value in coastal management.

The data collected at Ameland inlet during the Kustgenese 2.0 campaign and pilot nourishment, in combination with older datasets, has created an extensive dataset of bathymetric and hydrodynamic observations. This provides a unique opportunity for an in-depth analysis of the underlying physics that determine the meso-scale morphodynamic changes of the ebb-tidal delta, the pilot nourishment, and the interaction of the ebb-tidal delta with the adjacent coastlines

The (half)yearly bathymetric observations reveal how initial small-scale perturbations in the central part of the ebb-tidal delta (the ebb-chute and shield systems) develop, grow, migrate and start to dominate the developments of the entire ebb-tidal delta. Shoal instabilities are initially small morphodynamic changes and would not be considered to affect the ebb-tidal delta and inlet dynamics as a whole. However, the analysis presented in this report shows that complete relocation of ebb-tidal delta scale channels and shoals can be initiated through interactions that originate on the smallest scale of individual shoals. The ebb-tidal delta is therefore much more dynamic than what was expected from literature and existing conceptual models.

The ebb-delta nourishment was successfully placed on the Kofmansbult, which shows that it is technically feasible to place these large volumes of sand on the ebb-tidal delta platform. The nourishment did not visibly alter the morphodynamic behaviour of the Kofmansbult. Only through the continuation of frequent measurements and the subsequent integrated analysis, it is possible to start to understand the potential impacts of the ebb-delta nourishment on the coastal system.

Samenvatting

Het doel van dit Kustgenese 2.0 rapport is het huidige begrip van de rol van de buitendelta van het Zeegat van Ameland in het kustsysteem en de processen die ten grondslag liggen aan de meso-schaal buitendeltadynamiek samen te vatten. Deze kennis is niet alleen essentieel voor toekomstig duurzaam kustbeheer van het Amelander Zeegat, maar biedt ook waardevolle lessen voor de andere zeegaten van de Waddenzee en de (afgesloten) zeegaten in de Voordelta.

De synthese is bedoeld als technisch-inhoudelijke onderbouwing van het Kustgenese 2.0 technisch advies over de de mogelijkheden voor suppleties bij buitendelta's en de meerwaarde ervan voor het kustbeheer.

De gegevens die tijdens de Kustgenese 2.0 campagne en pilotsuppletie in het Ameland Zeegat zijn verzameld hebben, in combinatie met oudere datasets, een uitgebreide dataset van bathymetrische en hydrodynamische waarnemingen gecreëerd. Deze dataset biedt een unieke kans voor een diepgaande analyse van de onderliggende fysica die de meso-schaal morfodynamische veranderingen van de buitendelta, de pilotsuppletie, en de interactie van de buitendelta met de aangrenzende kusten bepaalt.

De (half)jaarlijkse bathymetrische waarnemingen laten zien hoe de aanvankelijke kleinschalige verstoringen in het centrale deel van de buitendelta (de ebgeul- en plaatsystemen) de ontwikkelingen van de gehele buitendelta kunnen bepalen en uiteindelijk beginnen te domineren. Instabiliteiten zijn in eerste instantie kleine morfodynamische veranderingen, waarvan voorheen niet werd gedacht dat zij de buitendeltadynamiek als geheel zouden beïnvloeden. De analyse gepresenteerd in dit rapport toont aan dat volledige verplaatsing van geulen en platen op buitendeltaschaal kan worden gestart door interacties op de kleinste schaal. De buitendelta is hiermee veel dynamischer dan verwacht op basis van literatuur en bestaande conceptuele modellen.

De buitendeltasuppletie werd met succes geplaatst op de Kofmansbult, waaruit blijkt dat het technisch haalbaar is om deze grote hoeveelheden zand op de buitendelta te plaatsen. De suppletie veranderde het morfodynamische gedrag van de Kofmansbult niet zichtbaar. Alleen door de voortzetting van frequente metingen en de daaropvolgende geïntegreerde analyse is het mogelijk om de mogelijke effecten van de buitendeltasuppletie op het kustsysteem te begrijpen.

Understanding the morphological processes at Ameland Inlet
1220339-008-ZKS-0008, 4 March 2020

Deltares

Table of Contents

Deltares

1   Introduction and Objective

The Wadden Sea is one of the last large tidal regions where natural forces have free reign without a dominating influence from human activities. Elias et al. (2012) point out that natural processes have free reign in shaping the Wadden Sea morphology, but this shaping can only take place within established boundaries. Over the last centuries, multiple large- and small-scale interventions, such as coastal defence works, closure dams, dikes, sea-walls, and land reclamations have reduced and essentially fixed the basin and barrier dimensions in place. The geological roll-over mechanisms of landward barrier and coastline retreat (Van Straaten, 1975; Flemming & Davis, 1994; Van der Spek, 1994) can therefore no longer be sustained. So far, despite the large continuous sedimentation in the tidal basins, nearly 650 million m^3 since 1935 (Elias et al. 2012), the individual inlets were sustained in location and similar channel-shoal characteristics of the basins were retained. These observations illustrate that the Wadden Sea has been resilient to anthropogenic influence and pressure.

An important observation by Elias et al. (2012) is that much of the basin fill is supplied by the eroding ebb-tidal deltas. These ebb-tidal deltas are limited in size and rapidly reducing in volume. Increased coastal and barrier-island erosion is to be expected when an insufficient volume of sand is supplied by the ebb-tidal delta. Repeated beach and shoreface nourishments and potentially ebb-tidal delta nourishments may be used to mitigate shoreline erosion and add to the sediment budget of both islands and basins. However, to successfully design and construct such nourishments, it is essential that the ebb-tidal delta (morpho)dynamics and particularly the process of sediment-bypassing is better understood. This is one of the motivations for a pilot project that includes placement of 5 million m^3 of sand on the ebb shoal of Ameland Inlet as part of the Kustgenese 2.0 project.

The objective of this report is to bring together the current understanding of the role of the ebb-tidal delta in the coastal system, and the processes underlying meso-scale ebb-tidal delta dynamics. Our analysis is based on high-resolution bathymetric and hydrodynamic datasets obtained at Ameland Inlet. Intensive monitoring of the inlet by Rijkswaterstaat has created a globally unique dataset of long-term, high-quality bathymetric observations. In combination with recently obtained high-resolution observations of hydrodynamics (water levels, wind speed and direction, waves, currents and discharges) and morphodynamics (bathymetry, bedforms and sediment characteristics) during the Kustgenese 2.0 field campaign, this provides a unique opportunity for an in-depth analysis of the underlying physics that determine the morphodynamic changes of the ebb-tidal delta. Such knowledge is not only essential for future sustainable coastal management of Ameland Inlet, but also provides valuable lessons for the other inlets of the Wadden Sea and the (closed-off) inlets in the Voordelta.

This report summarizes various studies of Ameland Inlet (Elias, 2018; Elias et al. 2019; Van Weerdenburg, 2019; Van der Werf et al., 2019) that were conducted as part of the projects KPP Beheer en Onderhoud Kust and Kustgenese 2.0. Where needed, the results presented in these reports were updated with an additional analysis of the measurements collected during the Kustgenese 2.0 measurement campaign and the ebb-tidal delta nourishment monitoring.

Deltares

2 Study area

2.1 General setting

The Wadden Sea (Figure 2.1) consists of a series of 33 tidal inlet systems. These inlets extend over 500 km along the northern part of the Netherlands (West Frisian Islands), and the North Sea coasts of Germany and Denmark (the East Frisian Islands and North Frisian Islands). The Frisian islands separate the Wadden Sea from the North Sea. Although dissected by several major estuaries, such as Ems, Elbe and Weser, the Wadden Sea is the world's largest uninterrupted system of tidal flats and barrier islands. Over a period of more than 7000 years, a wide variety of barrier islands, tidal channels, sand and mud flats, gullies and salt marshes formed under a temperate climate, rising sea level, and, especially during the last century, human interventions.
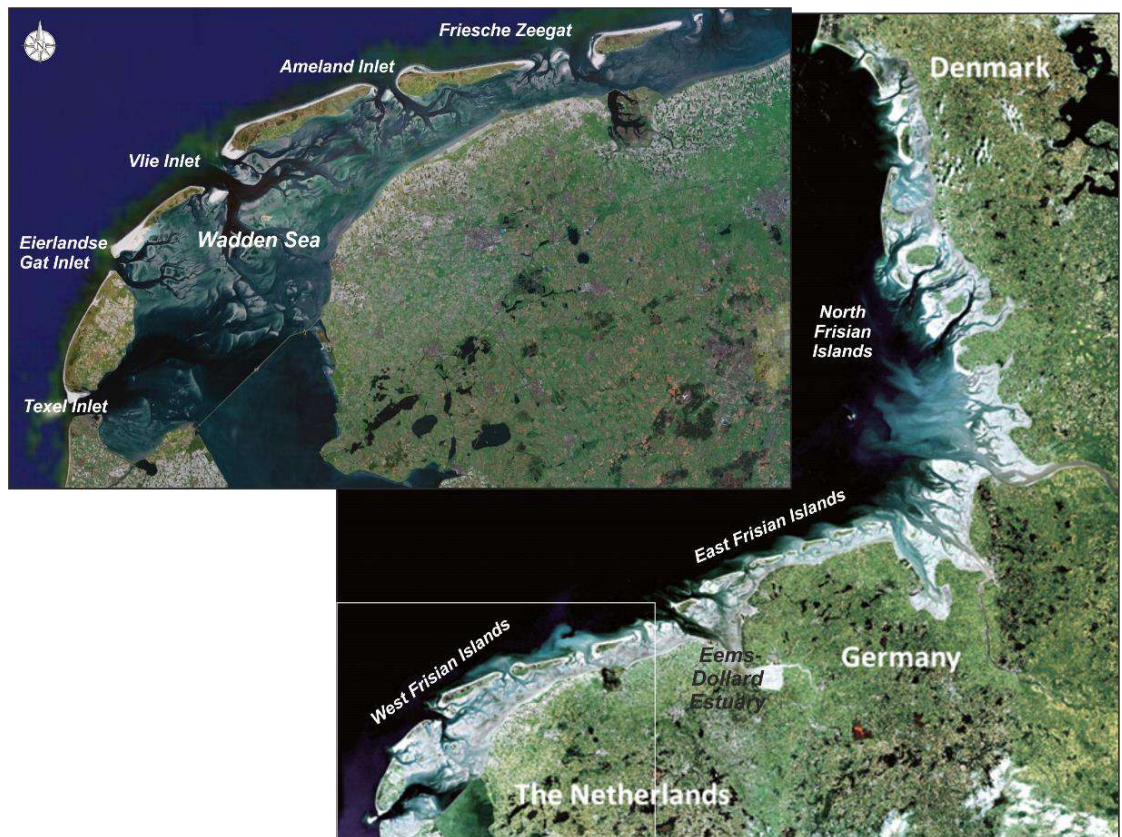
Figure 2.1   bottom panel: An overview of the islands and inlets that form the Wadden Sea (based on picture from www.waddensea-secretariat.org). Top panel shows the 5 most westerly inlets of the Dutch Wadden Sea.

Ameland Inlet is centrally located in the chain of West Frisian Islands and bordered by the islands Terschelling to the west and Ameland to the east (Figure 2.1, Figure 2.2). With a tidal range increasing from 1.4 m at Den Helder (Texel Inlet) to 4.4 m near Bremen, and waves with an average significant wave height around 1.4 m, the Frisian Inlets fall in the mixed-energy category (Hayes, 1975; Davis and Hayes, 1984). Characteristic of mixed-energy inlets systems is the presence of large and stable inlets, with barriers typically being short and 'drumstick'-shaped (Hayes, 1979). The associated Ameland tidal basin has a length of about 30 km and covers an area of 270 km^2. Approximately 60% of the basin area consists of intertidal shoals (Eysink, 1993). The present-day location of the Frisian coastline was formed around 1600 AD. Historically, Ameland Inlet was the

Deltares

outlet of the medieval Middelzee tidal basin, which reached its maximum size around 1000 AD (Van der Spek, 1995). Infilling with marine sediments and subsequent dike building on these new deposits resulted in the reclamation of the landward part of the basin, decreasing tidal prisms, constriction of the inlet and extension of the updrift barrier island Terschelling. The geometry of both adjacent islands shows the typical drumstick-shape described in the model of Hayes (1979), having a bulbous updrift side and a long, narrow downdrift end that formed through spit accretion. An eastward littoral drift dominates along the islands as a result of the prevailing winds out of the westerly quadrants. Estimates of the longshore drift vary considerably. Along the Terschelling island coastline values of 0.5-0.6 to 1.0 million m^3/year were reported by Tanczos et al. (2000) and Spanhoff et al. (1997), respectively. Ridderinkhof et al. (2016) estimate the longshore drift rate to range between 0.3-0.5 million m^3/year along the Terschelling coast and 0.8-1.2 million m^3/year along the Ameland coast. Based on a recent reanalysis of the Wadden Sea sediment budget, Elias (2019) indicates that the longshore drift maybe considerably higher than previously assumed. Note that in this paper the terms updrift and downdrift refer to the direction of the longshore drift along the islands, which for the Frisian islands means that updrift is to the west of the inlet (i.e. Terschelling coast) and downdrift is to the east (i.e. Ameland coast).

The tidal processes of flooding and draining are the driving force shaping the inner basin. These flows result in fractal channel patterns there (Cleveringa & Oost, 1999). The basins are more-or-less separated by higher elevation and finer grain size, so-called tidal divides or watersheds. These tidal divides form where the tidal waves traveling through two adjacent inlets meet. Here, sedimentation due to near-zero velocities results in preferred tidal-flat accretion (e.g. Pinkewad in the east and Terschellinger Wad in the west). These tidal divides are often considered to form boundaries that separate inlet systems and are located somewhat eastward of the center of the barrier islands due to the amplitude differences between the neighbouring inlets (Wang et al., 2013) and the prevailing eastward wind direction. Both recent field measurements (van Weerdenburg, 2019) and the model study of Duran-Matute et al. (2014) show that these tidal divides do not form hydrodynamically closed boundaries, as exchange of water and suspended sediment exchange still occurs. Especially during strong wind events, considerable throughflow over the divides and thus between the inlets occurs. Elias (2019) estimates that net sand transport over the tidal divides bordering Ameland basin is directed to the east and ranges between 0.2 and 0.5 million m^3/year

2.2 Present day channels and shoals

Figure 2.2 provides a detailed overview of the main channels and shoals that form the present-day Ameland Inlet. In the inlet gorge, between the islands of Terschelling and Ameland, a deep main ebb-channel is located along the west coast of Ameland (Borndiep, see Figure 2.2 [1]). The deepest parts of this channel exceed 25 m in depth. In the basin, Borndiep connects to Dantziggat [2] that curves eastward into the basin towards the tidal divide of Ameland (Pinkewad). To the west, separated by the shoal Zeehondenplaat [16], a smaller channel system is formed by Oosterom [3] and Boschgat [4], both curving southward towards the tidal divide of Terschelling (Terschellinger Wad). In the present bathymetry, Boschgat does not directly connect to the Westgat flood channel [6]. A shallow platform dissected by a series of smaller, dynamic channels and shoals is present between the eastern island tip of Terschelling (Boschplaat [15]) and Borndiep.

The main channel on the ebb-tidal delta is called Akkepollegat [7]. Akkepollegat had a pronounced seaward outflow in the past, but recently two ebb-chutes [9,10] have formed along its western margin. The most seaward, oldest, ebb-chute [9] and its associated ebb-shield (from hereon called Kofmansplaat [22]) now covers most of the shoal area known as Kofmansbult [11]. To the north the ebb-delta nourishment is visible as a shallow platform just seaward of the Kofmansplaat [21]. Eastward migration of Kofmansplaat has distorted the outflow of Akkepollegat and rotated the channel eastwards [7]. Extensive sedimentation has occurred in the distal part of the channel and in the 2019 bathymetry the channel has almost disappeared. The deepest part of Borndiep, the

Deltares

main inlet channel, is now curved towards the younger, southern ebb-chute channel [10]. The latter channel may have already taken over the role as main ebb channel on the ebb-tidal delta.

The main ebb-tidal delta shoal area lies to the east of Akkepollegat, which is downdrift in relation to the littoral drift. This large shoal area or swash platform is named Bornrif [12]. Along its eastern margin, now connected to the coast of Ameland, the remnants of the shoal Bornrif Bankje [13] are still visible. This shoal had formed and migrated as a narrow swash bar, along the seaward margin of the ebb-tidal delta shoal and attached to the Ameland coast just east of the Bornrif Strandhaak [14]. The Bornrif Strandhaak was a large ebb-delta shoal that attached to the coastline around 1985. This natural mega-nourishment resembles the "Zandmotor" (Stive et al., 2013) both in dimension and layout, and has supplied the (downdrift) coastline of Ameland with sand over the past decades. Just to the west of this location, at the northwest tip of Ameland island, repeated sand nourishments [20] and extensive shore-protection works are needed [19] to maintain the coastline. In the 2019 bathymetry (Figure 2.2, lower panel), a recent (2019) large nourishment is still visible along the coastline. While shoal attachments built out the coastline of Ameland, the opposite was observed along the coastline of Terschelling. The eastern tip of this island, Boschplaat [15], has receded over 1.5 km since 1975.

Deltares

(1). Borndiep	(8). ebb-chute 1	(14). Bornrif Strandhaak	(20). Location of beach
(2). Dantziggat	(not on map)	(15). Boschplaat	nourishments
(3). Oosterom	(9). ebb-chute 2	(16). Zeehondenplaat	(21). Location of ebb-tidal
(4). Boschgat	(10). ebb-chute 3	(17). Koffiebonenplaat	delta nourishment
(5). Blauwe Balg	(11). Kofmansbult	(18). Vrijheidsplaat	(22). Kofmansplaat
(6). Westgat	(12). Bornrif platform	(19). Coastal protection	
(7). Akkepollegat	(13). Bornrif Bankje	works Ameland West	

Translations of Dutch names: 'plaat' = shoal; 'bankje' = (sand) bar; 'geul' = channel; 'gat' = channel or creek; 'diep' = deep (channel); 'strand' = beach; 'haak' = 'hook', 'eiland'= island.
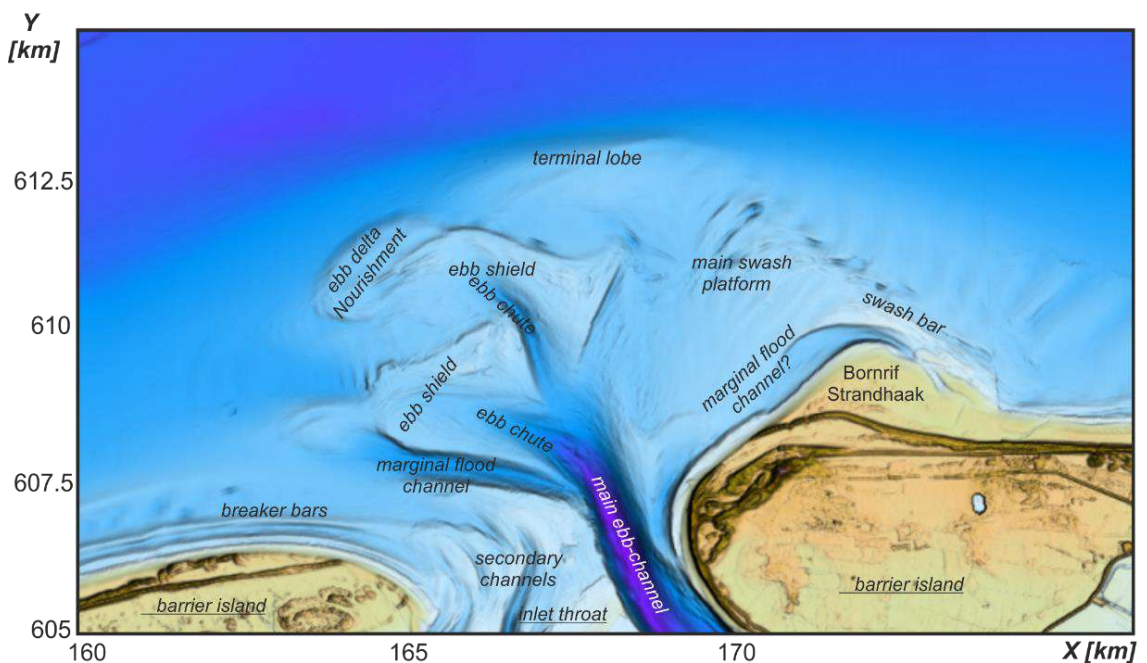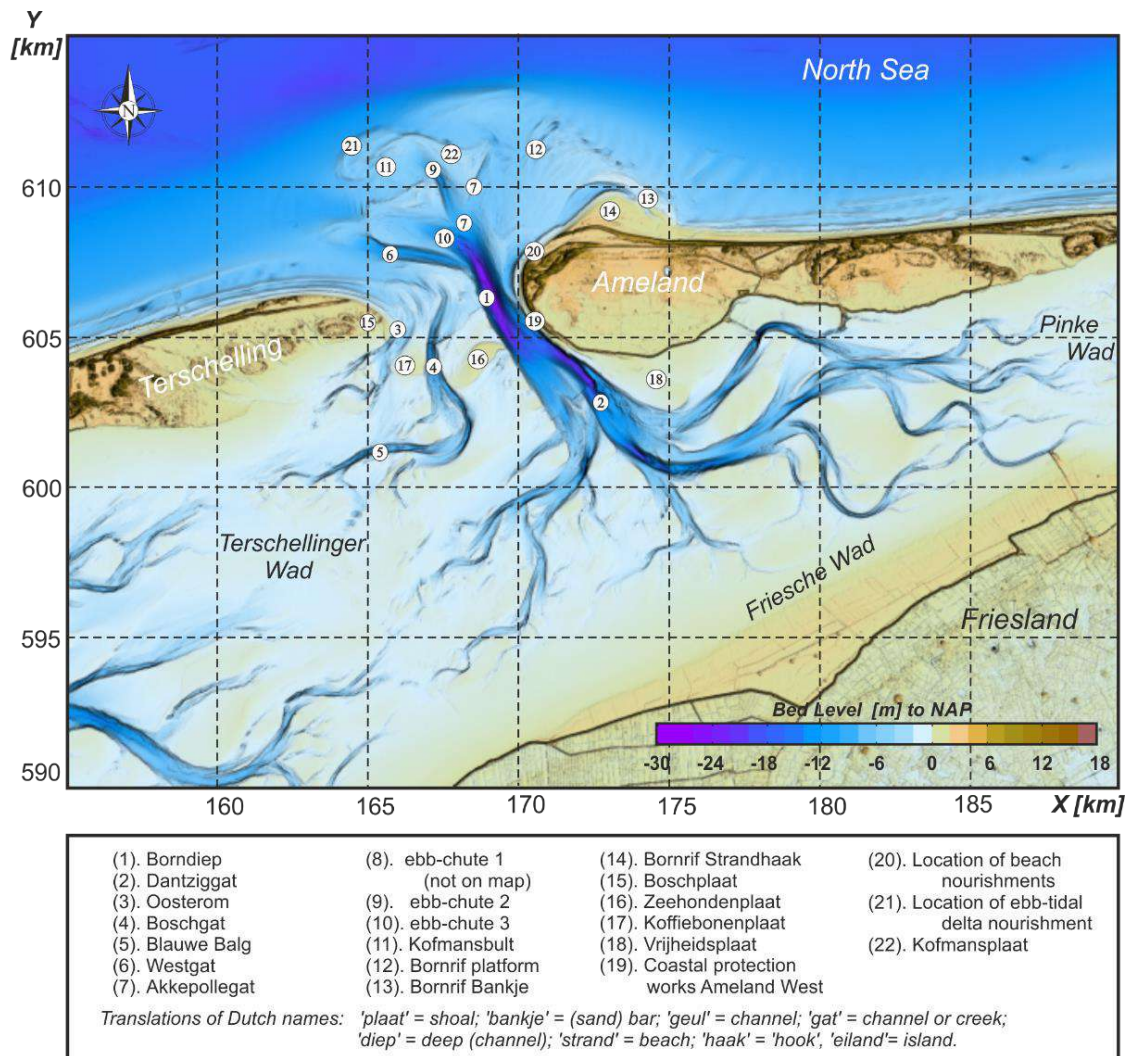

Figure 2.2   Overview of the channels and shoals that form the present day Ameland Inlet. The underlying Digital Elevation Model (DEM) or bathymetry is based on the 2019 Kustgenese 2.0 spring dataset (missing data and the basin are filled in with 2017 measurements).

Deltares

2.3   Sediment-bypassing processes at Ameland Inlet.

Ameland Inlet has a long history of bathymetric surveying. The first maps were probably drawn in 1558, followed by a series of maps and charts that increase in detail with time. Nautical charts were produced between 1798 and 1958 based on surveys by the Hydrographic Service of the Royal Netherlands Navy. Since 1958 data have been collected by Rijkswaterstaat. Up to 1985, these data were stored as paper charts, although some of the underlying analogous data used to construct the charts were digitized in 1991-1992 (De Boer et al., 1991a,b; Rakhorst et al., 1993). Since 1986 all bathymetrical surveys are collected and stored digitally.
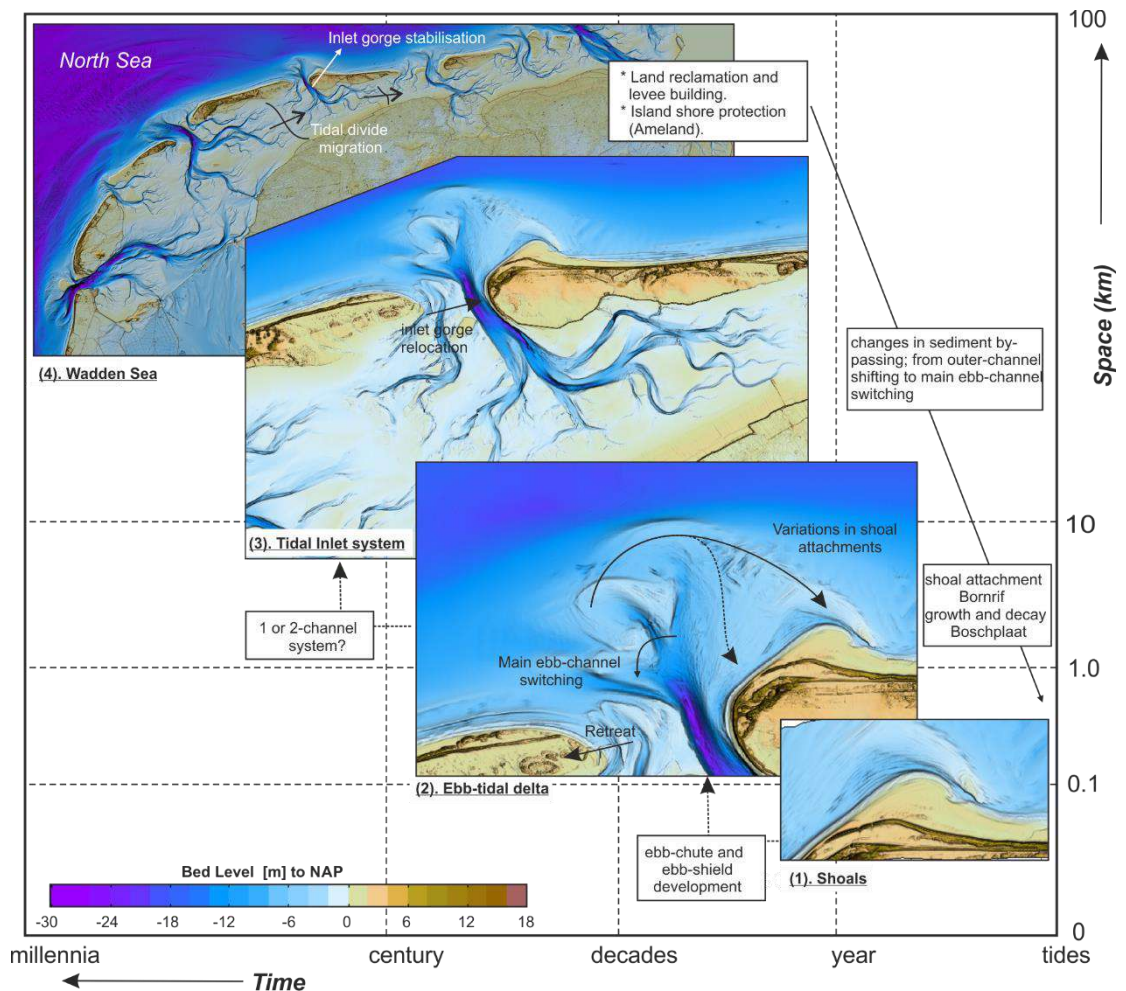
Figure 2.3   A cascade of scales and relevant processes to describe the change in inlet dynamics over various time and spatial scales for Ameland Inlet.

An analysis of the long-term morphodynamic behavior of Ameland Inlet is presented in Elias et al. (2019). This paper analyses in detail the sediment-bypassing that occurs at Ameland Inlet using both bathymetric charts and high-resolution digital data spanning a period of nearly 200 years. This study is especially relevant for Kustgenese 2.0 as the sediment-bypassing exerts a large influence on the updrift and downdrift shorelines, and the ebb-delta nourishments directly interact with the sediment-bypassing process. In this section, a summary of the main research findings is therefore provided.

An important conclusion from the study concerns the (lack of) predictability of the sediment-bypassing process. Predictability of sediment-bypassing appears to be limited. The observed 'cyclicity' in growth and decay of the adjacent islands results from unique sets of ebb-tidal delta

Deltares

configurations and the underlying sediment-bypassing processes differ fundamentally. Moreover, both large-scale and small-scale morphodynamic interactions can alter or initiate the sediment-bypassing process. To explain the various processes that influence Ameland Inlet over a range of time and spatial scales, a scale-cascade model was proposed (Figure 2.3).

This scale-cascade model consists of four levels of aggregation, increasing from the level of (1) individual shoals, to (2) the ebb-tidal delta, (3) the inlet system and finally (4) the Wadden Sea as a whole. Based on the analysis presented by Elias et al. (2019), it can be concluded that ebb-tidal delta-scale changes (level 2) can be driven by both morphodynamic interactions resulting from the larger scales of the inlet (level 3) and the Wadden Sea (level 4), and through interactions that originate on the smallest scale of individual shoals (level 1).

The principle of large- to small-scale interaction in tidal inlets is well described by the conceptual models of e.g. Dean (1988) and Stive and Wang (2003). The barrier islands, ebb-tidal delta, inlet gorge, and basin all form part of the same sand-sharing system and strive to maintain a balance or (dynamic) equilibrium state between these elements. A distortion in one of the elements, either natural or anthropogenic, imposes sediment exchange between the elements until a new equilibrium state is attained. This new equilibrium state imposes different extrinsic conditions on the smaller-scale processes.

A large-scale geomorphic transition in the morphodynamic behavior of Ameland Inlet was first visible around 1926 as the main channel in the inlet gorge shifted to the east, from an updrift to a downdrift location. This shift is related to the eastward migration of the tidal divides in the basin, which had been ongoing since 1600 AD as a result of land reclamation and levee building (Van der Spek 1995). In a natural, non-engineered system, systematic migration of the channels in the basin would induce a similar movement of the tidal inlet and ebb-tidal delta and, hence, migration of the barrier islands. However, at Ameland, as Borndiep migrated eastward, intensive shore-protection works were constructed that stabilized the inlet channel in that position. About the same time, the sediment-bypassing mechanism changed from "outer channel shifting" to "main ebb-channel switching" thereafter. Both sediment-bypassing mechanisms eventually produce bypassing shoals, but the location of shoal attachment to the downdrift island Ameland may differ.

Recent measurements show that (changes in) sediment-bypassing can also be initiated through interactions starting at the smallest scale levels. High-resolution observations taken between 2005 and 2017 illustrate the initiation of a new sediment-bypassing cycle triggered by an initial small-scale distortion or shoal instability in the central part of the ebb-tidal delta. The Kustgenese 2.0 observations presented in this report help us to better understand these small- to meso-scale interactions. The meso-scale is hereby defined as the scale in which typical morphological ebb-tidal delta elements (e.g., ebb and flood channels, channel-margin linear bars, terminal lobes and swash-bar patterns) form and migrate. The associated time-scales are years to decades and the spatial scales are kilometers. The meso-scale dictates the evolution of the channels and shoals on ebb-tidal delta scale.

Deltares

3 Morphodynamics of Ameland Inlet (2005-2016)

The focus of this Chapter is on the meso-scale morphodynamics of Ameland Inlet; see Figure 2.3 for definition. Studies in the past such as Hayes (1975); Hubbard et al. (1979); Sha (1989); FitzGerald (1996), and recently Elias and van der Spek (2017) have shown that the distribution, evolution, shape and size of typical meso-scale ebb-tidal delta elements provide useful insights in sediment transport patterns. The analysis of Elias et al. (2019) showed that smaller-scale distortions can develop in meso-scale features (ebb-shield and chute systems), that can drive ebb-tidal delta wide change. The ebb-tidal delta nourishment can be considered a meso-scale element, and therefore it is essential to understand the morphodynamic processes on this scale level in enough detail.

The analysis presented in this section is focused on the data available over the 2005-2016 timeframe; the more recent changes 2016-2019 are provided in the next Chapter as part of the Kustgenese 2.0 analysis.

3.1 Bathymetric measurements

Since 1986 all bathymetrical surveys are stored digitally following a strict protocol. The digital maps are based on regularly collected data, in approximately 3-year intervals for the ebb-tidal delta and 6-year intervals for the basin (Dillingh, 1990). Each inlet system is measured with approximately 200 m transect spacing using a single-beam echo-sounder. Following quality checking for measurement errors, data are combined with nearshore coastline measurements and lidar data for the tidal flats in the basin and interpolated to 20x20 m grids. The grids are then stored digitally as 10x12.5 km blocks called Vaklodingen (De Kruif, 2001). In addition to the 3-yearly Vaklodingen, bathymetric data were also collected by RWS over the interval 2007-2010 in the framework of the SBW-Waddenzee project (Zijderveld and Peters, 2006). These data were processed and saved in the Vaklodingen format. Half-yearly bathymetric surveys of the ebb-tidal delta started in 2016 and were continued until the end of 2019 as part of the Kustgenese 2.0 project. Table 3.1 provides an overview of survey data collected since 2005. Note that the recent data (2016-2019) is discussed in the next Chapter.

Table 3.1   Overview of the available bathymetric data for basin and ebb-tidal delta ETD.

Year	Dataset	Coverage		Date	Dataset	Coverage	
		Basin	*ETD*			*Basin*	*ETD*
2005	Vakloding	X	X	31-10-2016	KG2	-	X
2006	SBW	channels	X	21-06-2017	vakloding	X	X
2007	SBW	X	X	23-09-2017	KG2	-	Partial
2008	Vakloding	X	X	05-06-2018	KG2	-	X
2009	SBW	channels	X	14-10-2018	KG2	-	Partial
2010	SBW	channels	X	18-07-2019	KG2	-	X
2011	Vakloding	channels	X				
2014	Vakloding	X	X				

Even for the digitally available data, it is difficult to estimate their accuracy. Over time, surveying techniques changed several times, the accuracy of both instruments and positioning systems increased, and variations in correction and registration methods have occurred. Perluka et al. (2006) provided an analysis of the present-day survey accuracy in the Wadden Sea. These authors estimated the vertical accuracy of measured (raw) wet data at 0.11 m and 0.40 m for the final interpolated data. Similar error estimates for the Western Scheldt estuary show inaccuracies of 0.19

Deltares

– 0.23 m for low-gradient channel slopes and intertidal areas. Errors along the channel slopes are larger (up to 0.39 m) because of the steep gradients in bathymetry there.

3.2 Morphodynamic changes between 2005 and 2016

An analysis of the meso-scale morphodynamics of the ebb-tidal delta since 2005 (Figure 3.1) is based on the bathymetries obtained between 2005 and 2016. The choice of the 2005 bathymetry as a starting point is two-fold. Firstly, based on the analysis of the volumetric change of the ebb-tidal delta Elias (2018) indicates that inaccuracies may exist in the bathymetries prior to 2005. Secondly, the 2005 bathymetry is the last bathymetry, prior to the ebb-chute and shield formation (see below for explanation). Besides the formation of the ebb-chute and shield systems some of the main characteristics of the 2005 bathymetry are retained over the measurement period (Figure 3.2). The latter include:

(1) The inlet gorge consists of a shallow western part along the tip of Terschelling and a deep eastern part along the Ameland coastline that contains the main ebb-channel Borndiep.
(2) Borndiep has a north-westerly outflow onto the ebb-tidal delta.
(3) The main ebb-delta volume is located north-eastward (downdrift) of Borndiep in the Bornrif platform.
(4) In the shallow western part of the inlet, between Westgat and Boschgat, smaller secondary channels occur that do not directly connect to a channel on the ebb-tidal delta.
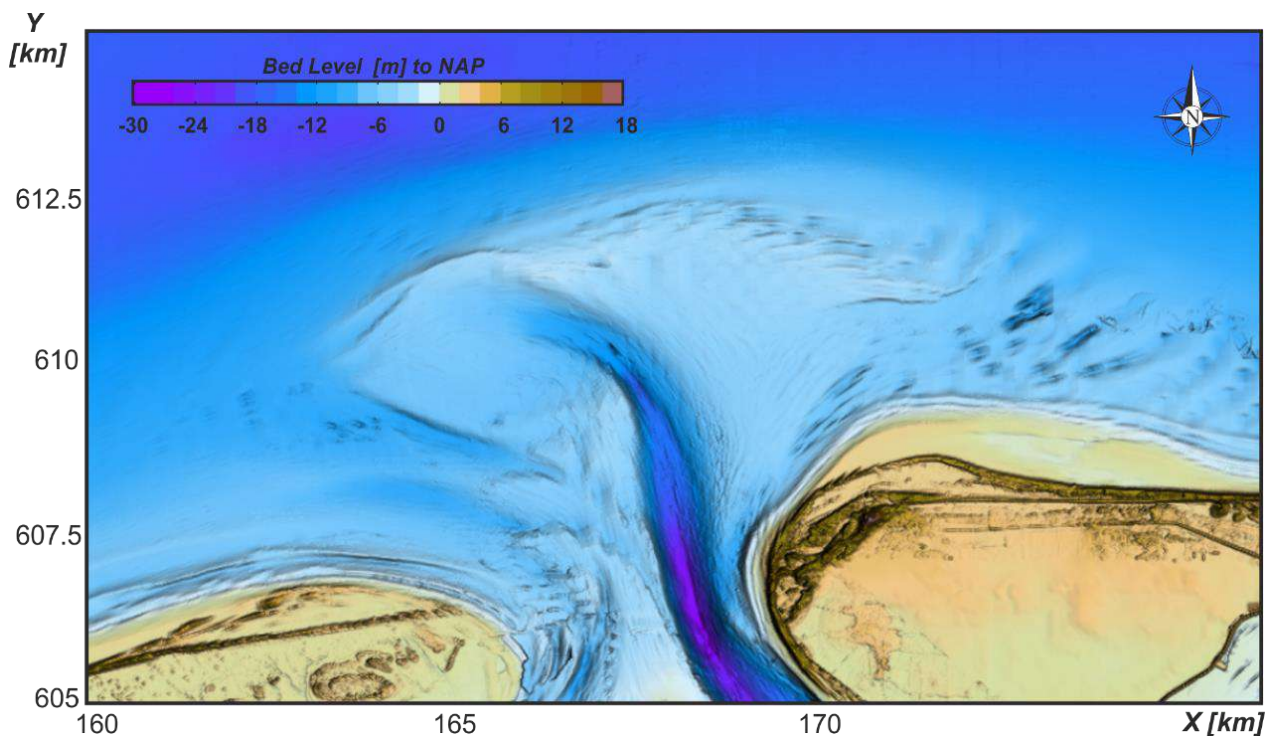

Figure 3.1   Bathymetry of the ebb-tidal delta based on the 2005 Vakloding.

Despite these commonalities, the bathymetries also display significant changes. These changes have been related to the initiation of a new sediment-bypassing cycle (Elias et al. 2019). In the 2005 bathymetry, a relative long and shallow shoal extends along the western margin of Borndiep and Akkepollegat on the ebb-tidal delta (Figure 3.2 [a]). On this shoal, small instabilities develop, triggering the formation of a series of initially small ebb-chutes and ebb-shields (2006, 2008, 2014). A first ebb-chute formed between 2005 and 2006 as a small spill-over channel just north of Westgat (Figure 3.2 [b]). As this channel grew, it pushed sediments seaward, forming a small ebb-shield onto the Kofmansbult shoal. By 2008, a second ebb-chute and shield (Figure 3.2 [c]) had formed that

Deltares

overwhelmed the first system. In total, the second ebb-chute migrated more than 3 km onto the ebb-tidal delta with rates varying between 160 m/year and 500 m/year. By 2014, the ebb-shields of the first and second ebb-chute merged, forming a large shoal just west of Akkepollegat (Figure 3.2 [e]). This ebb-shield development on the Kofmansbult continued to steer the morphodynamic changes of the central-downdrift ebb-delta platform; the combined ebb-shield expanded seawards, rotated clockwise, and by 2014, the ebb-shield covered the major part of the Kofmansbult [e]. This large shoal increasingly affected and constricted flow in Akkepollegat that subsequently reduced in size and was deflected downdrift, to the east. As a result, by 2016 a downdrift-curved channel remains. Using the -10m contour as a proxy for channel displacement, a near 1.3 km eastward displacement of the seaward end of Akkepollegat can be observed.

The growth of a large shallow shoal (Bornrif Bankje, Figure 3.2 [g]) suggests that the ebb-delta deposits in front of the channel were transported to the east along the north-eastern margin of the ebb-delta shoal.

Sandwiched between Westgat and the second ebb-chute, a new (third) ebb-chute (Figure 2.2 [10]) started to form between 2011 and 2014 (Figure 3.2 [d]). This new ebb-chute quickly grew and expanded to the (north)west. The -10 m contour migrated nearly 900m westward between 2011 and 2016. While the shallower part of the Akkepollegat channel primarily rotated eastward (up to the -10 m contour), the deepest part significantly reduced in length; over 300m between 2005 and 2009. As flow in Akkepollegat was increasingly restricted, a new outlet for Borndiep was needed. While the distal part of Akkepollegat rotated clock-wise (to the east), the proximal part, near the inlet gorge, rotated anti-clockwise (Figure 3.2 [f], revealing the likely new course for the main ebb channel south of the main shoal areas at the location of the third ebb-chute.

Large changes were also observed on the Bornrif platform. Although the outline of the Bornrif platform remainsunchanged, between 2011 and 2016 the formation, migration and eventual merger of Bornrif Bankje dominated the developments. The origin of Bornrif Bankje can be traced back to the period 1989-1999. During this period the northern ebb-delta front prograded seawards and increased in height at the seaward end of Akkepollegat. This outbuilding continued until 2011. It is likely that wave-breaking on this shallow shoal area resulted in downdrift sand transport along the ebb-tidal delta margin, and Bornrif Bankje slowly started to emerge on the north-east side of the ebb-tidal delta (2008-2010; Figure 3.2). The shoal continued to migrate eastward and landward (2011-2014). Migration rates based on the -5 m contour range from between 150 and 430 m/year. By 2014, only a small channel remained between the Bornrif Strandhaak and Bornrif Bankje. The associated transport of sand is likely caused by a combination of wave-driven and tidal flow on the shoal edge and by transports due to flow contraction and acceleration of the along-shore North-Sea tides around the steep slope of the ebb-tidal delta. The map of 2016 shows that the tip of Bornrif Bankje nearly attached to the Ameland coastline, just downdrift of the Strandhaak.

An opposite behavior is observed at the island tip of Terschelling. Here the Boschplaat continues to erode. This Boschplaat erosion is linked to the, at this location, relative deep ebb-tidal delta north of it. As a result, waves can propagate relatively undisturbed towards the coast. This means that wave breaking-related transports can induce significant coastal erosion and eastward transport towards Borndiep.
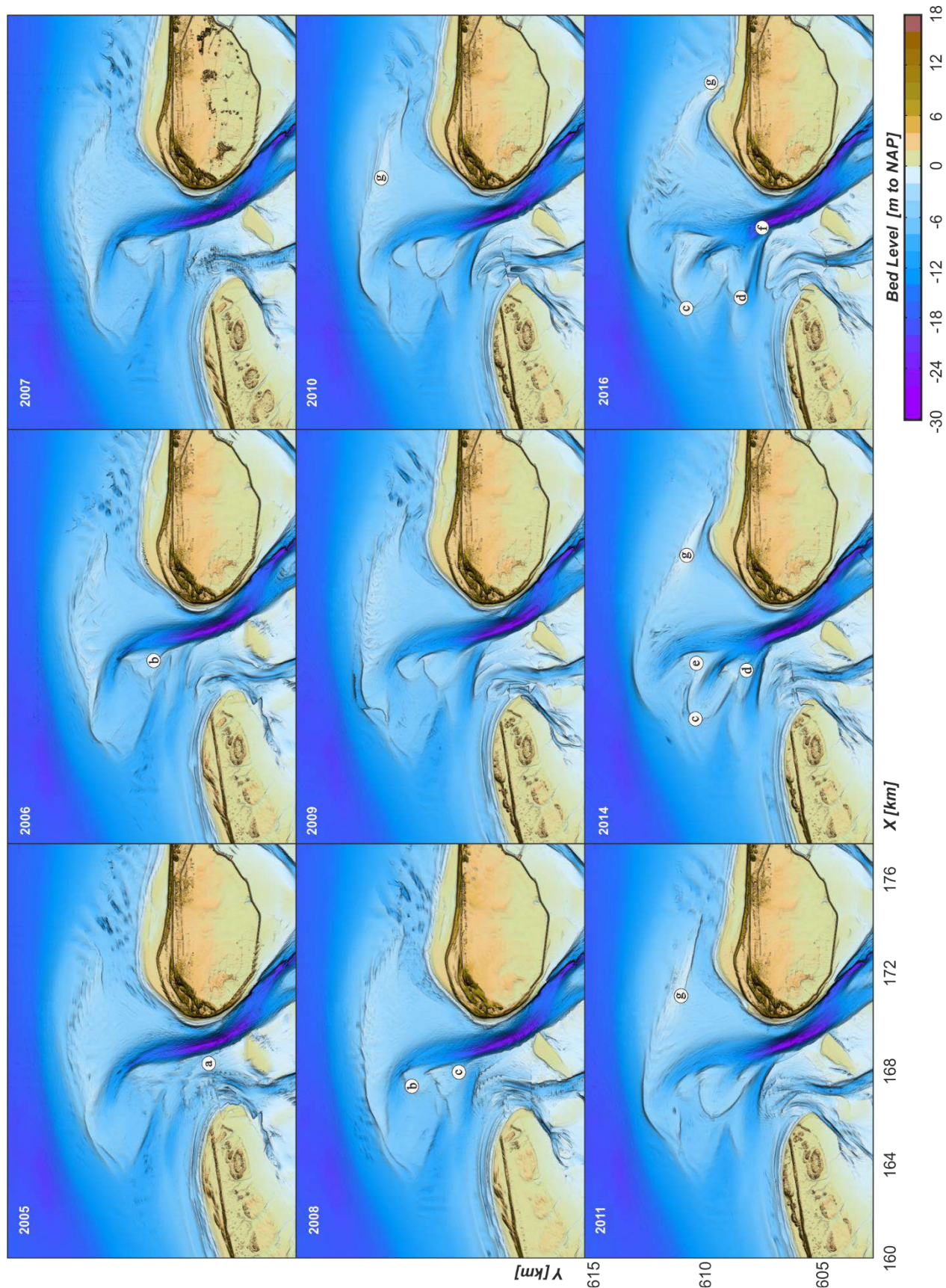
Deltares

Figure 3.2   Complete bathymetries of the ebb-tidal delta based on measurements over the time-frame 2005-2016.

Understanding the morphological processes at Ameland Inlet
1220339-008-ZKS-0008, 4 March 2020

Deltares

3.3   Sediment budget analysis 2005-2016

An extensive analysis of the sediment budget of the Wadden Sea including Ameland inlet is presented in Elias (2019). Our goal in this Chapter is not to replicate those efforts, but to provide insight in volume changes at the meso-scale by focusing on the individual shoals and channels. Estimates of the volumes associated with certain morphodynamic features such as channels and shoals are often difficult to make as these depend on the selection of an arbitrary reference level. In this study, the sedimentation-erosion patterns over the period 2005-2016 are used as an indication of the volume changes. The numbers between square brackets [..] in the following paragraphs refer to the numbers indicated in Figure 3.3.

In total, the ebb-tidal delta and coast show a net increase in sediment volume of 11.1 mcm. The majority of this gain was observed along the island coastlines, to the north and south of the ebb-tidal delta. The ebb-tidal delta gained 6.6 million m^3 (mcm) of sediment but correcting for 4.7 mcm of nourishments a net gain of around 1.9 mcm would have occurred. The volumetric change of the ebb-tidal delta is small compared to the observed gross changes of ~140 mcm.

Erosion is observed along the adjacent coast of Terschelling, where the Boschplaat loses 11.0 mcm of sediment [17,23]. Most of these losses occur on its seaward side 7.7 mcm [17], while an additional loss of 3.3 mcm from is observed along the basin side. A volumetric gain of 5.9 mcm to the east in the Boschgat area [16], suggests that sediment from Terschelling, and supplied through the littoral drift, are transported from the island tip eastward and towards the basin.

Severe erosion is also observed just to the north of Westgat, where the two ebb-chutes developed. In total this area loses 17.7 mcm [14]. Part of this erosion is caused by a small rotation and migration of the main channel Borndiep/Akkepollegat. With a decreasing efficiency of the northward extending Borndiep/Akkepollegat, the channel dimensions become too large. This channel is consequently filled with sediments that are transported southward (by waves) over the Bornrif platform. A total volume of 12.4 mcm is deposited along the channel's eastern (Bornrif) side [18], that is at least partly provided by the over 25 mcm of erosion of the seaward Bornrif platform [11]. The Bornrif shoal area shows alternating patterns of erosion and sedimentation. The ebb-delta front due north of the early Akkepollegat location [10] gains 7.6 mcm of volume. This accretion is caused by the rotation of Akkepollegat that temporarily expanded north what resulted in a migration/outbuilding of the delta front. The shallower portions of this shoal (roughly above -5 m NAP) were eroded and transported landward by the wave-driven transports resulting in a loss of 25.1 mcm [11]. Part of these sediments were transported in the form of a shoal (Bornrif Bankje) along the delta margin towards the coast of Ameland. This contributes to the 14.1 mcm of sedimentation observed here [20,8]. The deeper part of these deposits is less easily moved and a sediment accumulation of 7.6 mcm remains [10].

Sediment accretion on the Kofmansbult due to ebb-shield formation is estimated to be 17.8 mcm [12]. An initial 6.9 mcm accreted to its south as part of the deposits related to the southern ebb-shield and the Westgat ebb-shield [13].

An important conclusion from this sediment budget is that the net morphodynamic changes are small compared to the gross changes. On the ebb-tidal delta about 140 million m^3 of volume change occurred, but net change is limited to 5.1 million m^3. The dynamics of the channels and shoals are much more dominant for the morphological behavior than the actual exchange with the coast. These large gross changes also provide an indication of the systems sensitivity to nourishments. Nourishments in the order of 2-5 million m^3 are of such size that they are unlikely to significantly influence the ebb-tidal delta dynamics.

The sediment budget of the tidal inlet and ebb delta also facilitates the calculation of the sediment exchange on a larger scale. The main developments in the period 2005-2016 are (1) the erosion of

the east end of the island of Terschelling, (2) the development of the ebb chutes and -shields and (3) the sand transport towards Ameland over the shoal Bornrif.

Erosion east end Terschelling
The erosion of Boschplaat (Figure 2.2, [15]), both under water and above, produces a total sand volume of 12.6 mcm (polygons 15, 17, 2)[1]. The gain in polygon 16, directly downdrift of Boschplaat, is only 5.9 mcm. This implies that 6.7 mcm has been transported further, into the tidal basin and/or onto the ebb delta.

Ebb chute and -shield development
Formation and continued scouring of the ebb chutes produced a substantial amount of sand: 17.7 mcm (polygon 14). The total sedimentation on the ebb shields is larger, a volume of 24.7 mcm (polygons 12, 13). The surplus of 7.0 mcm has been transported here from other sources, probably erosion of Boschplaat or export from the tidal; basin. The 'missing' volume of 6.7 mcm that eroded from Boschplaat (see above) fits very well with this surplus volume, suggesting that the former volume ended up on the ebb shields.
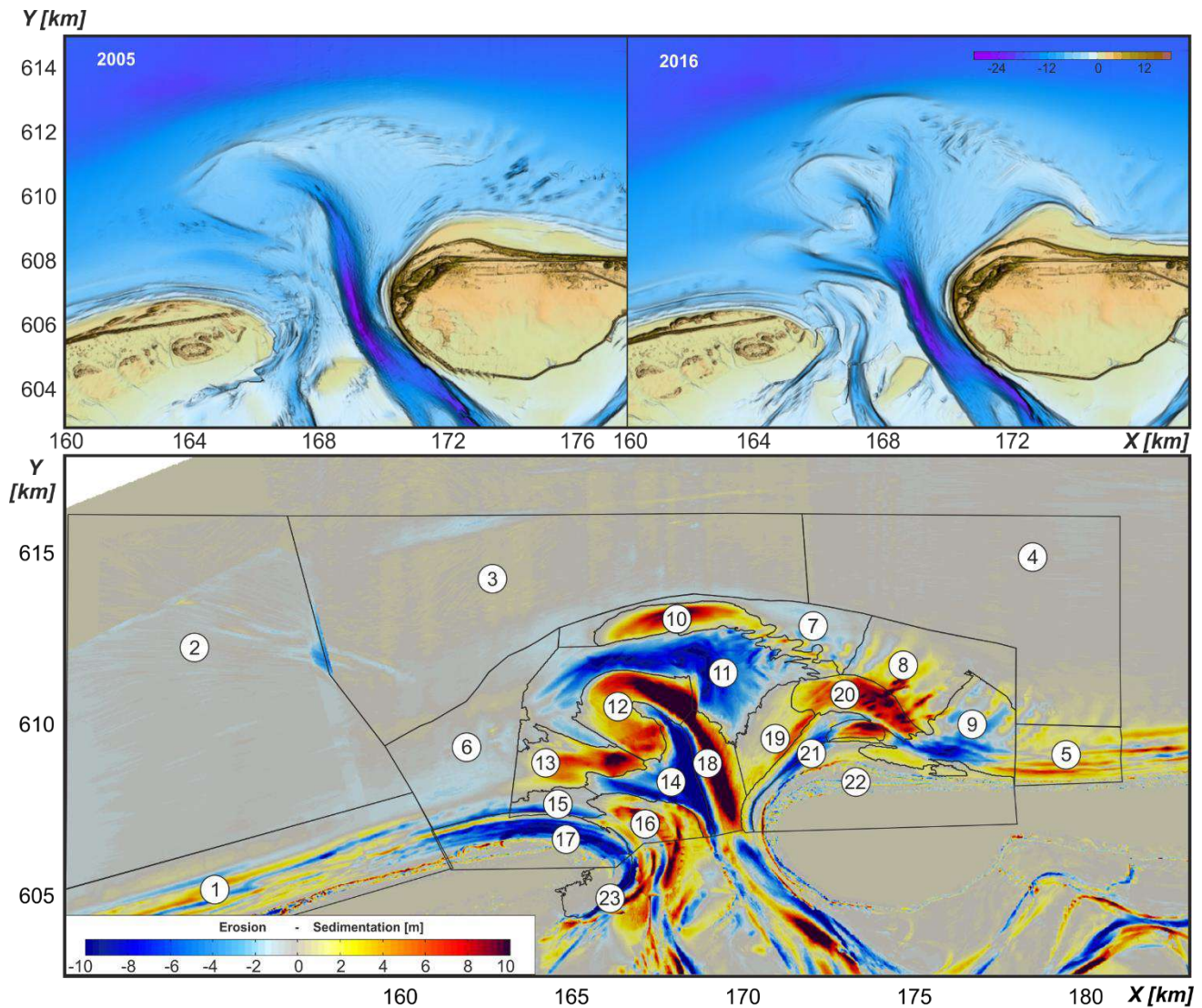
Bornrif sand transport
The erosion on Bornrif shoal (polygon 11) comprises a large volume: 25.1 mcm. However, this is the result of two developments, the northward expansion of the Akkepollegat ebb shield and the more regular transport from the seaward edge in the direction of west Ameland. Hence, the eroded volume can be split in two sub-polygons. The sand volume that was deposited during the expansion of Akkepollegat is 7.6 mcm (polygon 10). That amount will have been produced by scouring and subsequent transport by ebb currents. Therefore, it is assumed that c. 8 mcm of the total eroded volume of 25.1 mcm in polygon 11 ended up in polygon 10. This means that c. 17 mcm was available for transport to the southeast, over Bornrif shoal, in the direction of west Ameland. Moreover, erosion in polygon 7 delivered an extra 2.5 mcm. The total sand accumulation at the landward part of Bornrif is 17.6 mcm (polygons 8, 19, 20). The erosion in polygon 21 will have contributed to this. The total volume gain is slightly smaller than the total erosion, but part of that volume will have been transported either into the infilling Borndiep channel (polygon 18) or to the coastal zone of Ameland (polygons 9, 5 and beyond)

Combination these 'transport cells' sketches the bigger picture of sand exchange around Ameland Inlet between 2005 and 2016. Erosion of Boschplaat produces a surplus of 7 mcm which corresponds with the sediment gain in the ebb shields. The sediment exchange over Bornrif shoal is also approximately balanced. This implies that the major part of the sedimentation in the infilling Akkepollegat (polygon 18), say 10 mcm out of 12.4 mcm, has been transported here from sources outside of the ebb delta. Export by the tidal basin seems most likely. However, a contribution of the eroding seaward part of the delta (polygon 6) is possible. This also holds for the volume of the sand nourishments on northwest Ameland (c. 4 mcm). The latter two sources add up to a total of 9 mcm, which means that if their contributions ended up in Akkepollegat entirely, the contribution of the tidal basin will have been small.

---

[1] Note that the eroding area at the southside of Boschplaat is larger than polygon 23. Hence, the total volume can be larger.

Understanding the morphological processes at Ameland Inlet
1220339-008-ZKS-0008, 4 March 2020

Deltares

Figure 3.3 *Observed sedimentation-erosion patterns and volume changes over the time period 2005-2016. Tables show the values for the individual polygons (left) and aggregated features (right). Based on Elias (2018).*

Poly-gons	Volume change [mcm]			Poly-gons	Volume change [mcm]		
	Wet[1]	Beach[2]	Dune[3]		Wet[1]	Beach[2]	Dune[3]
1	0,9	0,7	2,0	12	17,8	-	-
2*	0,4	-	-	13	6,9	-	-
3	-0,9	-	-	14	-17,7	-	-
4	1,1	-	-	15	-1,6	-	-
5	4,1	0,6	0,3	16	5,9	-	-
6	-4,9	-	-	17	-5,6	-1,5	-0,6
7	-2,5	-	-	18	12,4	-	-
8	3,8	-	-	19	3,5	-	-
9	-5,4	1,7	-	20	10,3	-	-
10	7,6	-	-	21	-3,3	-0,4	-
11	-25,1	-	-	22	0,2	0,2	0,1
				Total	7,9	1,3	1,9

Name	Polygons	Volume change [mcm]			
		Wet[1]	Beach[2]	Dune[3]	Total
Coast	1,2,3,4,5,6	0,7	3,0	2,3	6,0
ETD	7-22	7,2	-1,7	-0,4	5,1
		7,9	1,3	1,9	11,1
Bornrif	8,9,19-22	9,1	1,5	0,1	10,7
Boschplaat	15,16,17	-1,4	-1,5	-0,6	-3,5
Westgat	13,14	-10,8	-	-	-10,8
Kofmans-bult	12	17,8	-	-	17,8
					-
Borndiep	18	12,4	-	-	12,4
Bornrif (front)	11,10,7	-20,1	-	-	-20,1
		7,2	0	-0,4	6,6

(1). Wet = volume change for bed level <+1 NAP.
(2). Beach = volume change for bed level between +1 and + 3m NAP.
(3). Dune = volume change for bed level > +3m NAP.
* erosion in polygon 2 (2005-2007) is unrealistic. Therefore a zero change is assumed over this time frame.
(23). Polygon 23 - erosion of basin side of Boschplaat = -3.3 mcm.

Deltares

4 Analysis of Kustgenese 2.0 field data

Further insight into the processes underlying the observed meso-scale morphodynamic changes can be gained from analysis of measurements obtained during the Kustgenese 2.0 Amelander Zeegat (AZG) campaign. Note that in this report, only a selected portion of the data collected is used. As of this writing part of the data is still being processed and studied by the university partners in the SEAWAD research program. Where needed the analysis of older datasets (e.g. discharge, wave and tide measurements) was combined with the recently obtained data from Kustgenese 2.0.

4.1 The setting of the Amelander Zeegat campaign

4.1.1 Location and general description of the measurements

An extensive field campaign was conducted at Ameland Inlet between August 29 and October 10, 2017. Bathymetric, hydrodynamic and sediment data, and benthic species distributions were collected. Figure 4.1 presents the instrument locations. A complete overview of the KustGenese data is presented by Van der Werf et al. (2019) and the data can be retrieved at http://waterinfo-extra.rws.nl/.

Multiple instrument deployments, surveys and mapping cruises were undertaken. The bulk of the measurements were made using five frames equipped with instruments to study flow and waves (ADCP, ADV), turbidity and sediment concentration (OBS, LISST), and bedforms (3D SONAR). These frames were placed at various locations in Ameland inlet (see Figure 4.1). Note that data from frame 2 could not be retrieved since the frame was buried in sand and lost during a storm. This is an unfortunate demonstration of the shoal migration into Akkepollegat discussed in Section 3.2 and highlights how dynamic the ebb-tidal delta is.

In addition to the frame measurements, several roving ADCP measurements were carried out simultaneously over two transects just seaward of the inlet gorge (see dashed lines in Figure 4.1). Current velocities were measured using a downward-looking ADCP over a period of at least 13 hours to cover a full tidal cycle, which allows for the calculation of the tidal prism through the inlet. In the basin, upward-looking ADCPs were placed on each watershed to measure the flow and water levels. Wave-measurements were performed through a series of wave buoys, and stand-alone pressure sensors in the vicinity of frame 4 and 5. Flow patterns were obtained using Lagrangian drifter experiments around frame 4 and 5, and by a single large-scale experiment conducted over the entire inlet during a single tidal cycle.

In addition to the AZG campaign, additional bathymetry and X-Band radar measurements were collected between 2016 and 2019. The bathemetry of the ebb-tidal delta was surveyed every 6 months between 2016 and 2019 (Table 3.1). These surveys are an extension of the regular bathymetric (Vaklodingen) monitoring. In addition, high-resolution multi-beam data was collected along 4 transects at varying intervals. This included repeated surveys over the tide-cycle in Borndiep. The navigational X-Band radar on the lighthouse of west Ameland was used as a remote sensing tool to estimate depths in the outer delta. The area that is captured by the radar covers a circle with a radius of approximately 7.5 km (Gawehn, 2019; Gawehn et al. 2020).
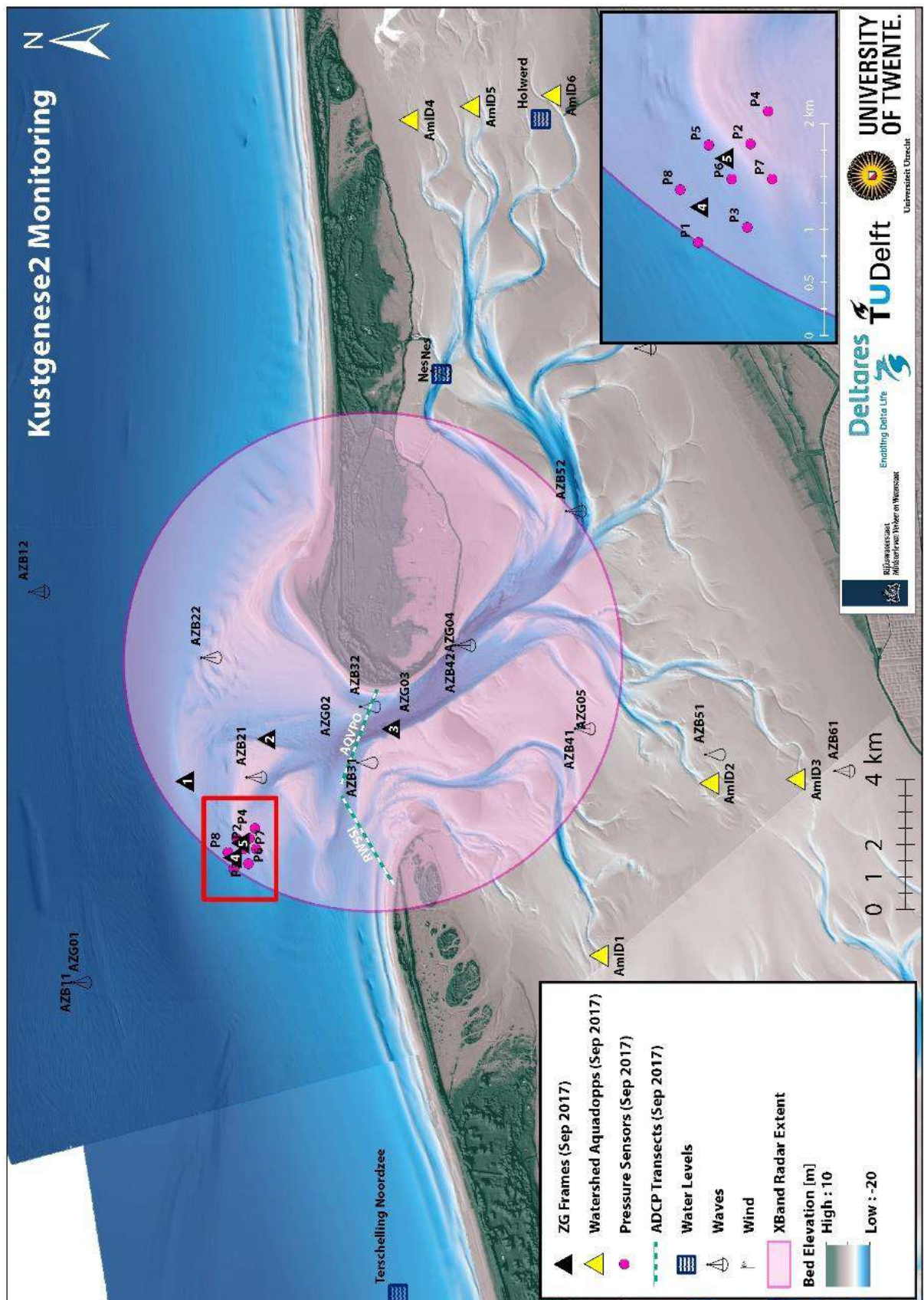
Deltares

Figure 4.1 Locations of hydrodynamic and sediment measurements carried out during the 2017 Ameland Zeegat campaign.

Understanding the morphological processes at Ameland Inlet
1220339-008-ZKS-0008, 4 March 2020

Deltares

4.1.2 Meteorological conditions observed during the campaign

Figure 4.2 provides an overview of the meteorological conditions during the Amelander Zeegat field campaign. During the measurements, both calm and storm conditions occurred (Figure 4.2 c,d). During most of the campaign, wind velocities were below 10 m/s with wind directions from south to west (180⁰-270⁰). Corresponding wave heights are small (below 1m) with wave periods of 4 s or less. From 11 to 15 September, the first major storm event occurred (Storm Sebastian). Winds from westerly direction peaked at velocities of 20 m/s, and the wave height reached 6 m at the buoy located just seaward of the ebb-tidal delta of Ameland Inlet (Buoy AZB11). This peak wave height is not representative for the entire storm event as waves mostly remained below 3 m. This storm event was followed by a relative calm period until the second storm event started on 30 September (Storm Xavier). The second storm event was less severe in maximum wind speeds. However, wind velocities of around 10 m/s from a west – northwesterly direction were sustained over a 5-day period. As a result, a prolonged period of 3 to 4 m wave heights was measured at the offshore buoy (AZB11).

The varying conditions had a clear impact on the observed water levels (Figure 4.2a). The semi-diurnal tidal movement is the main driving force for the open-sea tides and remains clearly visible throughout the timeseries measured at Nes, at the south side of Ameland. Part of the long-term fluctuation in water level is related to the spring-neap cycle, but also fluctuations can be seen that are related to the meteorological conditions. During the storm events air pressure reduces and the wind generates set-up or set-down of the water levels. This is reflected in the elevated mean water levels during both storm events, especially the increased water levels in the basin caused by northwesterly winds on 5-8 October (Figure 4.2a). Variations in set-up can drive complicated residual flow fields in the Wadden Sea and through the inlets. At first glance, such effects are not clearly visible in the velocities observed in the inlet gorge (Figure 4.2b). The measured velocity signal shows a typical semi-diurnal tidal modulation with slightly higher flood velocities compared to the ebb velocities. Velocities significantly reduce during neap tide and increase during spring tide. Only during the second storm event (around 6 October), enlarged ebb and flood velocities can be observed.
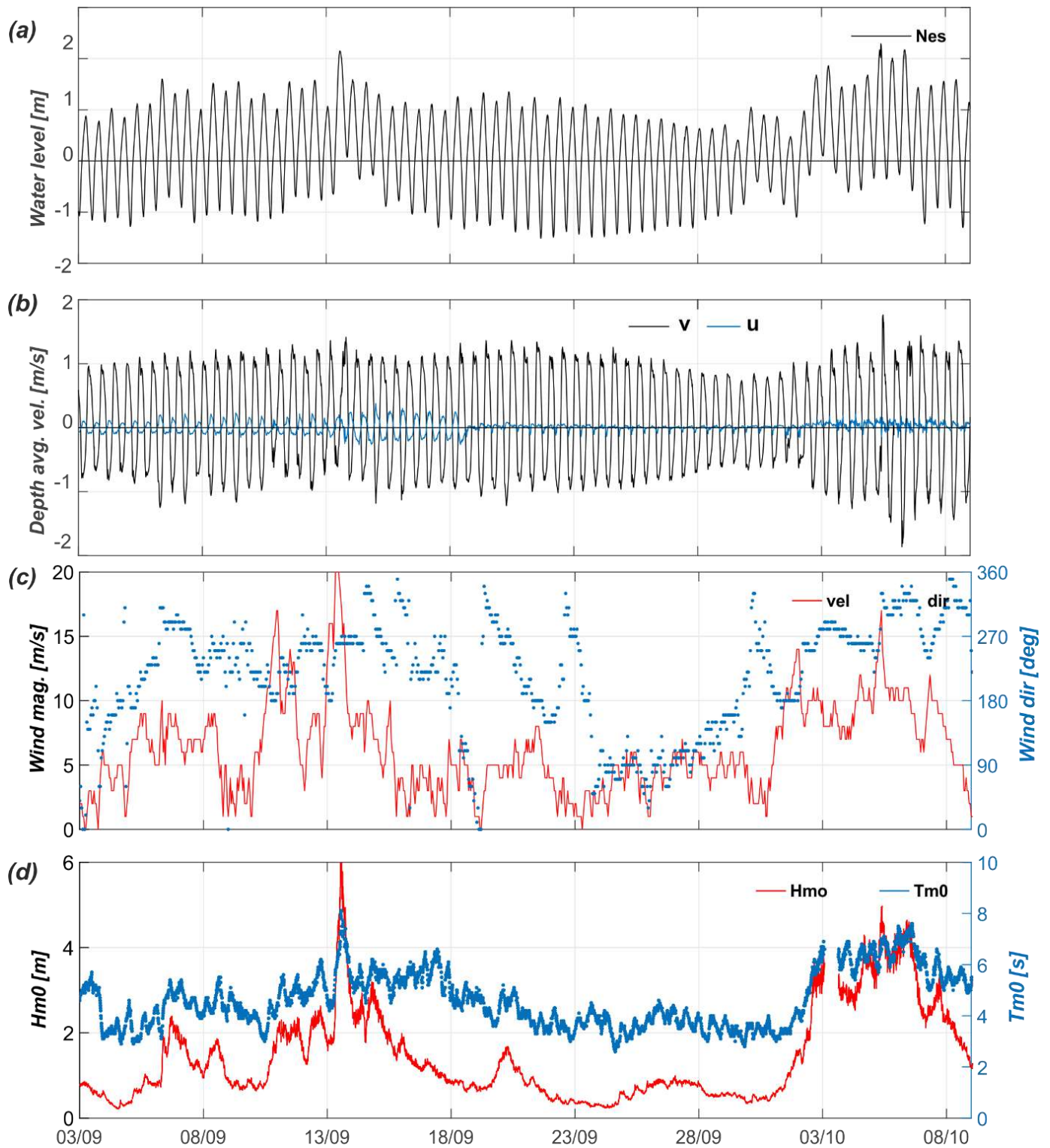
Deltares

Figure 4.2 An overview of the meteorological conditions during the 2017 main campaign. (a) Water levels measured at the nearby NES station, (b) Velocities observed at frame 3 (Borndiep channel) in along channel (v) and a crosschannel direction (v). (c) Wind speed and direction observed at the KNMI station of Terschelling.(d). Wave height and period at the offshore wave buoy B11.

Deltares

4.2 An analysis of the hydrodynamic measurements

4.2.1 Water levels during the campaign

The tidal movement at Ameland inlet is generated mainly by the tidal wave from the southern part of the North Sea that enters the Wadden Sea through the inlets. The North Sea tides are driven by tidal (Kelvin) waves entering from the Atlantic Ocean between Scotland and Norway in the north, and through the Dover Strait in the south. Interference of these two waves, distorted due to Coriolis effects and bottom friction, generates a complicated tidal flow pattern in the southern part of the North Sea (Pugh, 2004). The tides spin in a whirl with anti-clockwise rotation around 2 amphidromic points. Along the Holland coast, the flood-dominant tides propagate from south to north in a form that is between a standing and progressive tidal wave. This tidal wave generates maximum shore-parallel tidal velocities in the range of 0.5 to 1.0 m/s. Near Texel inlet this northward-travelling tidal wave meets the second eastward travelling tidal wave, that rotates around the second amphidromic point. The combined waves propagate from the west to east along the Wadden Sea Islands and into the basins. The mean tidal range thereby increases from 1.4 m at Den Helder to 2.15 m at Ameland inlet and 2.5 m in the Ems estuary (Eems-Dollard Inlet) and increases even further in eastward direction along the German Wadden coast.

Table 4.1   Overview 10 main constituents for Station Terschelling North Sea.

Constituent		Amplitude	Phase	Constituent		Amplitude	Phase
Name	ϕ	[m]	[deg]	Name	ϕ	[m]	[deg]
M2	28.98	0.86	234.07	L2	29.53	0.07	237.37
S2	30.00	0.24	296.12	K2	30.08	0.07	295.26
N2	28.44	0.15	211.71	MU2	27.97	0.06	321.76
O1	13.94	0.10	206.38	MS4	59.98	0.05	42.08
M4	57.97	0.08	330.04	SSA	0.08	0.05	233.59
K1	15.04	0.07	0.53	M6	86.95	0.05	60.42

The AZG campaign is too short for an accurate estimate of the tidal constituent values. Therefore, the analysis presented here is based on the long-term measurements at the 3 surrounding stations viz. Terschelling North Sea located offshore of Terschelling (TNZ), and the stations Nes and Holwerd in the basin. An overview of the 12 main tidal constituents for TNZ, based on T_Tide analysis (Pawlowicz et al., 2002) of the timeseries presented in Figure 4.3, is presented in Table 4.1. For a more elaborate analysis of the frames data see Van Weerdenburg (2019).

From the tidal analysis it can be concluded that the semi-diurnal tidal movement is the main driving force behind the horizontal water flow through the inlet (M_2 amplitude is 0.86 m). Distortion of the M_2 tide results in a significant asymmetry (M_4 amplitude is 0.08 m) and faster rise than fall of the tide. A considerable spring neap variation (S_2 amplitude is 0.24 m) results in an increase of the tidal range to 2.0 m during spring tide and a drop to about 1.0 m during neap. The tidal signal only partly represents the measured water levels. Meteorological distortion due to air pressure and wind-generated set-up or set-down can reach significant heights. At TNZ, set-up can exceed 1.5 m during major storm events (see Figure 4.3, bottom). In the Wadden Sea, with its complex bathymetry, set-up-gradients can drive complicated residual flow fields, generate shore-parallel velocities and throughflow between adjacent basins (Duran-Matute et al., 2014; Van Weerdenburg, 2019). In addition, the volume of water stored in the Wadden Sea due to the larger set-up can considerably enlarge the outflow velocities in the inlets following the storm events, thereby affecting channel dimensions, the ebb-tidal delta development and adjacent beaches. The morphological analysis presented in section 4.3 indicates that surge (and its associated larger ebb outflow) may play a bigger role in the morphological developments of the ebb-tidal delta than anticipated up until now.
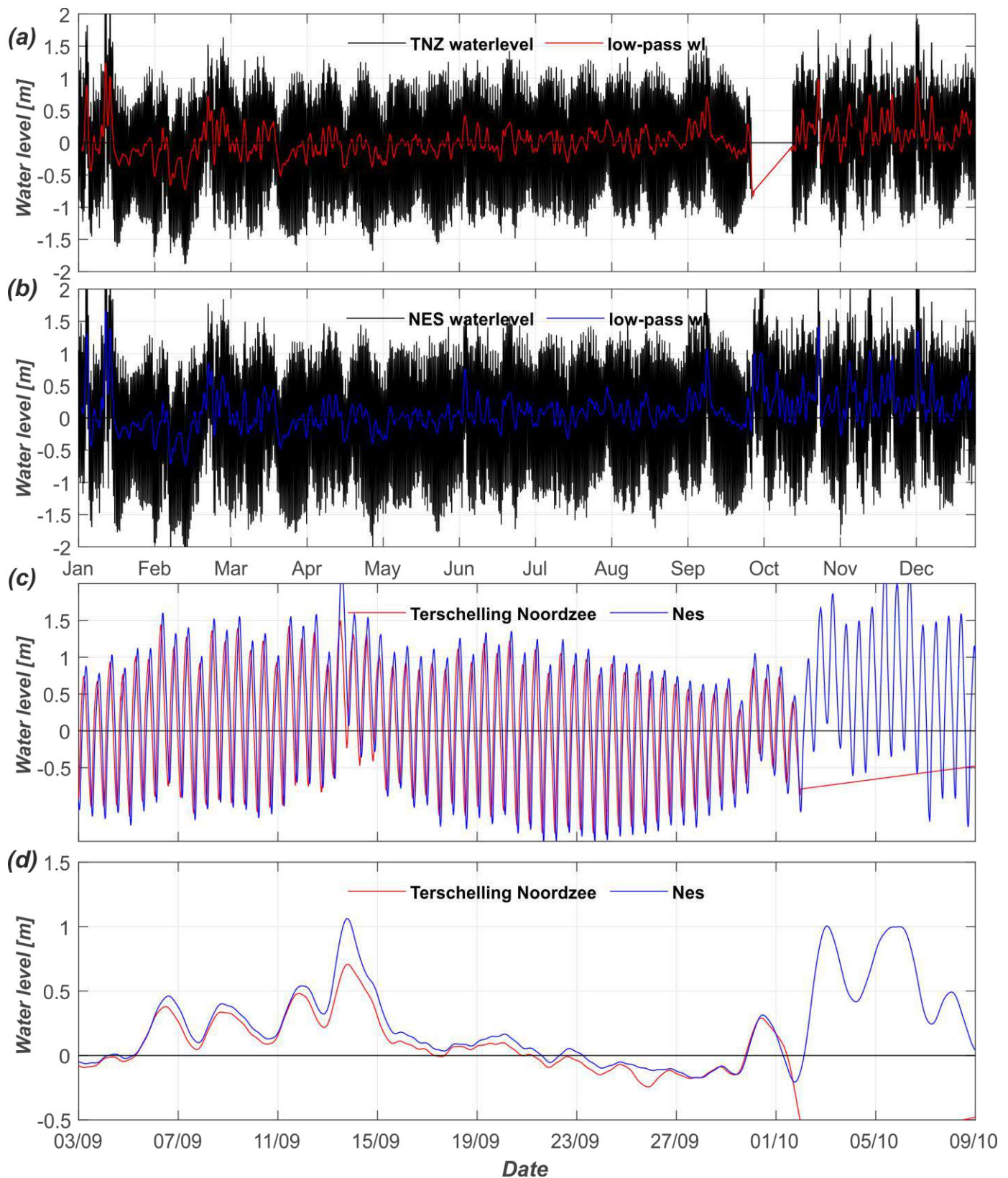
Deltares

Figure 4.3 An overview of the measured water levels near Ameland. Top to bottom: (a) water levels observed during 2017 at Terschelling Noordzee + low-pass filtered results (b). water levels observed during 2017 at NES + low-pass filtered results. (c) Details of the observed water levels at TNZ and NES during the AZG campaign, in September-October 2017, and (d) low-pass filtered water levels at TNZ and NES during the KG2 campaign.

Deltares

4.2.2 Current velocities

This analysis of current velocities is based on the depth-averaged ADCP data collected at the instrumented frames 1, 3 and 4.

Frame 1 and Frame 4 are both deployed on the seaward side of the ebb-tidal delta at depths of 8 m and 9 m below NAP. Frame 1 is positioned on the northern margin of the ebb-delta in front of the Akkepollegat channel. Frame 4 is positioned more westward on the Kofmansbult facing the seaward ebb-chute channel. At both locations flow through the ebb channels and alongshore-directed open-sea tides are likely to affect the velocity structure. Wave effects may be important as well as the frames are exposed to waves from the North-Sea but given the depths at both locations these effects are likely limited to major storm events only.
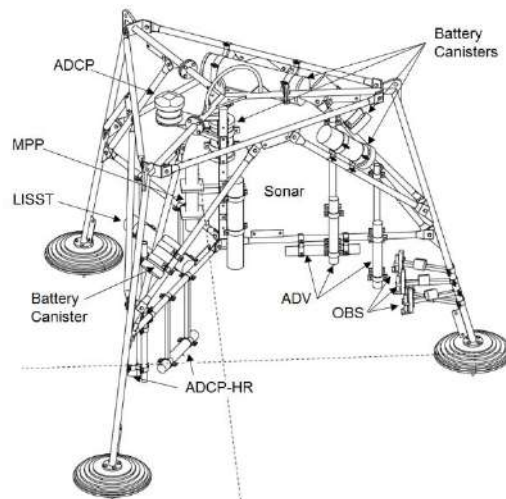
Figure 4.4   Design of the measurement frames used during the KG2 field campaigns. Each 2.4 m high stainless-steel frame was mounted with up to 14 instruments and their accompanying battery packs. This drawing indicates Frame 4 from the AZG campaign; not all instruments shown here were present on all other frames. From: Van der Werf, 2019.

At both frames, the ADCP was mounted near the top of the frame at a height of about 2.3 m above the seabed and recorded time-series of velocity profiles at 1 Hz intervals throughout the deployment. Depth-averaged velocities were calculated from the measured velocity structure by fitting a log distribution. Comparison of the near-bed velocity measured with the ADV illustrates the validity of this method (Van der Werf et. al., 2019).
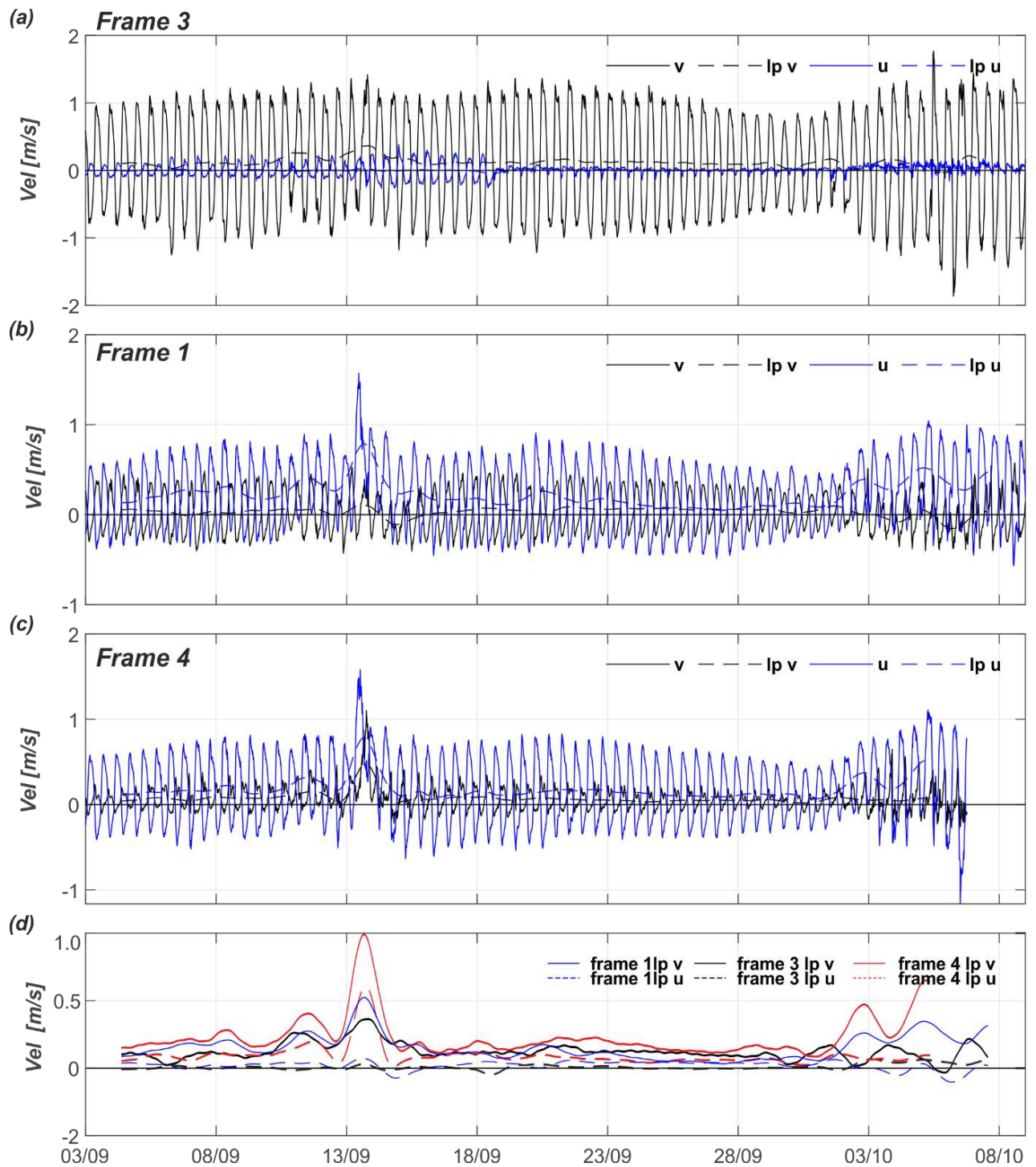
The tidal modulation dominates the velocity signal and shows a strong influence of the spring-neap variation (Figure 4.5 b,c). Both measurements show similar velocity timeseries with larger u (alongshore) versus cross-shore (v) velocities. Northward velocities dominate over the southward velocities, and seaward velocities are in general larger than the landward velocities. During neap tides, maximum ebb velocities are generally smaller than the flood velocities and below 0.5 m/s. During spring tides currents up to 0.8 m/s occur. Tidal velocities at frame 1 exceed the velocities at frame 4, but strong non-tidal contributions are also observed (Figure 4.5d). The contributions of the tidal and non-tidal components in the velocity fields can be estimated through tidal analysis and/or low-pass filtering of the data (Figure 4.5 d-g). Both methods show a relatively strong non-tidal signal at frame 1 with an average of 0.25 m/s over the recorded timeseries.

The significant influence of the non-tidal contributions (e.g. waves and wind-driven currents) are clearly visible in the maximum recorded velocities. These velocities exceed 1.0 m/s during storm events, while during the largest wave event (Storm Sebastian) a 1.5 m/s flow velocity was measured.

Deltares

Frame 3 was placed in the main channel Borndiep near its western slope at a depth of -20 m NAP. Detailed swath mapping revealed the presence of small scale bedforms at this location having average amplitudes of 0.40 m and wavelengths of 11 m (Elias, 2018). The bed forms indicate a flood dominant sediment transport. An upward looking ADCP was used to record the vertical structure of tidal currents. These data were analysed in a similar manner to frame 1 and 4 to obtain estimates of the depth-averaged tidal and non-tidal flow. The correspondence between the tidal velocity signal and measured data illustrates the dominance of tides at this location. Flow velocities are considerably larger compared to frame 1. During spring tide velocities exceed 1.35 m/s and reduce to around 0.50 m/s during neap tides. On average, ebb velocities exceed the flood velocities.

Non-tidal flow contributions peak during the 2 storm events, but the average response with a value of 0.12 m/s over the entire measuring interval is significantly smaller than at the more seaward frames. At this location, the non-tidal contribution is not directly linked to wave-breaking and wave-generated currents since most wave breaking occurs on the outer margin of the ebb-tidal delta. It is likely that wind-driven currents dominate the non-tidal flow in the inlet.
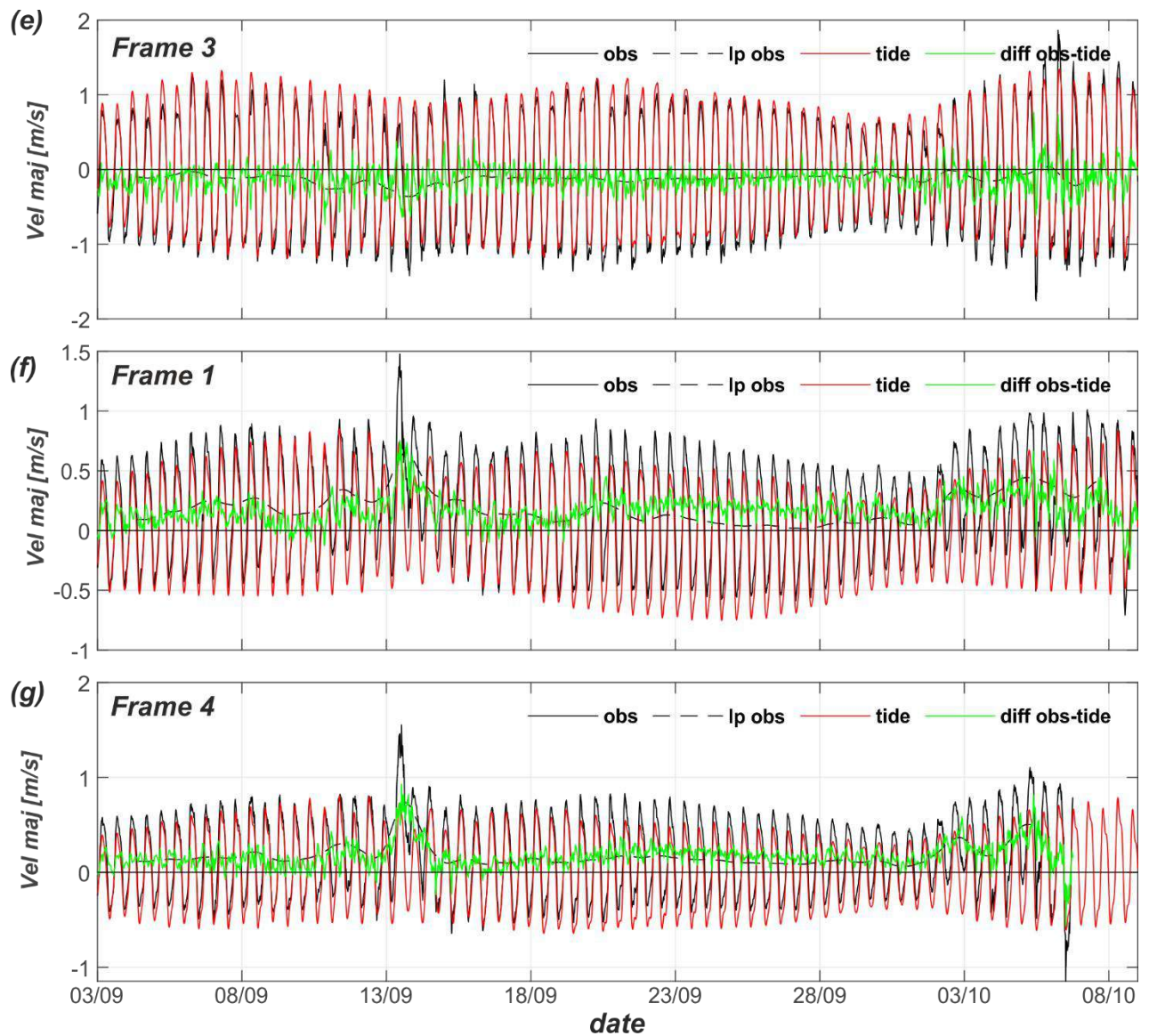
Deltares

Understanding the morphological processes at Ameland Inlet
1220339-008-ZKS-0008, 4 March 2020

Deltares

Figure 4.5   An overview of the observed (obs) depth-averaged velocities and low-pass filtered longshore (u) and cross-shore (v) velocities at frames 1, 3 and 4 (a,b,c), see Fig. 4.1 for locations. Summary of the low-pass filtered velocities at frames 1,3 and 4 (d). Measured, tidal velocities and non-tidal velocities at frames 1,3 and 4 (e, f, g).

Deltares

Flow over the tidal divides

In the basin tidal divides are formed where the tidal waves travelling through two adjacent inlets meet and sedimentation due to near-zero velocities results in tidal-flat formation. These tidal divides are often considered to form the boundaries at which the individual basins can be separated. The model study of Duran-Matute et al. (2014) already illustrated that a closed boundary at the Terschelling tidal divide does not really exist. In this study, model simulations driven by tides, wind and temperature over the 2009-2010 timeframe were made and estimates of the tidal prisms through the individual inlets and over the Terschelling watershed are presented. Duran-Matute et al. estimate that the averaged tidal prism through Ameland Inlet at 383 x10^6 m^3 (mcm), with a net seaward residual of -12 mcm. The tidal prism over the watershed is an order of magnitude smaller 33 mcm. However, the eastward residual flow of -23 mcm is of the same order magnitude to the residual flow through the inlets. It was concluded that this residual flow results from the wind effects and the variability in extreme events that can enhance, weaken or invert the tidally driven residual flow.

During the AZG campaign, flow over the tidal divides was measured by a series of 6 upward-looking Aquadopp ADCP-HR instruments; 3 on each tidal divide (see Figure 4.1). Results presented below are based on Van Weerdenburg (2019). Figure 4.6 shows the measured water levels at AmID1-T1, northern station Terschelling tidal divide, and AmID4-A1, northern station Ameland tidal divide. On average the maximum water depth is less than 2 m in both stations. The water depths increased to nearly 3 m during the Storm Sebastian (13 Sept.) (Figure 4.6). The measured discharges show a similar large peak (Figure 4.7). During this storm event discharges are almost an order of magnitude larger compared to the calmer conditions.
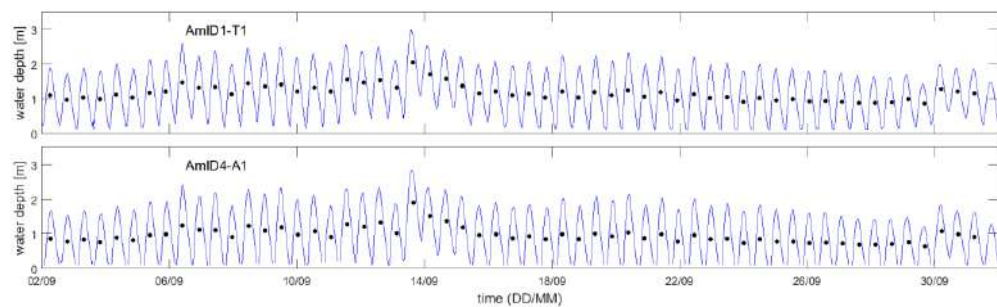

Figure 4.6   Time series of the local water depth measured at AQUADOPP AmID1-T1 (Terschellinger Wad) and AmID4-A1 (Pinkewad). Black dots indicate tide-averaged water depths (Van Weerdenburg, 2019).
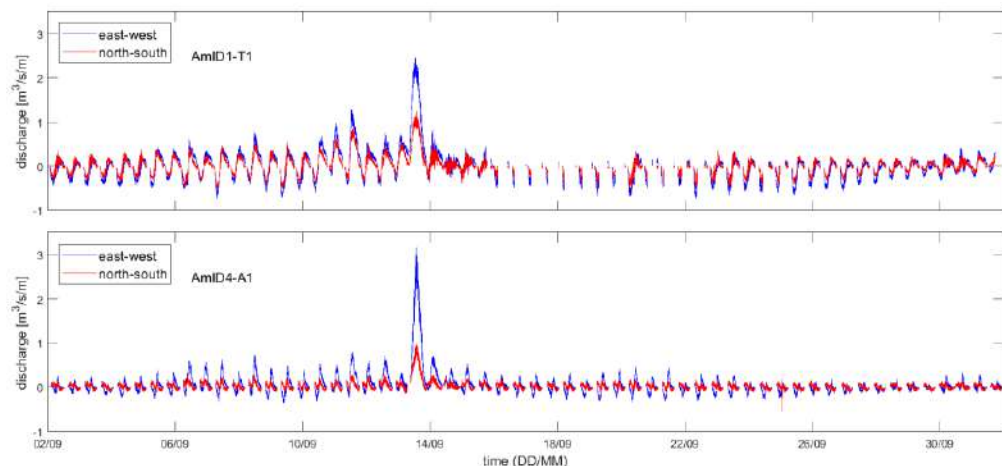

Figure 4.7   Time series of the instantaneous discharge in east- and northward direction per unit width as measured at AQUADOPP AmID1-T1 (Terschellinger Wad) and AmID4-A1 (Pinkewad). Gaps in the record indicate periods during which the water level did not exceed the blanking distance of the instrument (Van Weerdenburg, 2019).

Deltares

A residual current over the tidal divides was observed in the field observations. In general, the currents over the Terschelling watershed have a negative bias, indicating that the westward velocities are larger than the eastward velocities. As the station is placed in a channel that connects to Boschgat, this is an anticipated bias. This bias corresponds with the location of the station Based on a correlation between wind conditions and discharges, Van Weerdenburg (2019) concludes that residual discharge at Terschellinger Wad (represented by station AmID1-T1) is generally westward directed during calm conditions (Figure 4.8, left). Discharges are directed oppositely for wind velocities over 5 m/s from the southwest, and this eastward residual increases with wind speed. The isolated dot in Figure 4.8 shows Storm Sebastian.

Velocities at Pinkewad show a response similar to Terschelling Wad (Figure 4.8, right). Eastward flow is observed during wind conditions between south and northwest. Interestingly, similar magnitude of the residual discharge is observed during high wind conditions (> 10 m/s) from the south and milder conditions (5-10 m/s) from westerly direction. During low wind conditions residual discharges are near-zero, but a small westerly bias can be observed. This bias may result from the instrument location as a different response was observed between stations placed in the channels or on the tidal flats.

Both Duran-Matude et al. (2014) and Van Weerdenburg (2019) show that the large residual flow across the Terschelling watershed, especially during strong south-westerly winds is a crucial component in the overall circulation of the Dutch Wadden Sea. This residual flow is much larger than previously assumed. This suggests that the Wadden Sea is effectively one contiguous basin rather than a series of independent basins. Given this finding, assuming closed boundaries at the watersheds, common practice in morphodynamic model studies, may not produce realistic results for more energetic conditions.
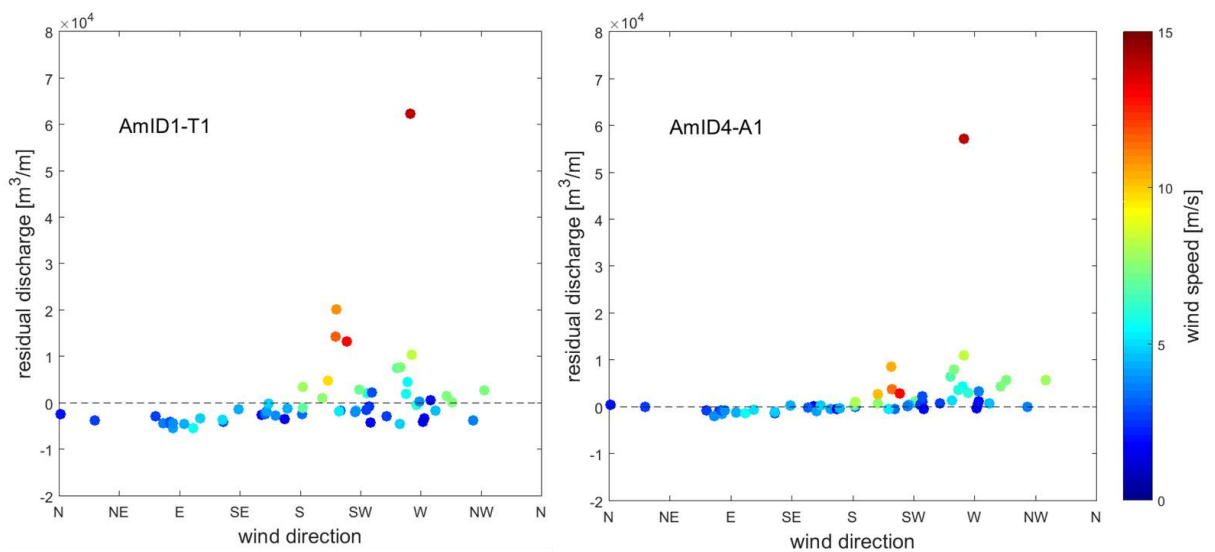

Figure 4.8   Residual discharge per unit width per tidal period as measured by Aquadopp instruments at AQUADOPP AmID1-T1 (Terschellinger Wad) and AmID4-A1 (Pinke Wad). Transport is defined positive in eastward direction (Van Weerdenburg, 2019).

Deltares

4.2.4 Drifter experiment

Lagrangian surface currents were measured using drifters equipped with GPS trackers. Positions of the drifters were recorded at 1 Hz intervals using an internal logger. The drifters were designed as floating devices that follow the top layer velocities but are minimally influenced by wind. The main experiments were carried out around frames 4 and 5, at the location of the planned nourishment. In this section, the results of a single large-scale experiment conducted on 9 September 2017 will be used. The goal of this experiment was to better understand the spatial variations in velocity on the ebb-tidal delta-scale circulation patterns and flow pathways. During this experiment drifters were retrieved after a full tidal cycle. From these experiments, velocity magnitudes and directions were determined.

Figure 4.9 illustrates the resulting flow pathways. Based on a series of numerical tracer experiments, Nederhoff et. al. (2016) hypothesize that Westgat forms a transition area on the ebb-tidal delta. Particles 'released' between Westgat and Terschelling mostly exchange with the southern part of the domain, while particles to the north exchange with Borndiep and are transported back onto the ebb-tidal delta.

The drifter experiment confirms this hypothesis for surface currents. All drifters deployed along the Terschelling coast follow the Boschgat channels into the basin. Drifters that are picked up by Borndiep are transported seaward into the ebb-chutes or through Akkepollegat onto the ebb-tidal delta. These patterns may differ for sediment travelling along or near the bed, but provide an additional line of evidence to explain likely suspended sediment pathways.
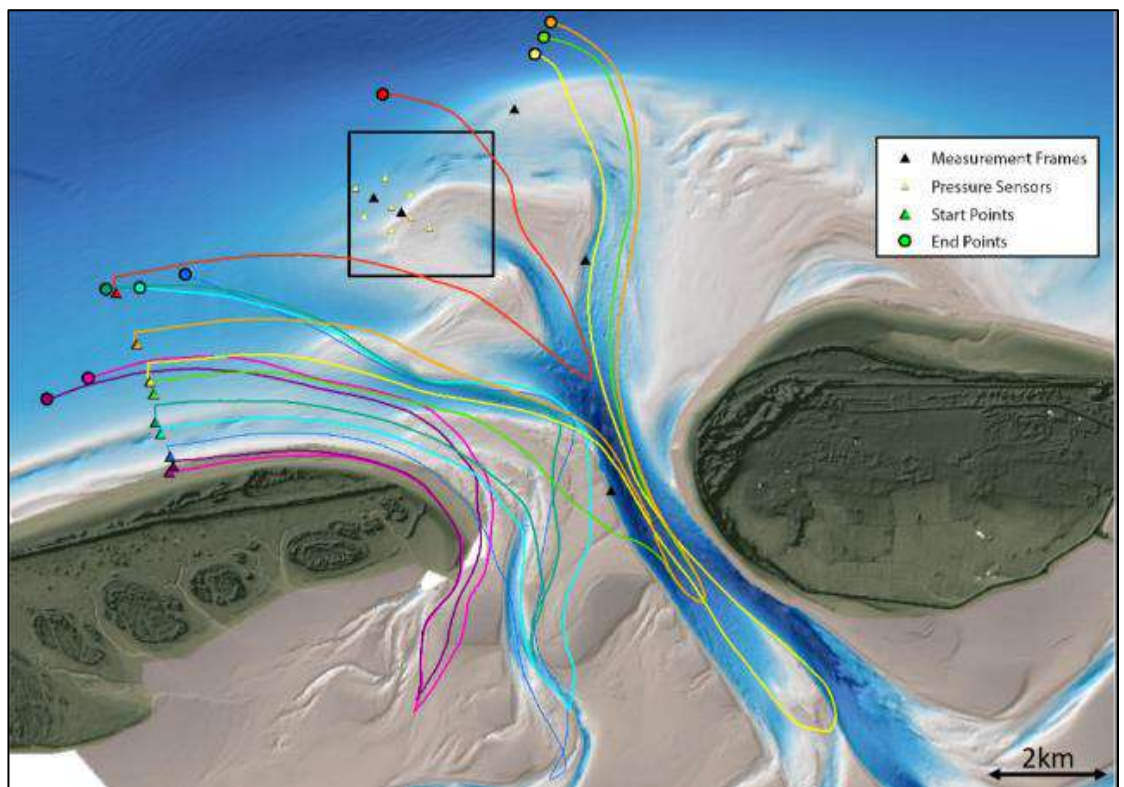

Figure 4.9   Large scale drifter experiment results. GPS tracks of the large-scale deployment on 9 September 2017 are shown. The drifters were released along a 3-km long transect north of Terschelling (triangles) and retrieved at different locations (circles) (source: Van der Werf et al. 2019; de Wit et al. 2018)

4.2.5   13-hour measurements.

The tidal motion is known to drive a significant flow through the inlet gorge. In the past, measurements of the discharge have been taken frequently in transects across the inlet gorge (Borndiep) by roving 13-hour ship measurements (see Table 4.2 for an overview based on Israel, 1998). All these older measurements were recalculated to a representative mean tide using a coherent method (Van Sijp, 1989). The oldest available measurement (1937) has a value comparable to the 2001 measurement (Briek et al., 2003). On average, ebb- and flood volumes through the inlet are c. 400-500 million m3. The residual discharges are small, less than 10 % of the gross ebb and flood volumes and both ebb dominance as well as flood dominance is observed.

The Kustgenese 2.0 discharge measurements were collected slightly different. In the present-day bathymetry, Boschgat is an area comprising small channels and subtidal shoals that cannot be measured accurately or safely traversed by boat. Therefore, current velocity and backscatter data were collected along 2 transects located just outside the inlet on the ebb-tidal delta (see Figure 4.1). These transects were sailed simultaneously by two survey vessels (Potvis and Siege) over a 13-hour time frame. Combined, the data of these two surveys provide an estimate of the total flow through the inlet (Figure 4.10). Each transect took roughly 20 minutes to complete. Raw ADCP data were transformed to earth coordinates using heading and tilt information supplied by the vessel. The recorded velocities were corrected to remove the motion of the vessel using the bottom ping, which estimates the vessel speed with respect to the seabed. The processed data allows us to quantify the discharges through the inlet, but small fluctuations in velocity vectors do not allow for the detailed analysis of the vector fields.

The experiments were conducted during three distinct phases in the tide. Measurement 1 was taken on 1 September 2017 during neap tide. As a result, the ebb and flood volumes were smaller compared to the measurements taken at an average tide (5 September or 19 September). All measurements show a small net flow that varied from ebb-dominance during neap tide and flood dominance during the other 2 experiments. Although the discharges were not recomputed to a mean discharge, they are of similar magnitude to the older measurements (see Table 4.2).

An important conclusion from these experiments is that, despite significant changes in the basin and ebb-tidal delta bathymetry, the discharges have not considerably changed over time. Present-day values of gross and net flow are in line with the older measurements. The ebb and flood volumes are almost similar, which results in a relatively small net residual discharge. A clear statement on ebb- and flood dominance of the inlet is difficult to make. The dominance of the inlet may rely on the phasing in the tide and especially the prevailing meteorological conditions. Similar conclusions were found in the study of Van Weerdenburg (2019).

Table 4.2   Overview of measured ebb and flood volumes in Borndiep based on 13-hours measurements.

| Survey year	dates	Measured Discharge [10⁶ m³]			Mean Discharge [10⁶ m³]		
		Flood	Ebb	Total	Flood	Ebb	Total
1937	-	-	-	-	406	-431	-25
1968-1973	109 flood - 110 ebb tides	-	-	-	518	494	24
1996	1996	502	-450	52	448	-395	53
1999	26-10-1999 04:00-18:00	542	-573	-31	416	-454	-38
2001	22-01-2001 05:30-18:30	557	547	10	407	418	-11
2017	01-09-2017 05:00-18:00	330	339	-9			
2017	05-09-2017 05:00-18:00	480	449	31			
2017	19-09-2017 05:00-18:00	545	506	39			
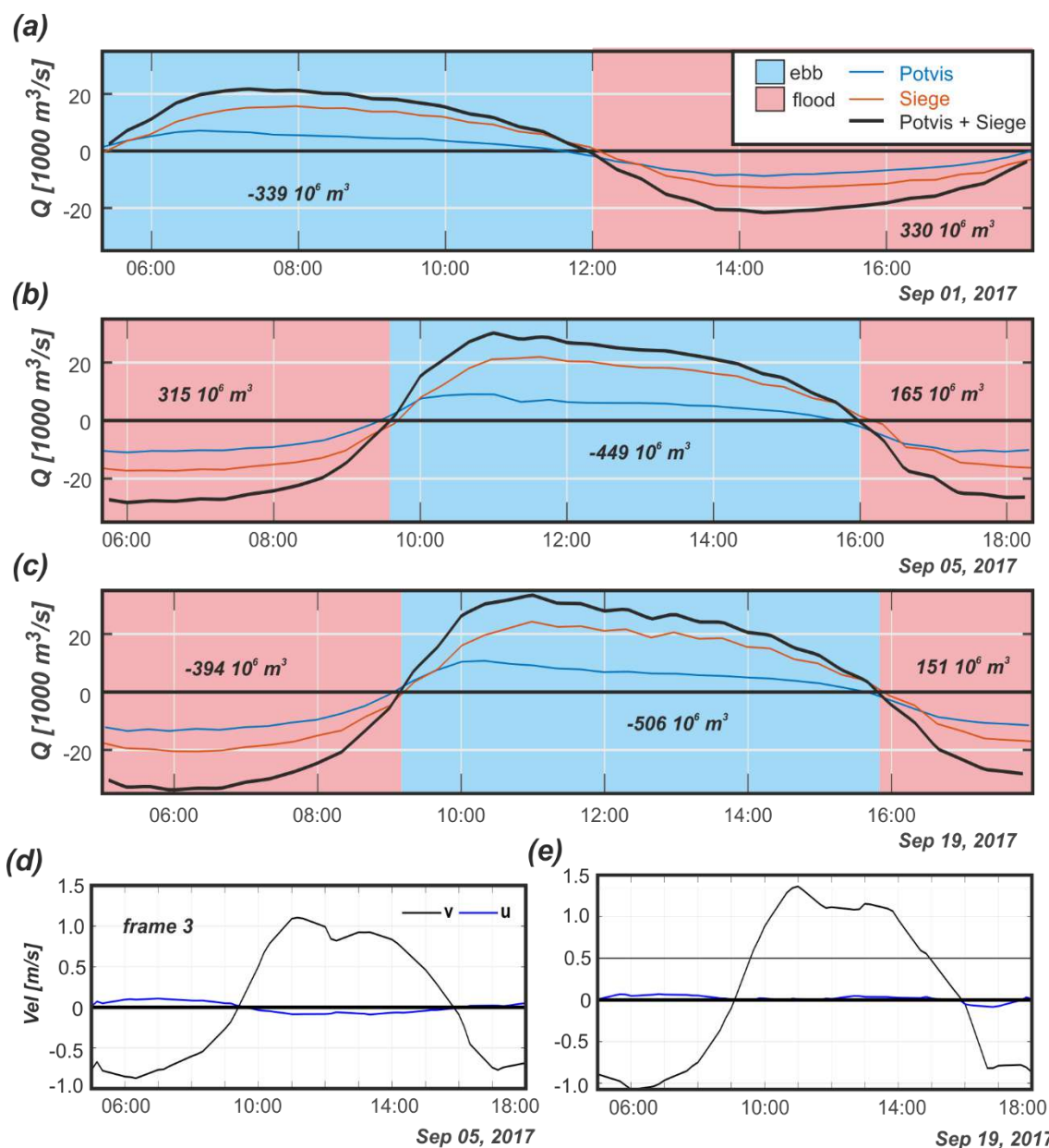
Figure 4.10 Discharge and flow measurement data grouped by measurement day: (a) September 1ˢᵗ 2017 (neap tide), (b) September 5ᵗʰ 2017 (mean tide) and (c) September 19ᵗʰ 2017 (spring tide). For the measurements on the 5ᵗʰ and 19ᵗʰ the depth-averaged velocity data derived from frame 3 are added (d and e).

Deltares

4.2.6 Waves

Wave data have been collected using wave buoys at the stations Eierlandse Gat (ELD) and Schiermonikoog (SON), respectively east and west of Ameland inlet, since 1979. Additionally, at Ameland inlet, waves have been measured in detail at multiple locations since 2007. Initially, these measurements were part of the SBW project (Zijderveld & Peters, 2006) but measurements have been continued since. Wave roses, summarizing the wave statistics for ELD, SON and 2 of the wave buoys located near Ameland Inlet are shown in Figure 4.11.

Due to the relative short record of observations at the Ameland buoys and missing data early summer, when the buoys are out of the water for maintenance, it is not possible to create a representative long-term wave climate for these buoys. Comparison of the wave direction and wave heights of ELD and SON with the Ameland wave buoys shows that SON resembles the Ameland wave climate best, with a close correlation in height and direction (Elias, 2018). For future wave climate schematizations, it is therefore recommended to use the SON data as basis.
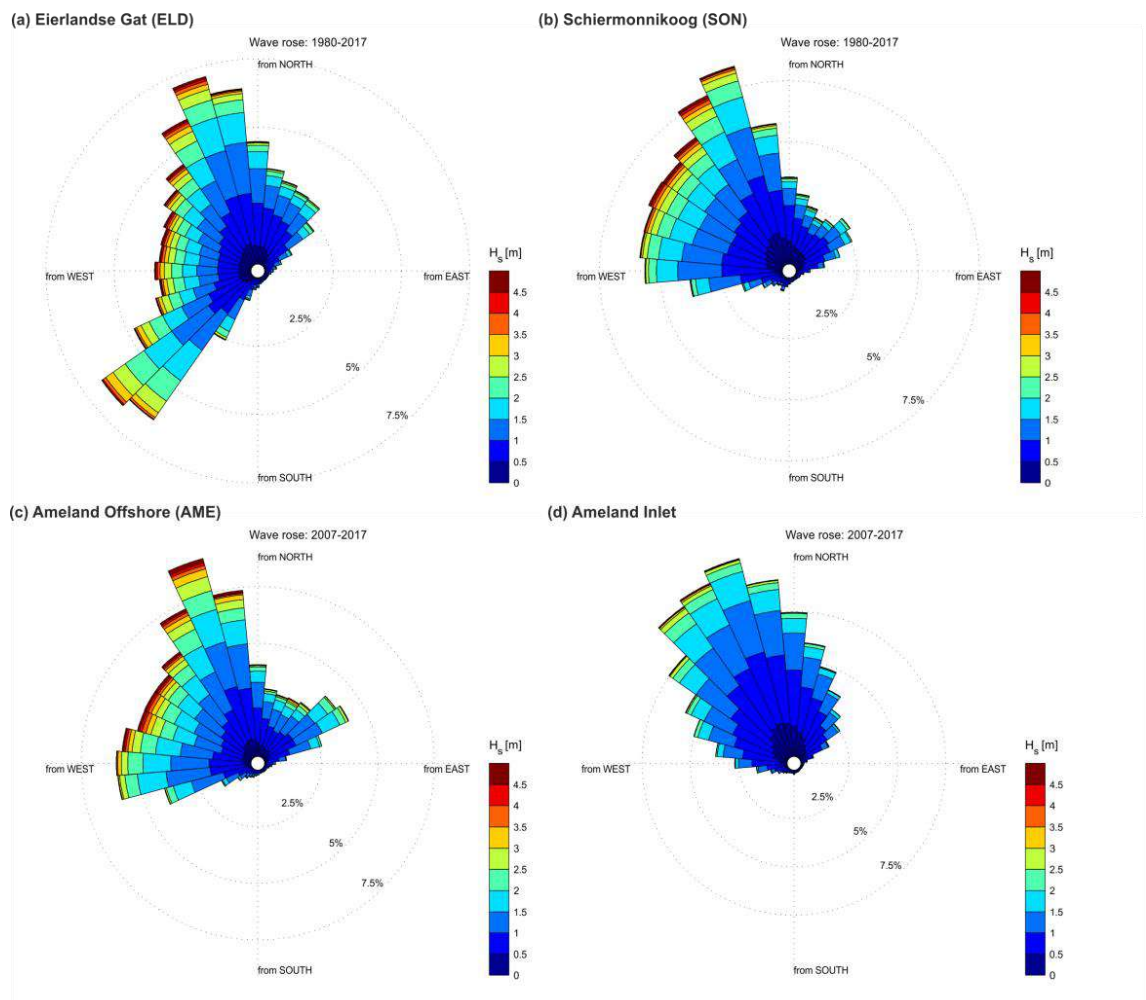

Figure 4.11 Wave roses for stations (a) Eierlandse Gat (ELD), (b) Schiermonnikoog (SON), and Ameland offshore (AME) and Ameland Inlet.

The offshore wave climate at Ameland shows a mean significant wave height of 1.37 m with a corresponding peak wave period of 7.2 s. Analysis of the measurements over the period 2007-2017, reveals that the wave climate mainly consists of locally generated wind waves. The shallow North Sea basin produces a mild wave climate. Typically, waves are below 2 m (83% of the record), only during severe storms significant wave heights can occasionally reach heights between 4.5 and 9.1

Deltares

m (less than 1 % of the record). Roughly 33% of the wave directions lie between west-southwest and north-northwest (235° – 305°). Most waves (62%) are from directions between north-northwest and North (305° – 0°). The remaining 4% is offshore directed and does not significantly contribute to the sediment transports. Waves from easterly directions (0°-180°) are smaller due to the sheltering by the mainland (offshore directed) and occur less frequently. Wave periods ($T_{1/3}$) typically vary between 3 to 6 seconds for lower wave conditions (89 % of the measurements). For typical storm waves (H_{sig}= 2-3 m), a mean wave period of 6,0 s occurs increasing to 7.6 s for severe storms (H_{sig} > 4m). Contributions of swell are minor. Wave periods over 9 seconds are only measured occasionally (0,1% of the record).

The dominant wind and wave directions differ considerably. The largest and most frequent winds come from the southwest, a direction hardly present in the wave record due to the sheltering of the mainland and the barrier islands.

During the AZG campaign not all wave buoys were available (see Figure 4.1 for locations). Figure 4.12 summarizes the available measurements for buoys AZB11, AZB21 and AZB32: Station AZB11 is located just offshore of Ameland inlet, station AZB21 is in the distal part of Akkepollegat, and station B32 just south of Westgat.

At buoy AZB11 a peak wave height of 6m was observed during storm Sebastian (13 Sept. 2017). During this storm wind directions were from the southwest and it is likely that the wave directions were similar. This explains the correlation with the measured wave height at the ELD buoy (Figure 4.12b). In general, the AZB11 measurements show a better correlation with the SON buoy. Only for waves from south(westerly) directions, notable lower values at SON are observed. Storm Xavier (1 – 9 Oct. 2017) resulted in sustained wave heights between 3 and 5 m.

The difference in wave height between stations AZB11 and AZB21 illustrate the important wave-dissipating effect of the ebb-tidal delta (Figure 4.12c). Wave heights at station AZB21 are strikingly smaller than at AZB11. Waves that exceed approximately 2 m in height apparently break on the ebb-delta front. Only limited additional dissipation of wave-energy occurs between station AZB21 and AZB32; this is due to the short distance and the presence of the relative deep channel between the two stations. A remarkable feature in the timeseries of stations AZB21 and AZB32 is the strong tidal modulation of the wave height (Figure 4.12c). The correlation between the peak in ebb-flow and the peak in wave heights suggests that this modulation is most likely related to wave-current interaction. The importance of wave-current interactions in wave-height amplification was also studied by Elias et al. (2012). Based on measurements and process-based models, these authors concluded that waves almost doubled in height in the Columbia River during opposing ebb tides. However, water level variations are probably important here as well. Comparison of the low-pass filtered wave heights and low-pass filtered water levels (Figure 4.12d) shows a correlation of larger wave heights and higher water levels. Since wave heights and surge both correlate to the wind velocity, this does not proof that higher water levels allow for higher waves, but it is an indication that higher waves generally coincide with a higher water levels over the ebb-tidal delta.
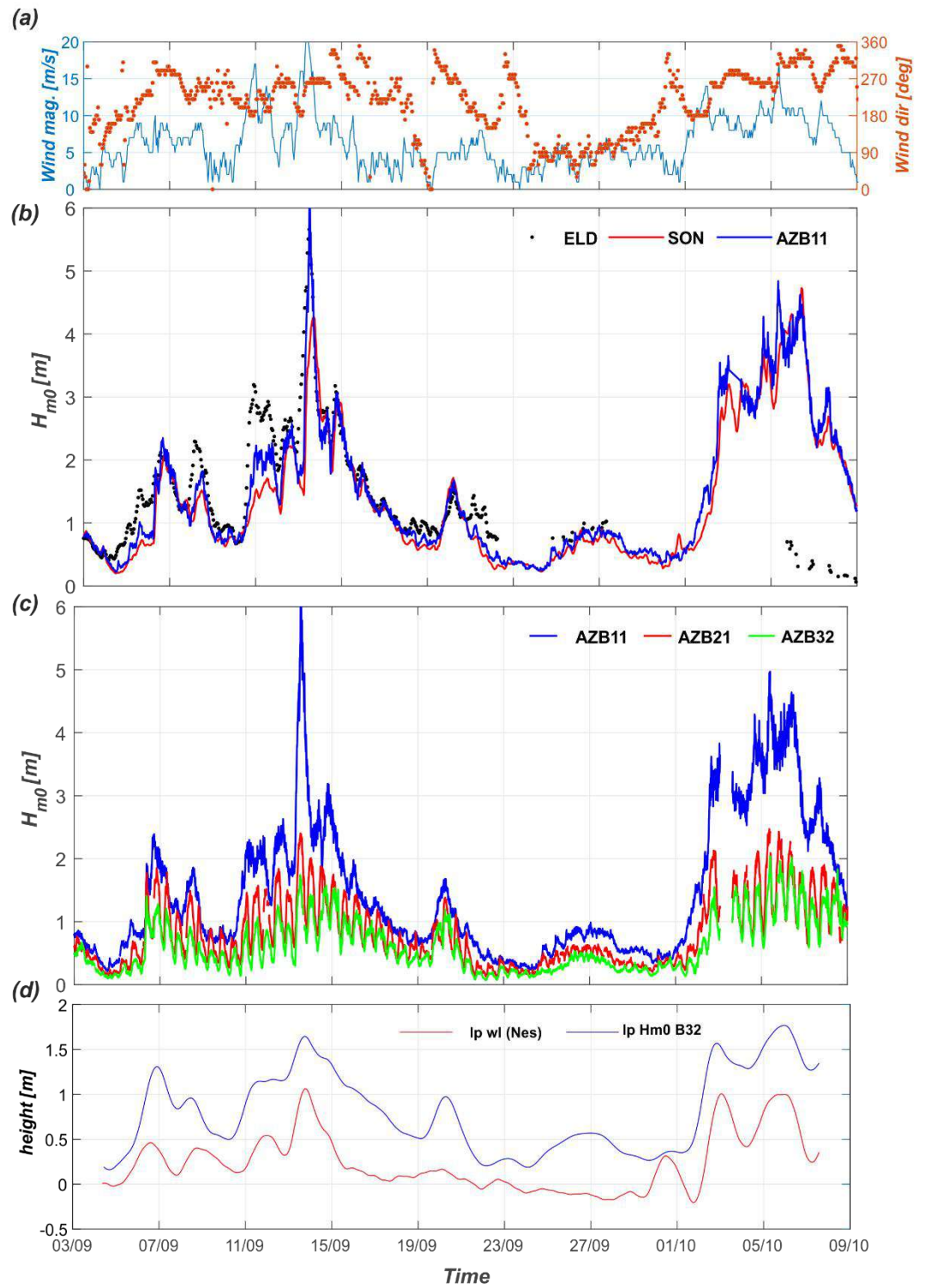
Deltares

Figure 4.12 Overview of the wave heights measured during the KG2 campaign. (a)Wind speed and direction observed at the KNMI weather station at Terschelling (b). "Deep-water" wave heights (H_{m0}) observed at station stations Eilerlandse Gat (ELD), Schiermonnikoog Noordzee (SON), and at the Amelander Zeegat buoy AZB11, (c) Wave heights observed at the Amelander Zeegat stations AZB11, AZB21 and AZB32. (d) Low-pass filtered water levels (Nes) and wave heights for buoy AZB32. Locations: see fig 4.1

Deltares

4.3 An analysis of the morphodynamics

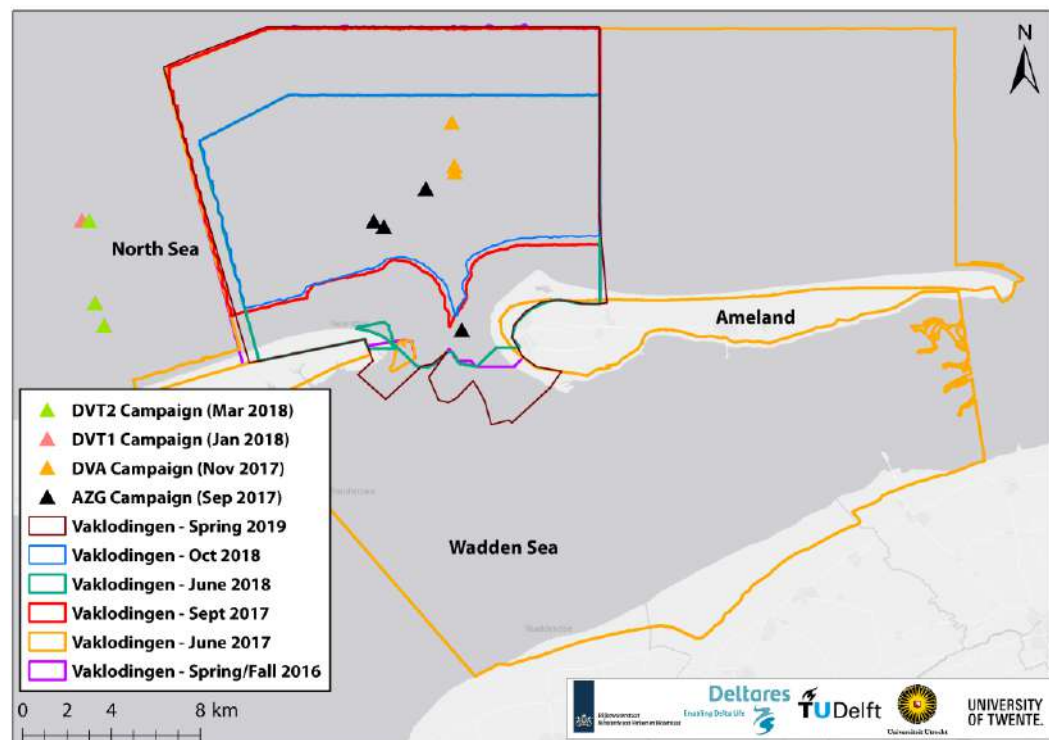### 4.3.1 Bathymetric measurements and volume changes

Figure 4.13 Overview of KG2 AZG Vaklodingen bathymetric measurements.

A description of the channels and shoals that are present on the Ameland Inlet ebb-tidal delta is provided in Chapter 2 and its evolution between 2005 and 2016 in Chapter 3. Figure 4.14 to Figure 4.19 illustrate the short-term evolution of the ebb-tidal delta between 2016 and 2019. For the Kustgenese 2.0 program, the ebb-tidal delta was surveyed at half yearly intervals (spring and fall measurements). Not all these measurements have a full coverage of the area (see Figure 4.13 and Figure 4.14). The spring 2017 and late spring 2019 surveys cover a larger domain as these were conducted as part of the regular Vaklodingen program. In 2017 the entire basin was measured as well. The high frequency of the Kustgenese 2.0 surveys provide a unique opportunity to study the short-term dynamics of the ebb-tidal delta and the response of the ebb-tidal delta to seasonal fluctuations in boundary conditions in particular.

Figure 4.15 shows the observed changes in bed height between the surveys. Despite the relatively short intervals, noticeable morphodynamic changes occurred on especially the distal part of the ebb-tidal delta. On delta scale, a difference in response between high-energy winter conditions versus low-energy summer conditions can be observed. The net volumetric change observed over the total interval, from 31 October 2016 to 18 July 2019, is 4.27 million m^3 (Figure 4.16). Most of this volume gain is observed on the ebb-tidal delta. The ebb-delta nourishment placed in 2018 (5.5 million m^3) and a large nourishment (2.4 million m^3) placed along the northwest coastline of Ameland in 2019 (see Figure 4.14, 18-07-2019) which must have contributed to this gain as well. Most of the net volume gain occurred in polygons 6,8 and 12 (Figure 4.16) on the ebb-shields and in Akkepollegat. The net volumetric change is small compared to the total erosion and sedimentation values (respectively -26 million m^3 and 30 million m^3). Both the erosion and sedimentation show near-linear trends over this interval.
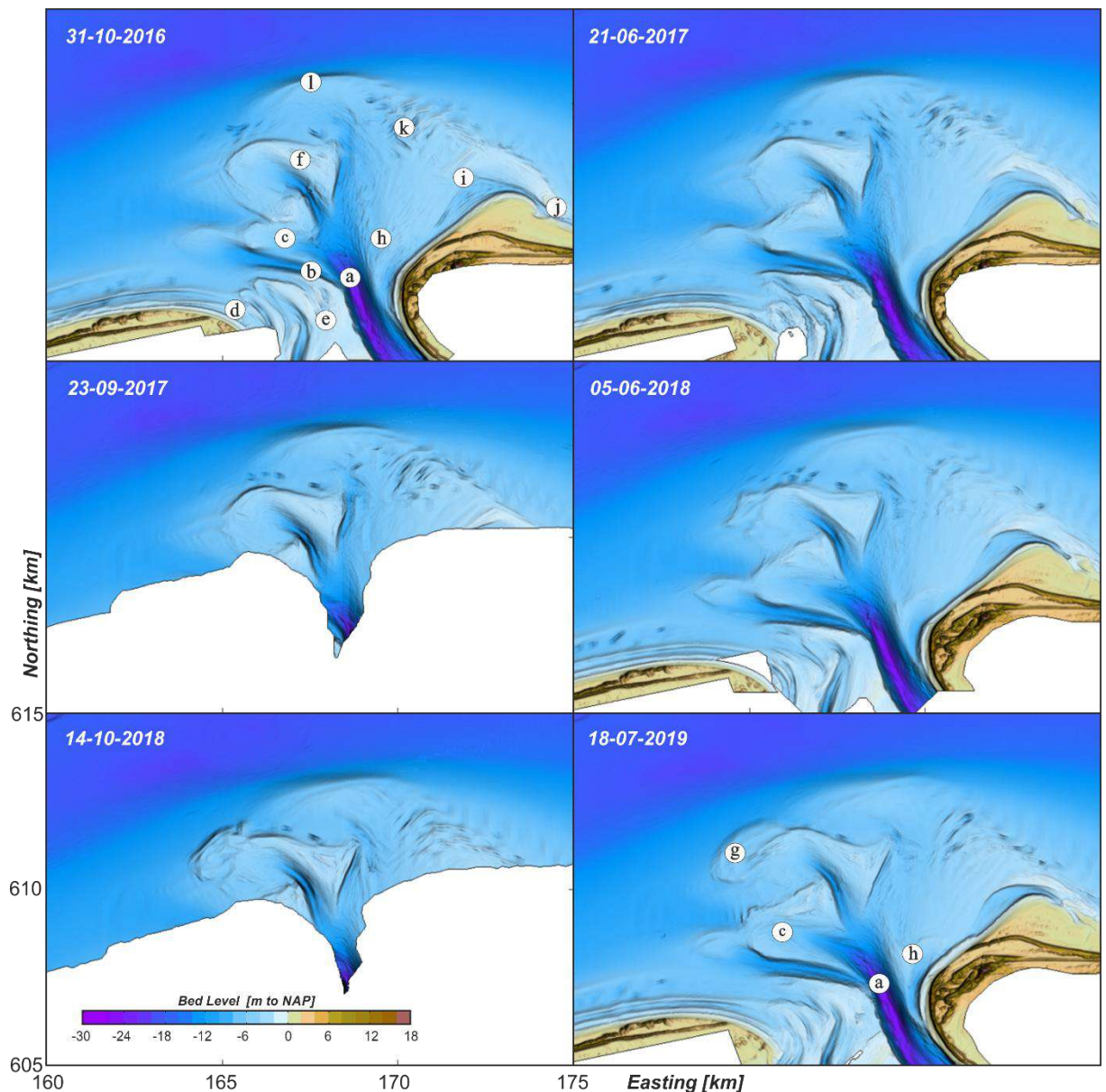
Figure 4.14 Overview of the measured bathymetries during the Kustgenese 2.0 campaign. Letters a-l indicate specific morphological developments that are analysed in the sections below.

Volumetric change during winter versus summer.

For the seaward part of the domain, the surveys allow for the reconstruction of the half-yearly volume changes and the difference in response to summer and winter conditions can be determined (see Figure 4.16, right lower panel). In polygons 7, 12 and 14 (Figure 4.16) a clear response to summer versus winter conditions can be observed. These areas have in common that they are all located on the seaward part of the domain were wave energy is most important. From the volume analysis it can be concluded that the infilling of Akkepollegat (polygon 12) mainly occurs during winter conditions. Over the winter period, the net sedimentation is 2.0 to 2.2 million m^3, while during the summer season the volume gain reduces to 0.2 to 0.7 million m^3. A similar response, however smaller in magnitude, is observed on the Bornrif platform (polygon 14). Here the erosion rate of 1.0 to 1.4 million m^3 during the winter period exceeds the observed erosion of 0.2 to 0.3 million m^3 during summer. A similar response is also likely for polygon 6, but due to the placement of the ebb-delta nourishment it cannot be observed this in the volume analysis.

Deltares
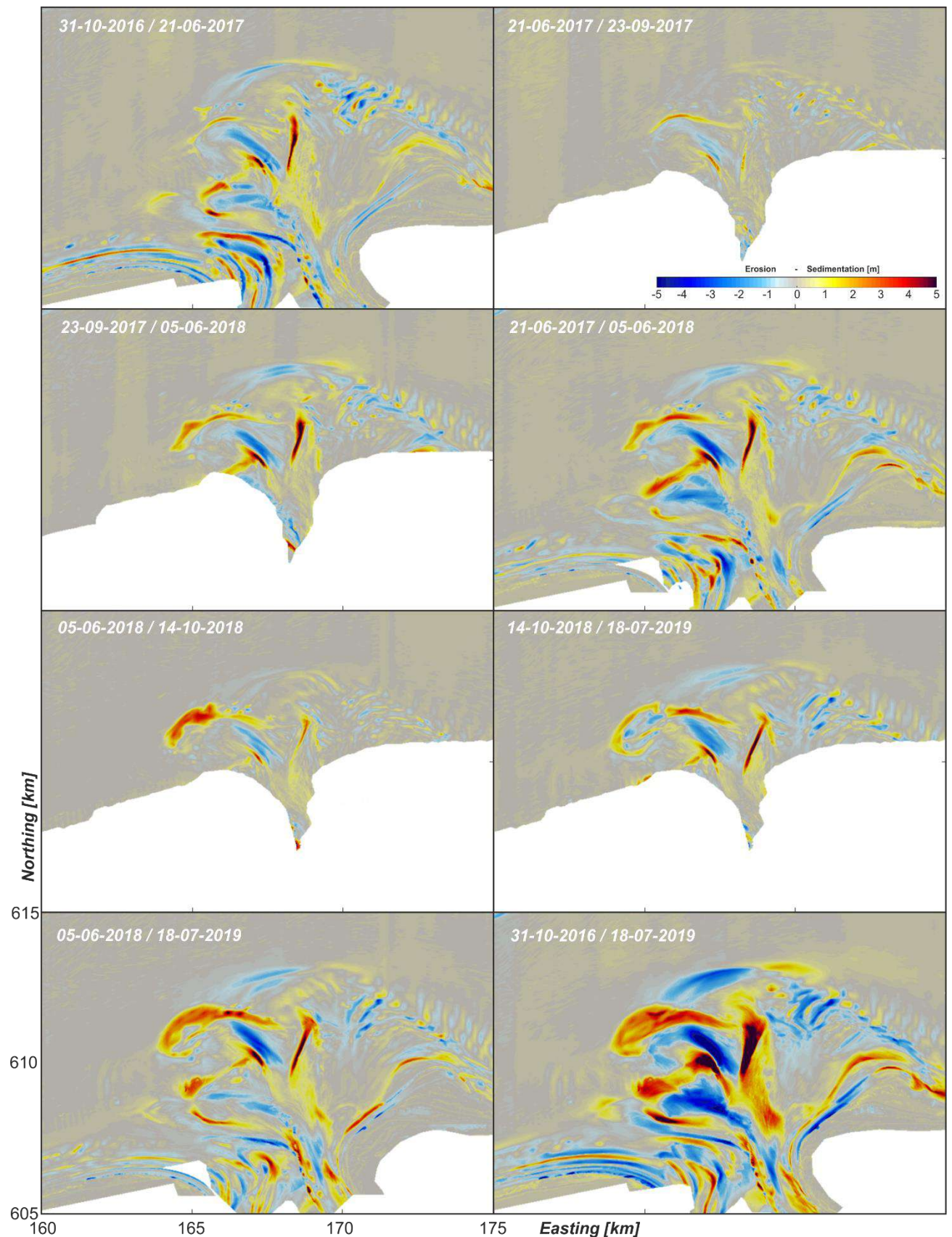
Figure 4.15 Overview of the sedimentation-erosion patterns obtained from differencing successive measurements taken during KG2. Time frames are indicated in the subpanels. The lower right panel illustrates the total change over the entire time-period (2016-2019).
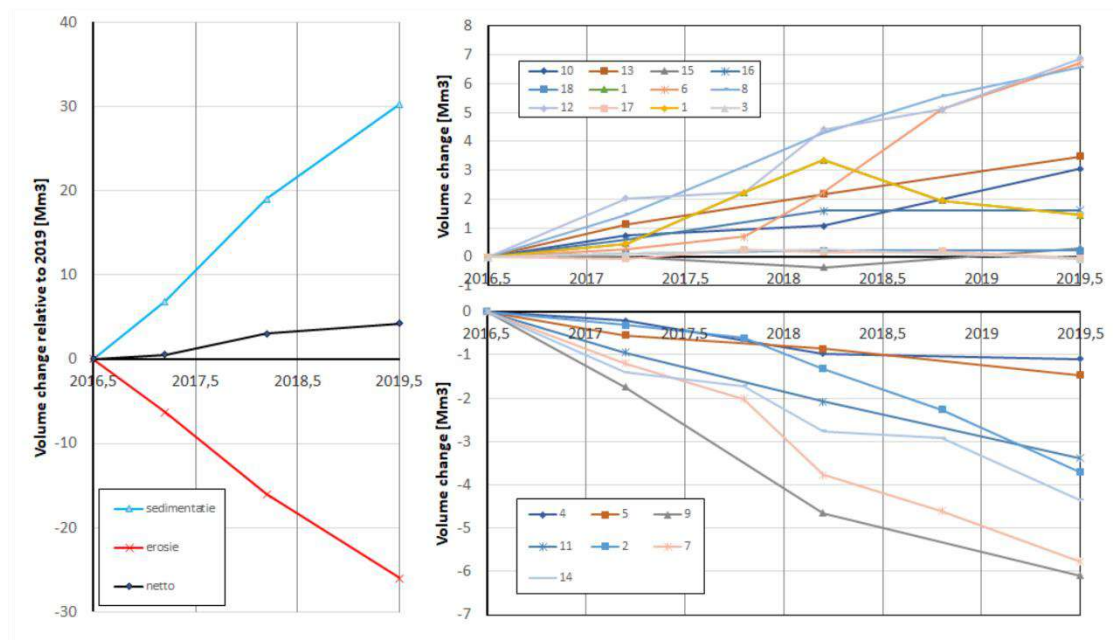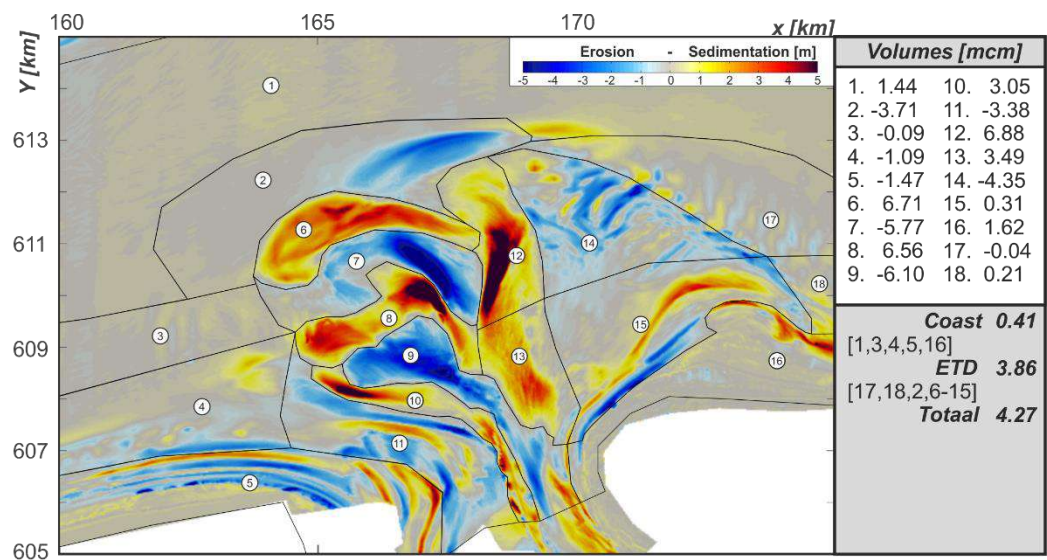
Understanding the morphological processes at Ameland Inlet
1220339-008-ZKS-0008, 4 March 2020

Deltares

Figure 4.16 A summary of the volume changes between October 2016 and July 2019.
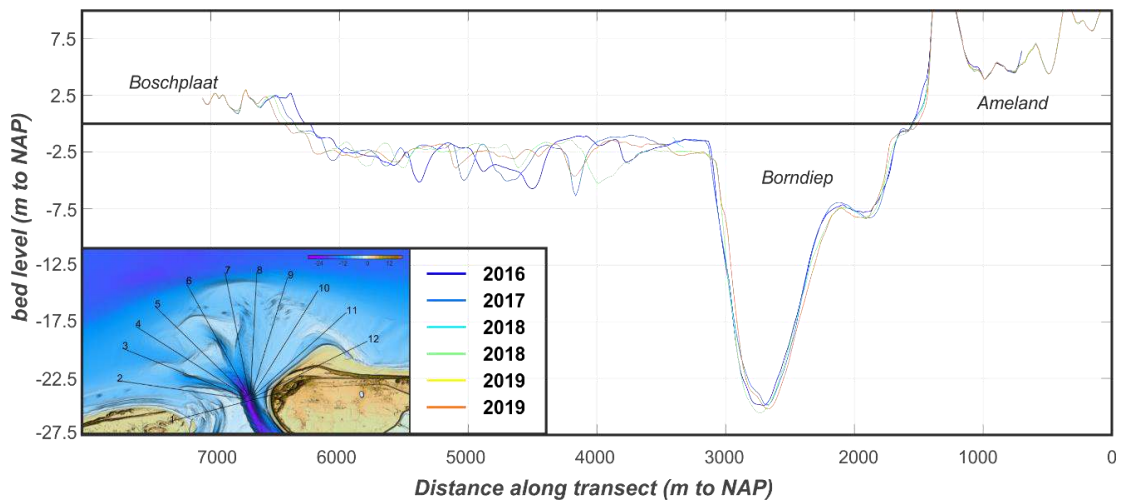
Figure 4.17 Bathymetric change for transect 1, located in the inlet gorge, over the timeframe 2016-2019

In the next section specific details of the morphological developments are discussed. These selected areas are indicated by a through l in Figure 4.14.

(a). Stability of inlet gorge (Borndiep).
The main inlet channel Borndiep (Figure 4.14 [a]) has retained a stable position in the inlet gorge (Figure 4.17, transect 1). Interestingly the deepest part of Borndiep, indicated by the purple colors in Figure 4.14, has developed a westerly outflow into the second, southern ebb-chute (*SEC*). This indicates that this ebb-chute is likely to develop as the main outflow channel.

(b). Stability of Westgat.
All measurements show a stable Westgat channel with a western orientation (Figure 4.14, [b]). The southern lobe of the *SEC* separates Westgat from the ebb-chute. This separation remains present throughout the survey interval and is indicative of an ebb and flood channel separation (Van Veen, 1950; Van Veen et al. 2005). Although the top view of the chart shows a stable Westgat channel, transect 3 that intersects it shows some noticeable changes. The ebb-shield shoal to its north increased in height; from -5 m to -4 m NAP. This part of the ebb-shoal builds out to the south, transforming the channel wall from a mild to steep slope. Despite these changes, the central, deepest part of Westgat has retained a constant location and depth. The shoals just south of Westgat, close to its connection to Borndiep, decreased in height. This indicates that the connection between Borndiep and Westgat is pushed basin-ward.

(c). Growth of the southern ebb-chute and ebb-shield system (SEC).
The *SEC* (Figure 4.14 [c]) have significantly expanded throughout the measurement period. In transects 4 and 5 (Figure 4.18) the ebb-shield is a shallow shoal with a height of -5 m, that moves over the underlying platform (located at -7 m). The outbuilding of the ebb-shield is indicated by its steep seaward slope. The seaward migration was nearly 1 km. Such a steep slope is characteristic of outbuilding due to ebb-transports and can be observed at other Wadden Sea inlets as well (e.g., Texel Inlet, Elias and Van der Spek, 2016)

In the last survey of 18 July 2019, a clear connection between the *SEC* and Borndiep can be observed. The deeper zone of Borndiep is now curved into the ebb-chute indicating that this route now forms the main ebb-channel of the system. The increasing importance of the ebb-chute may be reflected by the migration of 1 km of its ebb-shield. The associated volumetric change is an increase of 9.6 million m^3 on the ebb-shield since 2016 (Figure 4.16, [8,10]). Part of the sediments were delivered by expansion and deepening of the ebb-chute channel (-6.1 million m^3; Figure 4.16 [9]).

(d,e). Erosion of the coastal zone and Boschgat area.

Deltares

The nearshore area of the Terschelling coast, including Boschplaat and the Boschgat area, has experienced a net erosion. The near-shore polygon 5 has lost in total 1.5 million m^3 of sand (Figure 4.16). Large volume losses were also observed in the Boschgat – Westgat area with -3.4 million m^3 of erosion. Despite these large volumetric losses, the morphological character of the area did not significantly change as in all bathymetries a single, larger Boschgat channel and several shallow, dynamic channels between Boschgat and Boschplaat at the eastern end of Terschelling are observed (Figure 4.14 [d], [e]). Boschgat did not significantly increase in depth, but slowly continued to migrate eastward. The shallow channels with maximum depths of c. NAP -6 m, and bounding shoals that reach heights of around NAP-1 m, show smaller-scale dynamics. Boschplaat however, continued to retreat in westward direction (around 200 m). See transect 1, Figure 4.17.

(f). Migration of Kofmansbult ebb-shield (NEC) and closing of the Akkepollegat channel.
The *NEC* and associated ebb-shield (Kofmansplaat; (Figure 4.14 [f]) continued to expand seaward and eastward. The ebb-chute channel was retained, forming a narrow-curved channel that ends in Kofmanbult. In total -5.8 million m^3 of erosion was observed (Figure 4.16, [7]). The ebb-shield at the end of the channel showed an increase in volume of 6.7 million m^3 (Figure 4.16, [6]), but most of this increase is related to the placement of the ebb-delta nourishment (see next section for details). A large increase in volume also occurred to the east of the ebb-shield, where sedimentation of 6.9 million m^3 (Figure 4.16, [12]), has filled in the Akkepollegat channel (burying the second measurement frame). This large accretion shows that sediment transport from the *NEC* eastward must exist. As a result of the large infilling rates, a clear Akkepollegat channel is no longer visible in the 2019 bathymetry.

Transect 6 (Figure 4.18) shows the migration of both the young, *SEC* and the *NEC*. The *NEC* migrated over 800 m between 2016 and 2019. At this location, the volume and height of the ebb-shield reduces. The seaward migration has been ongoing even before placement of the ebb-delta nourishment. The ebb-delta nourishment is not present in this profile and no clear response to the placement can be observed. The ebb-delta placement can be observed in transect 5 as a large volume gain just seaward of the ebb-shield.

Transect 7 (Figure 4.19) provides more insight into the closing of Akkepollegat. The eastward migration of the ebb-shield is visible as the volume of the shoal increases. Both the proximal as well as the distal end of the channel filled in with sediments. This transect clearly illustrates the difference in response to summer and winter conditions. Both the movement of the ebb-shield and the lowering of the ebb-delta front occurs during (stormy) winter conditions, while a stable position is retained between the summer measurements. The large erosion of the ebb-shield during the winter season is reflected in the volume gain at Akkepollegat (Figure 4.19, [12]). On average the infilling rate during the winter season varies between 1.8 and 2,2 million m^3, while during the summer season this is -0.2 to -0.7 million m^3 (Figure 4.16, bottom panels).

(h,i). Development of nearshore shoals on Bornrif.
In addition to the infilling of Akkepollegat, the landward part of Bornrif near Ameland also shows an increase in shoal height. The landward part of Akkepollegat fills in with sediment (3.5 million m^3; Figure 4.16 [13]) and decreases in depth. The shoals along the entire landward margin of Bornrif increased in height and volume (0.3 million m^3, Figure 4.16 [15]). Note that the net volumetric change in polygon 15 is small, 0.3 million m^3, as the 2.9 million m^3 volume gain on the shoal is almost equaled by 2.6 million m^3 erosion in the bordering channel.

Transects 8 and 9 (Figure 4.19) clearly illustrate the growth of the nearshore shoals. Between 2016 and 2019 a near 4 m increase in height occured. In the past, shoals formed at this location grew and eventually attached as the Bornrif Strandhaak (see Elias et al. 2019). The large amount of sediment that bypassed the Akkepollegat channel and the shallowing in the nearshore are a first indications of the formation of a new attachment shoal. Given the location on the ebb-tidal delta, these shoals are likely to show a similar behaviour as the Bornrif strandhaak.

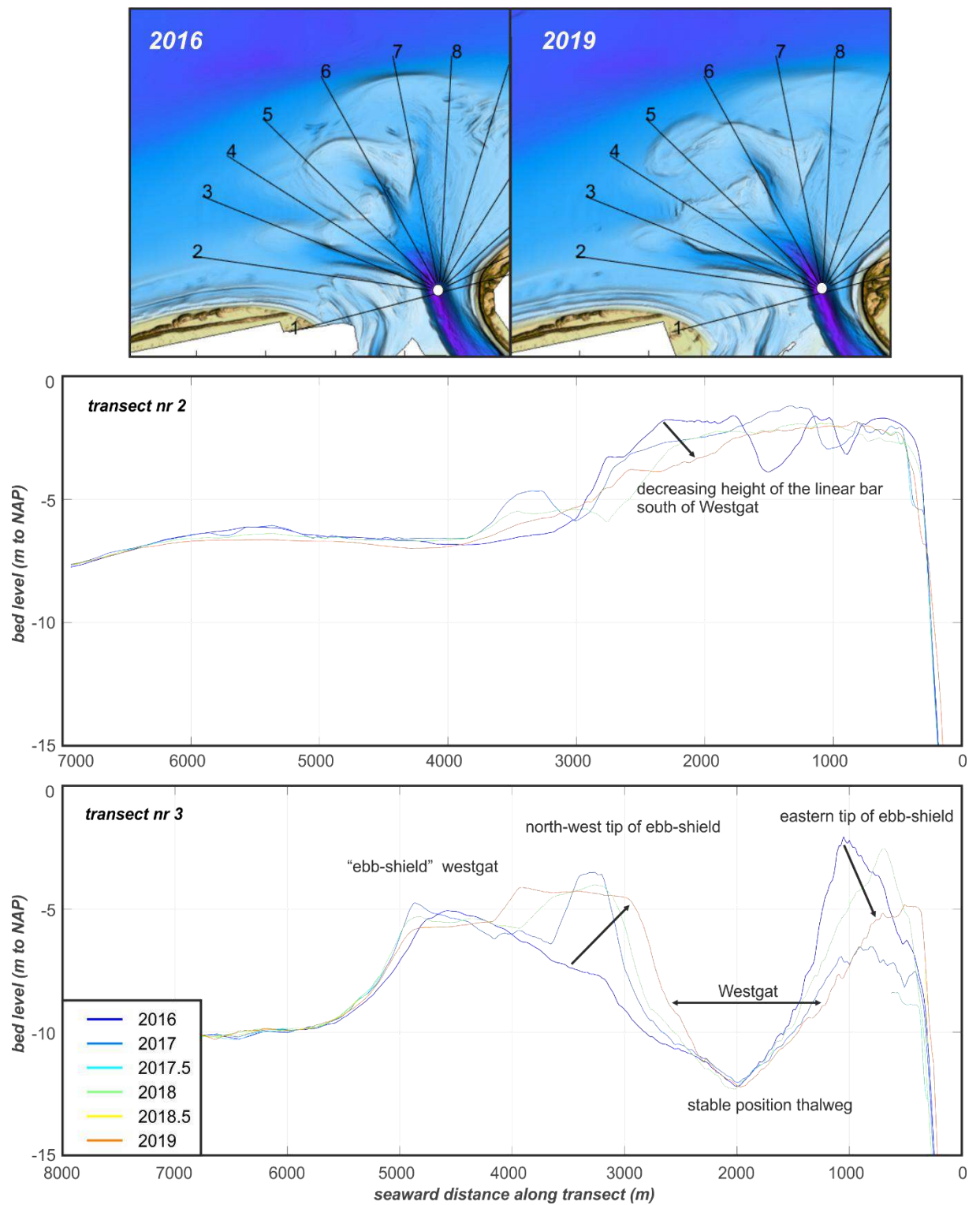**Deltares**

(j). Attachment of Bornrif Bankje

After years of migration across the Bornrif platform, Bornrif Bankje finally merged with the Ameland coast. The volume gain at the Ameland coast is small (0.2 million m^3; Figure 4.16, [18]), and is likely spread eastward along the Ameland coastline. To the west of Bornrif Bankje, shoals emerge that are laterally spread on Bornrif, along the coast (Figure 4.14, [i]). Parts of Bornrif Bankje can still be observed in profile 11 (Figure 4.19).

(k,l). Deepening of the offshore part of Bornrif.

The seaward part of Bornrif shows a distinct deepening. The ebb-delta front (Figure 4.14, [l]) erodes with 3.7 million m^3 (Figure 4.16, [2]). This front formed when Akkepollegat had a maximum seaward extension to the north. With the growth of the first ebb-chute and shield after 2006, Akkepollegat started to lose its dominance and the sediment flux was deflected to the new ebb-shield. , As waves continued to erode the ebb-delta front and redeposit these sediments landward, the loss of sediment supply resulted in substantial sediment loss. Also on the adjacent Bornrif shoal erosion can be observed (Figure 4.14, [k]). On Bornrif shoal, the formation and migration of large bedforms seems to dominate the patterns. The associated volume losses are 4.4 million m^3, which mostly occur during winter conditions (Figure 4.16, [14]).

Lessons Learned from the KG2 bathymetric measurements.

In conclusion, the high frequency of bathymetric surveying provides an unprecedented insight in short-term ebb-tidal delta dynamics. These surveys allow us to track and follow the development of the medium-scale channels and shoals that form the ebb-tidal delta. Half-yearly measurements may not be necessary to follow the migration of the features as both the 2016 and 2019 surveys still show comparable ebb-delta morphologies. However, within those 3 years substantial changes have occurred that it would not have been able to identify without the frequent measurements. The half-yearly surveys allow for an estimate of volume changes during the more energetic winter months versus the calmer summer period. Both erosion and sedimentation at the distal part of the ebb-tidal delta is to a large part driven by the winter conditions. The on average higher waves can stir up and transport large amounts of sand, that are subsequently deposited landward. The higher temporal resolution reveals the growth of small-scale perturbations to scales that affect the entire ebb-tidal delta. The ebb-tidal delta proved to be much more dynamic than what expected on the basis of literature and existing conceptual models.

Understanding the morphological processes at Ameland Inlet
1220339-008-ZKS-0008, 4 March 2020

Deltares

transect nr 2

decreasing height of the linear bar
south of Westgat

bed level (m to NAP)

transect nr 3

"ebb-shield" westgat

north-west tip of ebb-shield

eastern tip of ebb-shield

Westgat

stable position thalweg

—	2016
—	2017
—	2017.5
—	2018
—	2018.5
—	2019

seaward distance along transect (m)

Understanding the morphological processes at Ameland Inlet
1220339-008-ZKS-0008, 4 March 2020

Deltares

Figure 4.18 Bathymetric changes for transects 2-6 over the timeframe 2016-2019. Note that 0 corresponds to the Borndiep and 7000 to the open-sea.

Understanding the morphological processes at Ameland Inlet
1220339-008-ZKS-0008, 4 March 2020

Deltares

Understanding the morphological processes at Ameland Inlet
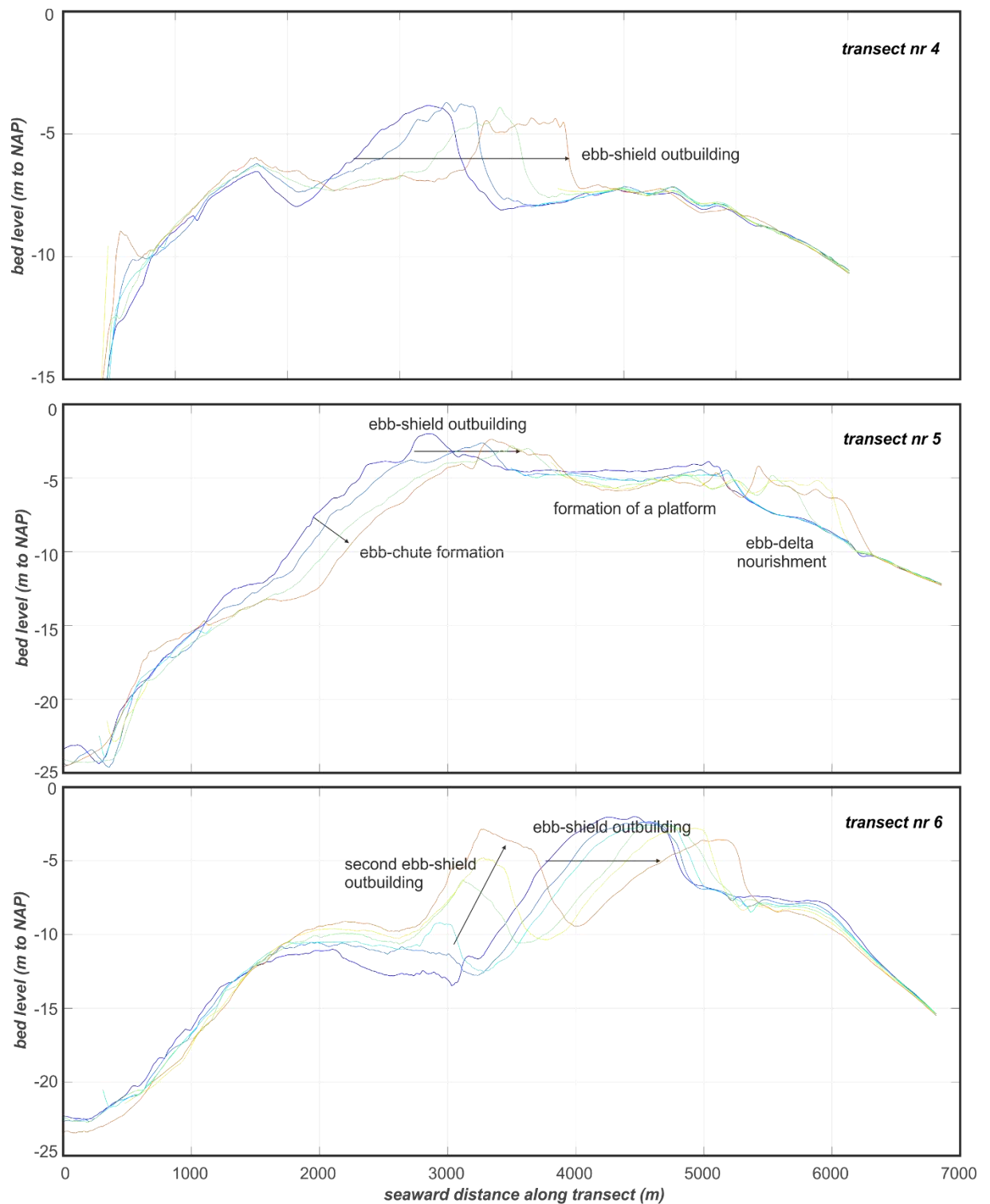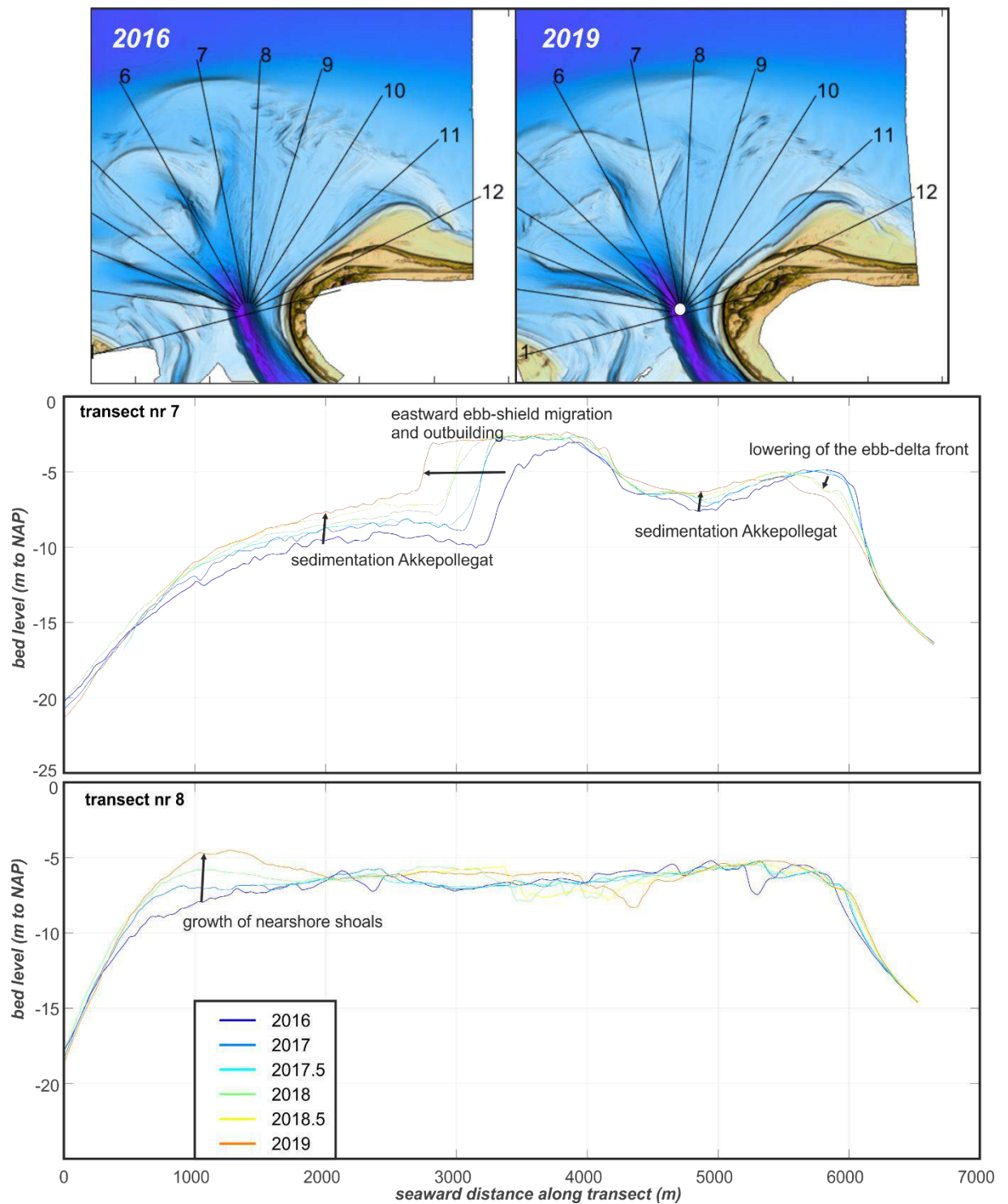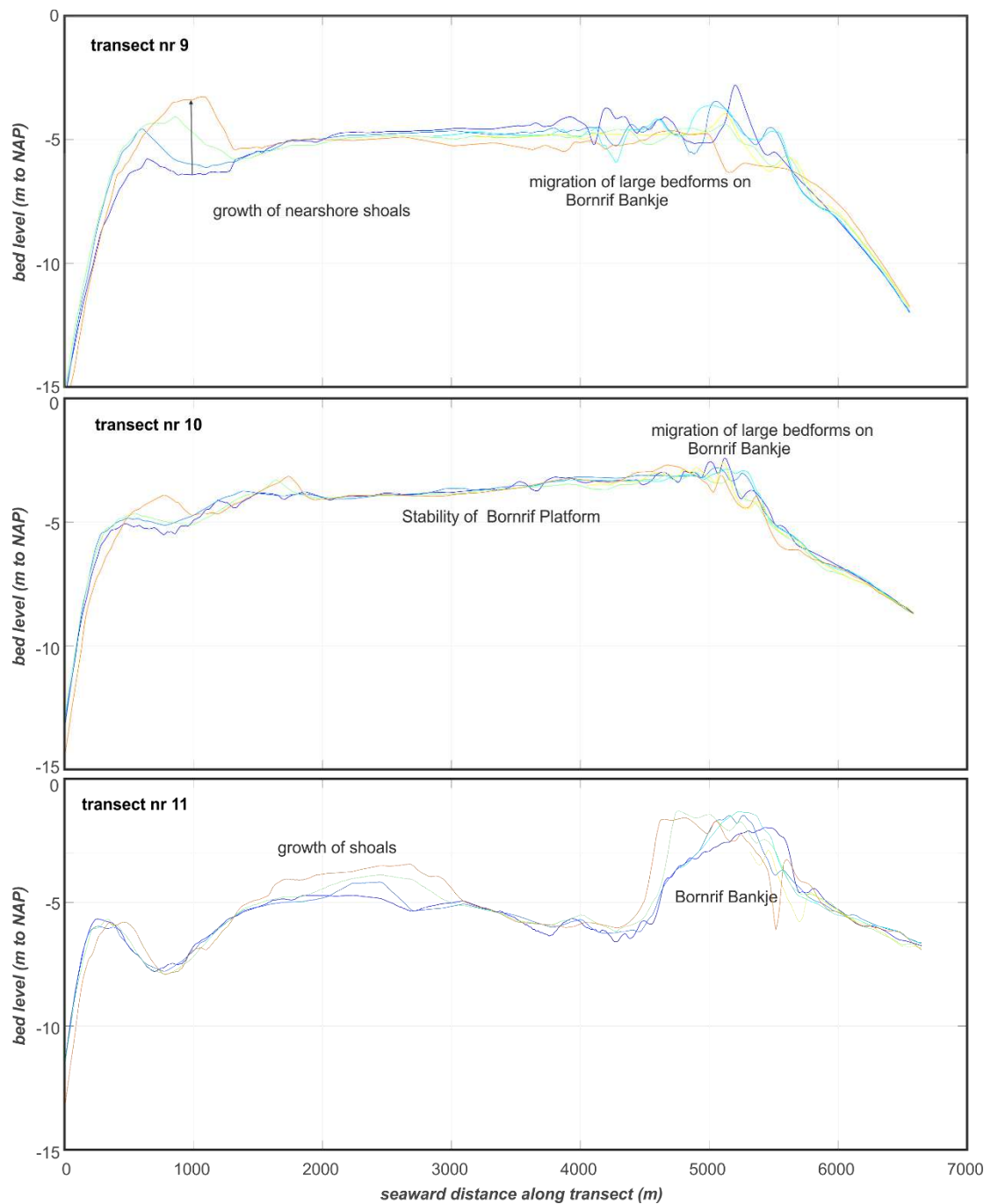1220339-008-ZKS-0008, 4 March 2020

Deltares

Figure 4.19 Bathymetric changes for transects 7-11 over the timeframe 2016-2019. Note that 0 corresponds to the Borndiep and 7000 to the open-sea.

4.3.2   An analysis of the ebb-delta nourishment.

The goal of this section is to summarize the development of the ebb-delta nourishment as a detailed analysis of the ebb-delta nourishment is provided by van Rhijn (2019). The most relevant findings of his study are summarized here and shown in Figures 4.19-4.28. In addition to the study of Van Rhijn, the surveys obtained in spring/summer 2019 are included.
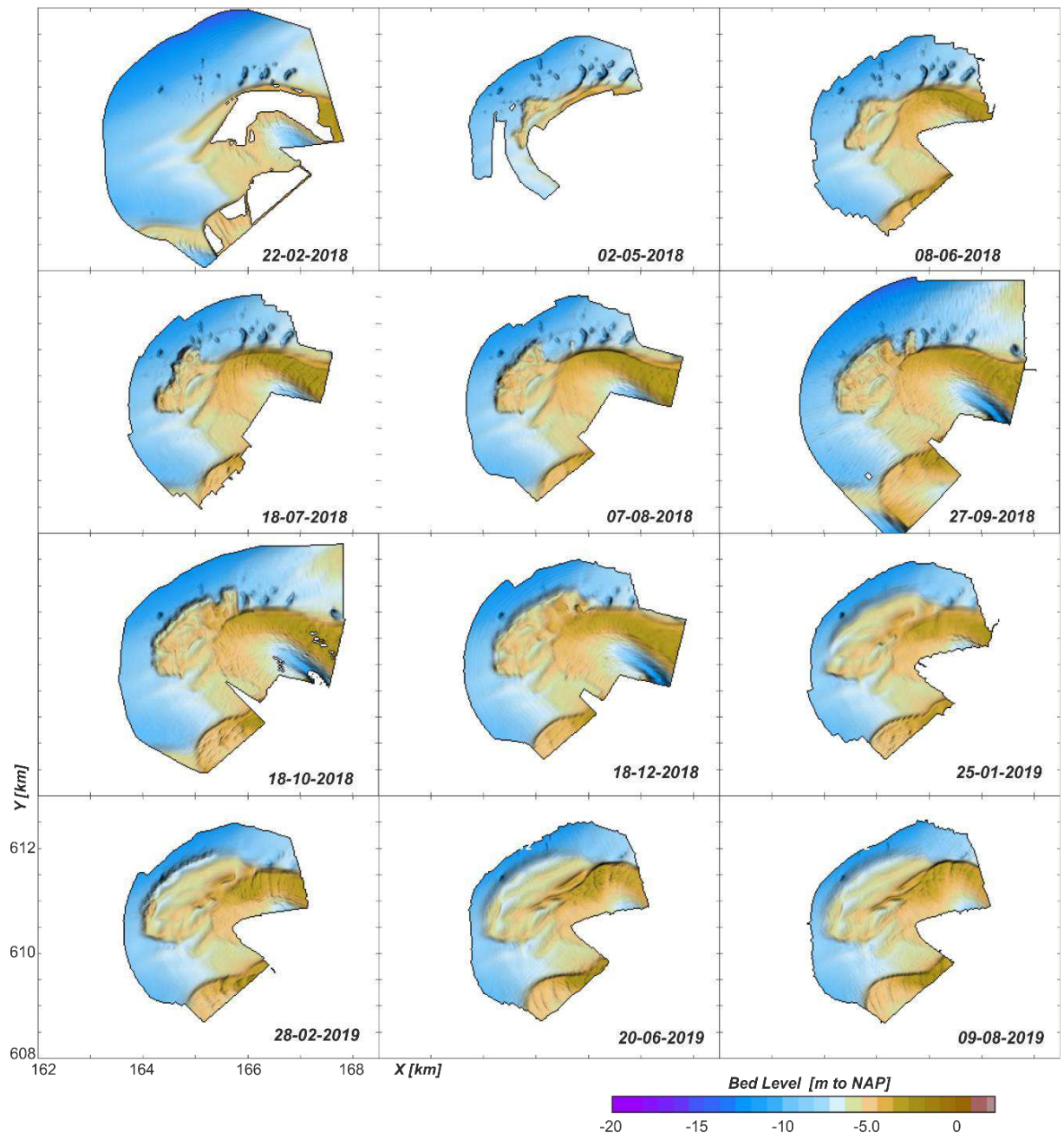
Figure 4.20 Overview of the bathymetries obtained from detailed mapping of the ebb-delta nourishment between 22-02-2018 and 09-08-2019.

From March 2018 through February 2019, nearly 5.5 million m³ of sand was placed on the seaward side of the Kofmansbult ebb-shield (see Figure 4.20 and Figure 4.21a). In the initial design, the nourishment was directly connected to the ebb-shield, but eventually it was placed slightly offshore, leaving a small channel between the ebb-shield and nourishment. This channel was filled in rapidly through natural sand redistribution. The nourishment design comprises an in-place volume of 5

Understanding the morphological processes at Ameland Inlet
1220339-008-ZKS-0008, 4 March 2020

Deltares

million m³ of sediment. To account for losses (typically 15%) due to e.g. settling, this means that in total 5.75 million m³ of sediment was dredged from the borrow areas. Based on volume changes in the survey data, Van Rhijn (2019) computed that 5.45 million m³, was actually placed on the seafloor. Most of the sediment (4.85 million m³) was found in the nourishment polygon, while an additional 0.6 million m³ was redistributed to fill in the trough.

As part of the project, the nourishment was surveyed regularly during placement and is followed for 2 years after completion. Figure 4.20 and Figure 4.21 provide snap shots of the surveys that are stored in the Kustgenese 2.0 repository. These maps show the formation of the ebb-delta nourishment between 22-02-2018 and 09-08-2019. The total change map over this timeframe (Figure 4.21a) is dominated by the placement. An interesting feature are the 2 large sandbars that can be observed in the pre-nourishment survey (Figure 4.20, 22-02-2018). These bars connect to the ebb-shield and extend in a southwesterly direction. In the most recent map of 09-08-2019, the nourishment is visible as a large extension of the ebb-shield. On this platform similar large bars can still be observed. A third and possibly fourth bar form seaward of the original 2 bars.
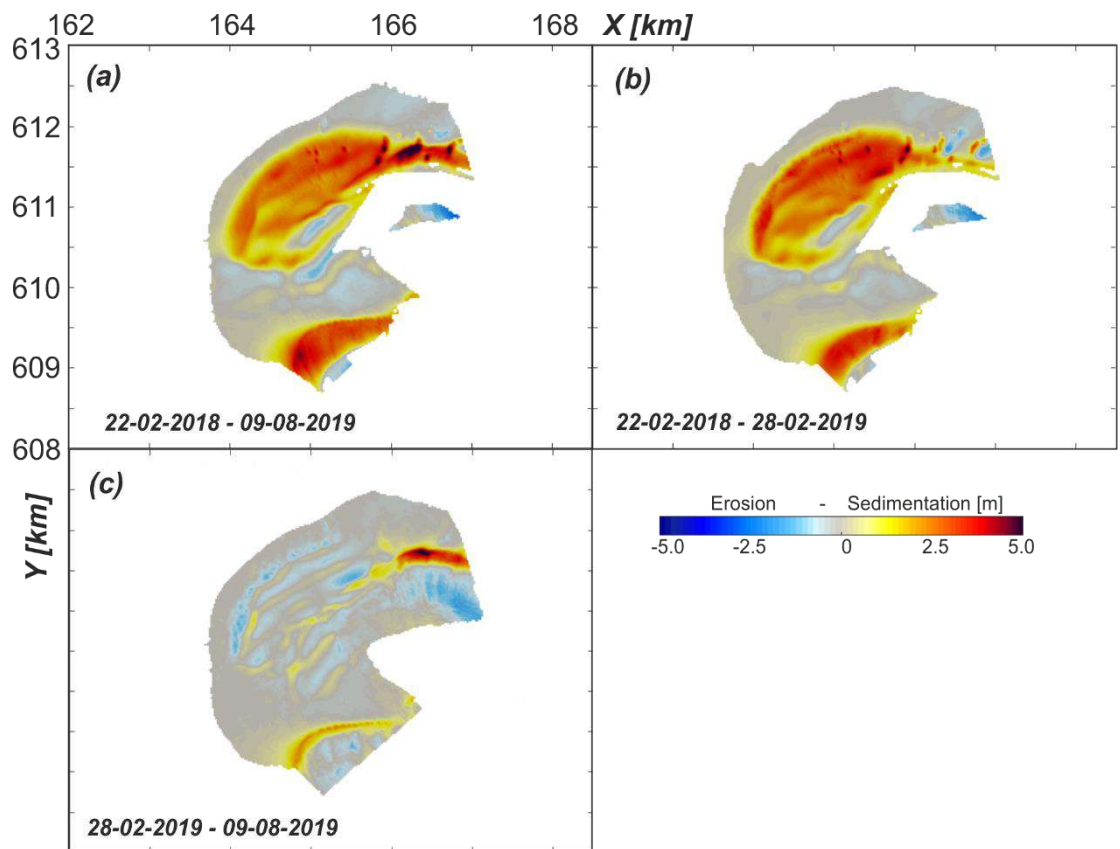

Figure 4.21 Overview of the observed sedimentation-erosion patterns of the ebb-tidal delta nourishment. (a) Total period: 22-02-2018 – 09-08-2019, (b) During construction (22-02-2018 – 28-02-2019) and (c) after construction (28-02-2019 – 09-08-2019).

The bathymetries of 28-02-2019 and 09-08-2019 (Figure 4.21c) provide a first indication of the changes after placement. These changes show that a small erosion prevails on most of the nourishment, while accretion is observed on its downdrift side. Most of this erosion occurs in the rougher winter/spring conditions between 28-02 and 20-06-2019. A similar, large response was also observed during the placement 18-12-2018 and 25-01-2019. Volume changes in summer, between 20-06-2019 and 09-08-2019, are near negligible. These findings correspond with the conclusions of Van Rhijn (2019) and are in line with the general ebb-tidal delta behaviour as described in the

Deltares

previous section. In the next paragraph, a detailed description of the development of the nourishment and the ebb-delta is provided through the analysis of cross-sections (Figure 4.22):
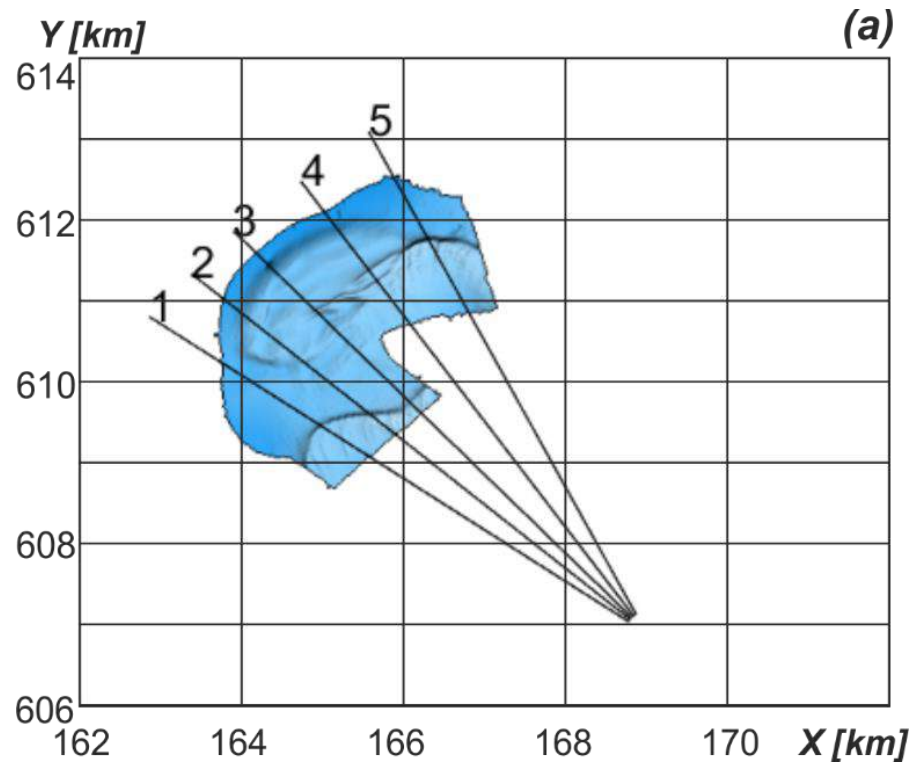
Figure 4.22 Overview of the selected transects taken over the ebb-tidal delta nourishment. See Fig. 4.23 – 4.28 for details of each transect.

Figure 4.23 Overview of the development of transect 1 between 22-02-2018 and 09-08-2019 (open sea is to the right).

*Transect 1 (*Figure 4.23*); Located just south (landward) of the nourishment. Here, an influence of the nourishment on the profile evolution is not observed. This transect intersects the southern ebb-shield *(SEC)* and provides a detailed view of its growth. At this location the ebb-shield outbuilding exceeded 500 m in 1.5 years. Distinct differences in migration rate between the measurements

Deltares

occur which seem related to the season. Significant migration is observed between February and June 2018 and from October to December 2018. During the summer season (May-October 2018) the migration is negligible. A constant migration rate is observed since December 2018.
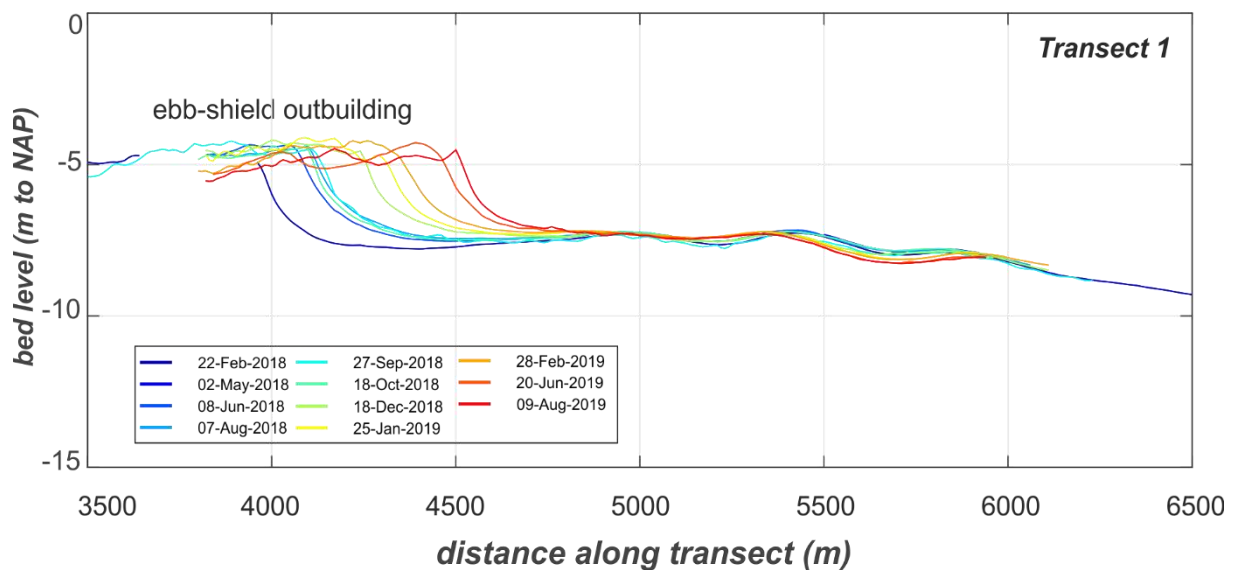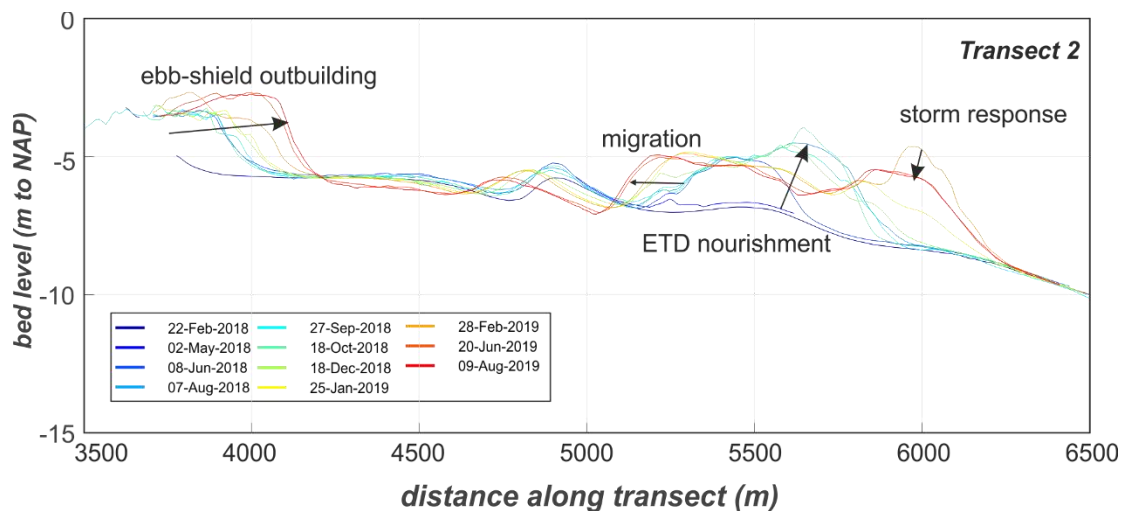

Figure 4.24 Overview of the development of transect 2 between 22-02-2018 and 09-08-2019. Open sea is to the right.

*Transect 2 (*Figure 4.24*);* Transect 2 crosses both the southern ebb-shield (distance 4 km) and the southern end of the ebb-delta nourishment (km. 5-6). Here, the migration of the ebb-shield is limited till January 2019. Between January and June 2019, a clear seaward movement occurs and the shoal increases in height. It is unclear if this development is initiated by the nourishment, as a 1 km platform still separates the ebb-shield and nourishment. It is therefore likely that the migration is part of the natural evolution of the ebb-shield. The ebb-delta nourishment shows two dominant evolutions. Initially, an increasing height and volume is observed, roughly at km. 5.5. Here the nourishment builds up to a height of -4 m around August 2018. Ever since, the height of the nourishment decreases and the shoal spreads out in both seaward and landward direction. Additional nourishments continue to add volume to the seaward part of the shoal reaching a maximum height in February 2019. After construction, an initial strong decrease in height at its seaward end is observed. Here, a small but high ridge lowered in height. The bulk of the nourishment however remains in place
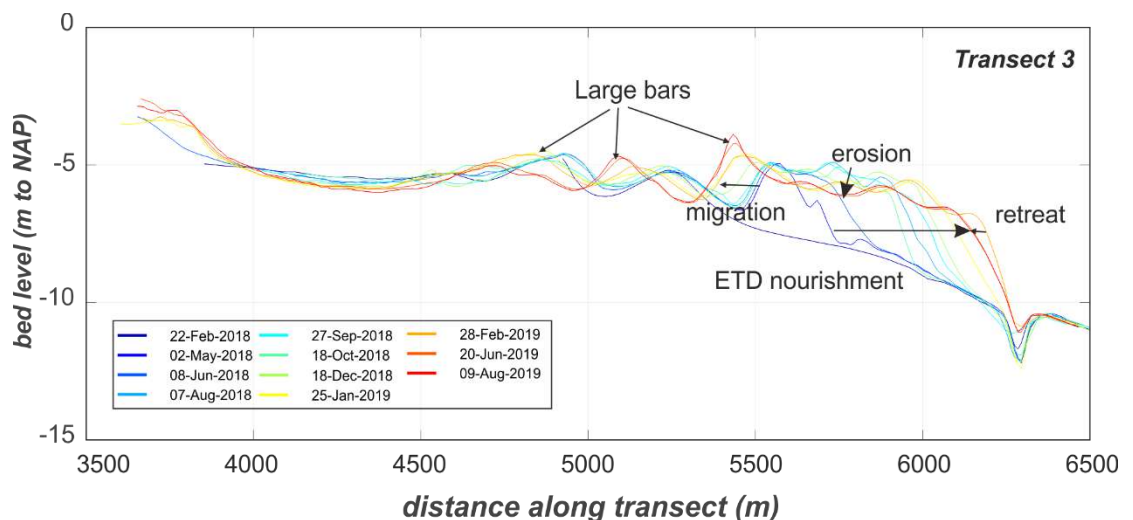

Figure 4.25 Overview of the development of transect 3 between 22-02-2018 and 09-08-2019. Open sea is to the right.

Deltares

*Transect 3 (*Figure 4.25*);* This transect is located centrally over the ebb-delta nourishment which can be observed between 5.5 and 6.3 km. The seaward outbuilding during construction is clearly visable. Also, large bars were present in the initial bathymetry (22 February 2018). These bars are retained even after nourishment and migrated landward. The ebb-tidal delta front shows a limited retreat between February and June 2019. The height of the central part of the nourishment decreases and part of this material seems to accumulate landward in the form of a large bar.
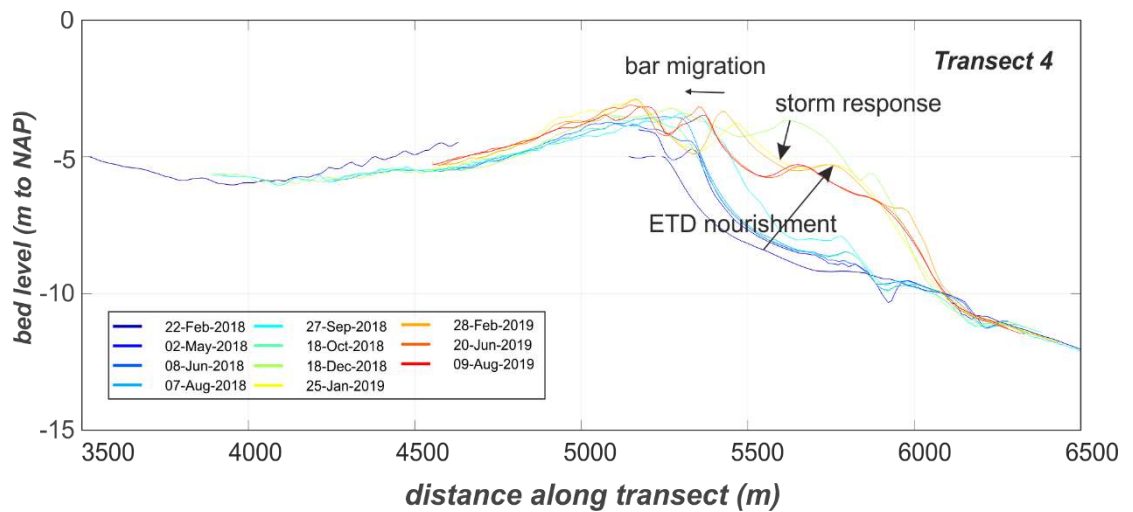
Figure 4.26 Overview of the development of transect 4 between 22-02-2018 and 09-08-2019. Open sea is to the right.

*Transect 4 (*Figure 4.26*);* Here, the ebb-delta nourishment is placed close to the northern ebb-shield. This ebb-shield continued to migrate seaward until September 2018. In this transect a clear storm response is visible as the height of the nourishment decreases significantly between December 2018 and January 2019. This material is partly transported landwards and forms a large bar that continues to migrate landward.
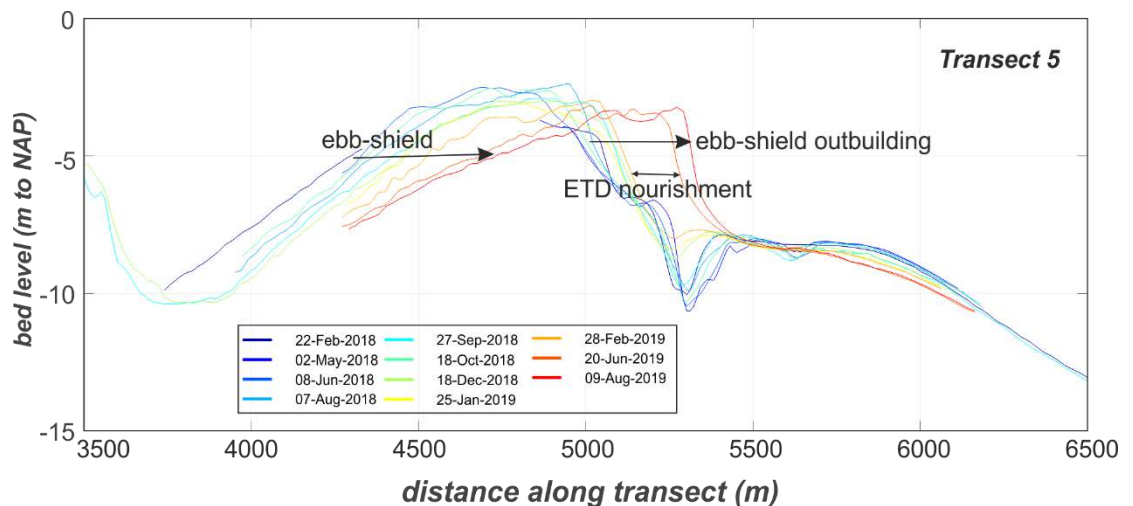
Figure 4.27 Overview of the development of transect 5 between 22-02-2018 and 09-08-2019. Open sea is to the right.

*Transect 5 (*Figure 4.27*);* Located to the north of the nourishment, this transect shows the ongoing seaward migration of the ebb-shield Kofmansplaat. The ebb-shield front moves 300 m seaward and decreases 1 m in height. Between 28 February 2019 and 20 June 2019, a strong seaward movement of the delta front can be observed. Part of this movement is likely the direct effect of the

Deltares

nourishment, but it partly results from the natural dynamics of the ebb-shield as during this timeframe the ebb-shield moved seaward.

Summary
Summary;

The conceptual model of Van Rhijn (Figure 4.28) corresponds with the insights in the natural behaviour of the ebb-chutes on the ebb-tidal delta (e.g. see Elias 2018 and Elias et al. 2019). The north-western margin of the ebb-tidal delta is governed by the behaviour of the 2 large ebb-chute and -shield systems that formed at this location. Prior to nourishment the seaward ebb-chute and shield system had reached a maximum extension and was subsequently pushed eastward by wave action. The second, southern ebb-chute and -shield is still developing and is being pushed seawards by the ebb current. This tide dominance results from the sheltering against strong wave action by the northern ebb-shield. Moreover, the ebb-chute channel developed an increasingly efficient connection with Borndiep.

The ebb-delta nourishment was placed as an expansion to the northern ebb-shield. It is not influenced by inlet tidal currents so waves and the tides on the open sea form the dominant sediment transport mechanisms. The open-sea tides may contribute to alongshore redistribution of sediments, but waves are the primary driver. This statement is clearly confirmed by the difference in change rates between the periods February 2019 through June 2019 versus June 2019 through August 2019. During the first period (winter/spring) conditions are more energetic. As a result, the volumetric changes are significantly higher than the changes during the less-energetic summer conditions. Van Rhijn made a similar observation during placement of the nourishment as the January 2019 storms from the north-west caused a considerable sediment transport in south-eastern direction. Wave-driven transports contribute to the eastward movement of the ebb-shield and the infilling of the Akkepollegat. Although not clearly presented in the conceptual model of Van Rhijn (Figure 4.28), it is likely that in addition to the landward component, waves also generate a downdrift transport along the nourishment. This downdrift nourishment likely contributes to the large infilling observed in the former Akkepollegat channel.

The frequent observations (in 2 to 4 month intervals) including the ebb-shield provide additional evidence of the functioning of the ebb-chute and -shield systems. Observations of both the ebb-shield and the ebb-chute channel show larger migration rates under winter conditions. Increased erosion of the shoals during winter can be easily explained by the more energetic conditions that occur. During winter, more and larger waves occur that break on the ebb-shield platform and drive a larger wave-driven sediment transport. The large outbuilding of the ebb-shield front and increased erosion of the ebb-chute channel during winter may be related to surge. In the North Sea a close correlation between wind speed and wave height occurs. In the winter season larger storms appear that do not only generate the larger waves but also can produce large-scale surges. These surges can considerably increase the exchange of water volumes through the inlet. As the basin drains after waining of the storm, ebb-velocities may be considerably increased resulting in strong current velocities over the ebb-tidal delta and increased seaward expansion and migration of the ebb-chute and shield systems. These findings raise questions of our general conceptual models describing tidal inlet systems.
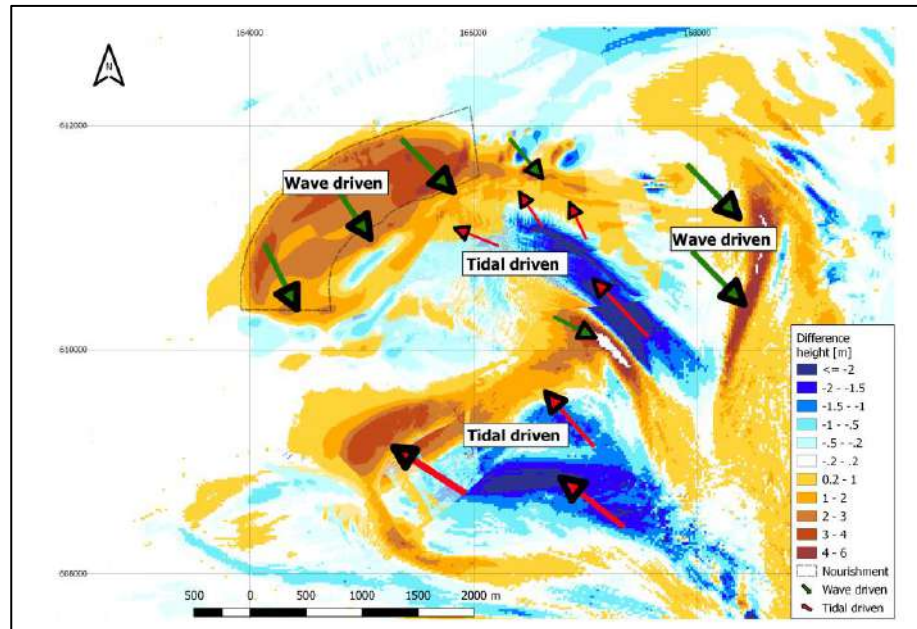
Deltares

Figure 4.28 Main sediment transport pathways and their underlying physical processes. The combined difference map of survey 0-9 and Vakloding 2017-05 - 2018-05 indicates the areas of deposit/sedimentation and erosion (source van Rhijn, 2019; Figure 6.1, page 54).

Understanding the morphological processes at Ameland Inlet
1220339-008-ZKS-0008, 4 March 2020

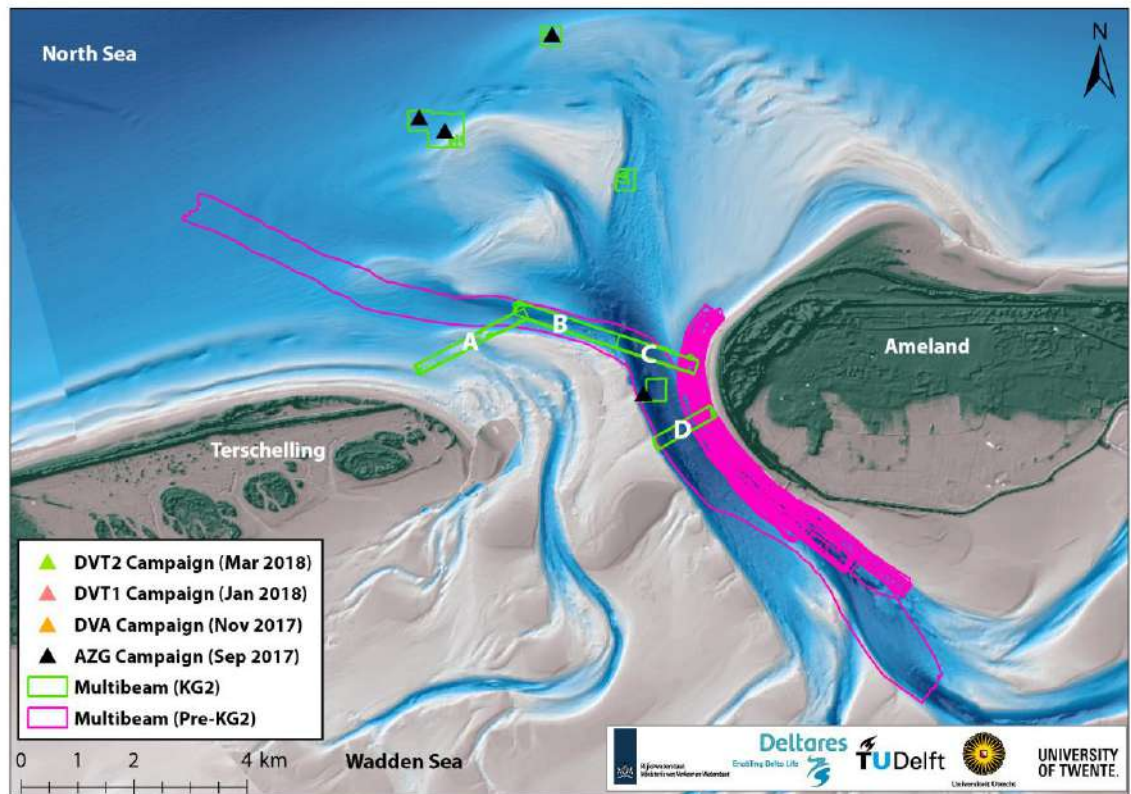**Deltares**

4.3.3 Bed forms

Figure 4.29 Overview of KG2 AZG multibeam measurements. ADCP transect measurements were carried out along Sections A, B, C, and D to determined water fluxes. (From Van der Werf et al., 2019)

Since 2005, regular surveys of the stone protection at NW Ameland have been made using Multi-beam echo sounding (MBES). Figure 4.29 provides a complete overview of the available datasets. These datasets do not cover the entire ebb-tidal delta but are limited mainly to specific parts of Borndiep channel. Most datasets cover the area directly adjacent to the shore protection works at Northwest Ameland. Especially relevant for this study is the MBES dataset taken on 17 April 2012 that covers the central part of the Borndiep channel and the outflow into the Westgat channel (Elias, 2018).

Table 4.3   Dates and locations of MBES surveys during Kustgenese 2.0.0 (see van der Werf et al., 2019).

Vak A	Vak B	Vak C	Vak D
30-08-2017	30-08-2017	30-08-2017	07-09-2017 7:54 - 8:26
31-08-2017	31-08-2017	31-08-2017	07-09-2017 8:36 - 9:27
02-09-2017	02-09-2017	03-09-2017	07-09-2017 9:37 - 10:17
03-09-2017	04-09-2017	04-09-2017	07-09-2017 10:24 - 11:08
04-09-2017	06-09-2017	06-09-2017	07-09-2017 11:13 - 11:52
06-09-2017			07-09-2017 11:57 - 12:31
			07-09-2017 12:37 - 13:14
			07-09-2017 13:18 - 14:13
			07-09-2017 14:15 - 14:55

Additional MBES datasets were collected during the Kustgenese 2.0 campaigns. MBES data was obtained at an additional 4 locations (see Figure 4.29 and Table 4.3) at several intervals. In the study of Elias (2018), the data obtained in areas A through D as summarized in Table 4.3 were

Understanding the morphological processes at Ameland Inlet
1220339-008-ZKS-0008, 4 March 2020

Deltares

analyzed. These data can be subdivided in 3 categories. (1) Individual measurements of the Vakken A, B, C. (2) Four repeated surveys of Vakken A, B, C in August and September 2017. (3) Repeated surveys of bedforms over a tidal cycle in Vak D on 7 September 2017. In addition, detailed measurements of the frames were also made, but these have not been analysed yet in the present study.

The multi-beam surveys obtained in Ameland inlet show the presence of multiple bedform fields (see Figure 4.30 and Figure 4.31 for examples). Analysis of these MBES surveys provides us with a detailed picture of the sediment transport directions in some of the major channels in Ameland Inlet as summarized in Figure 4.32. At the western outflow of Westgat sediments are flood dominant in the channel, transporting sediments towards Borndiep, and ebb-dominant to the south. The outflow of Borndiep towards the ebb-tidal delta is ebb-dominant. A flood dominant transport prevails only along the coast of Ameland. However, the coastline directly faced by Borndiep is governed by ebb-dominant bedform asymmetries. In the center of the inlet gorge, a flood-dominant transport prevails, except locally along the southern embankment a flood-dominant (basin-ward) transport is observed. Flood dominant transports are also observed onto the shoal that separates the eastern and southern fork of Borndiep (Dantziggat and Kromme Balg respectively). Measurements in Kromme Balg are not present, but the three profiles leading into the channel all point to a flood-dominant transport. Most of the profiles in the section of Borndiep that leads to Dantziggat show an ebb-dominance. The most basin-ward profiles show ebb dominant transport directed onto Kikkertplaat, and a flood dominant transport in the deepest parts of Dantziggat.

The analysis of Vakken A, B, C from the Kustgenese 2.0 MBES surveys provides us with: (1) corresponding areas in which bedforms are present, and (2) similar bed-form asymmetries and bed-form migration patterns. This correspondence illustrates that these bedform fields are consistent over time and can therefore help to identify sediment transport directions and patterns in the channels on the ebb-tidal delta. These conclusions are however not completely trivial. The detailed analysis of Vak D, in which bedform characteristics are determined over a tidal cycle, indicates that bedform asymmetry and migration can depend on the local flow velocities during the survey.

Lessons learned in relation to morphodynamic modelling:

- The consistent and coherent bedform fields and asymmetries on the ebb-tidal delta provide valuable (or maybe even our only) validation datasets for the larger-scale sediment transport patterns. Such datasets cannot be easily obtained otherwise.
- Only small bedforms are present in the central part of the inlet gorge where flow velocities are large. This observation is in contrast with the numerical models that tend to predict larger bedforms in the main channels (e.g., Wang et al. 2019).
- No clear migration of the bedforms seems to occur in the central part of the Borndiep channel over a tide cycle. This indicates that net bed-load sediment transports may be small. Larger bedforms and migration rates are observed along the sides of the channel. This may indicate that most of the net sediment transports occur along the sides of the inlet gorge. This provides valuable concepts for model testing and analysis.
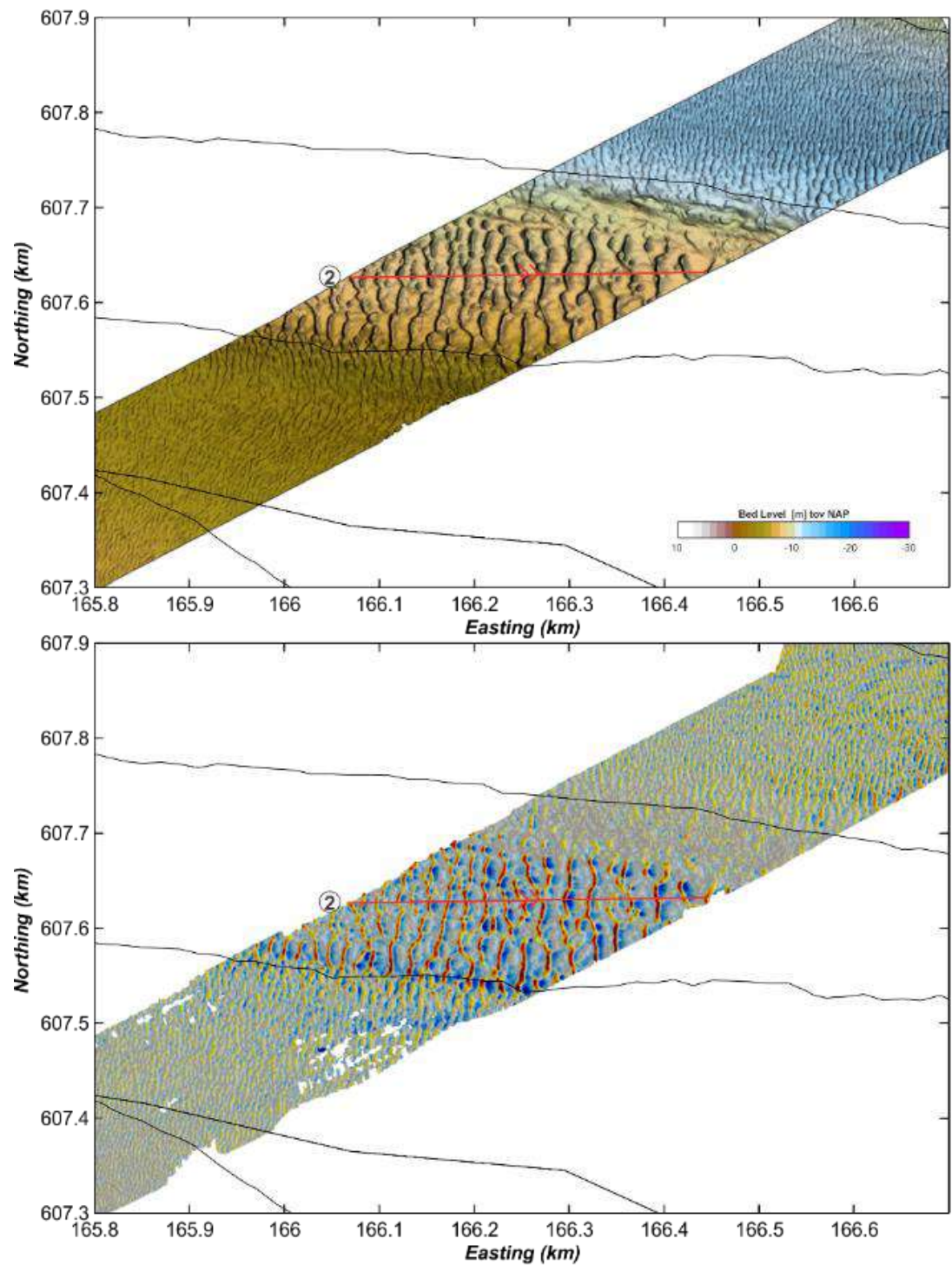
Deltares

Figure 4.30 (top): Example plot of the MBES data obtained for Vak C and bedform migration (bottom) between 30-08-2017 and 06-09-2017. Source: Elias (2018).
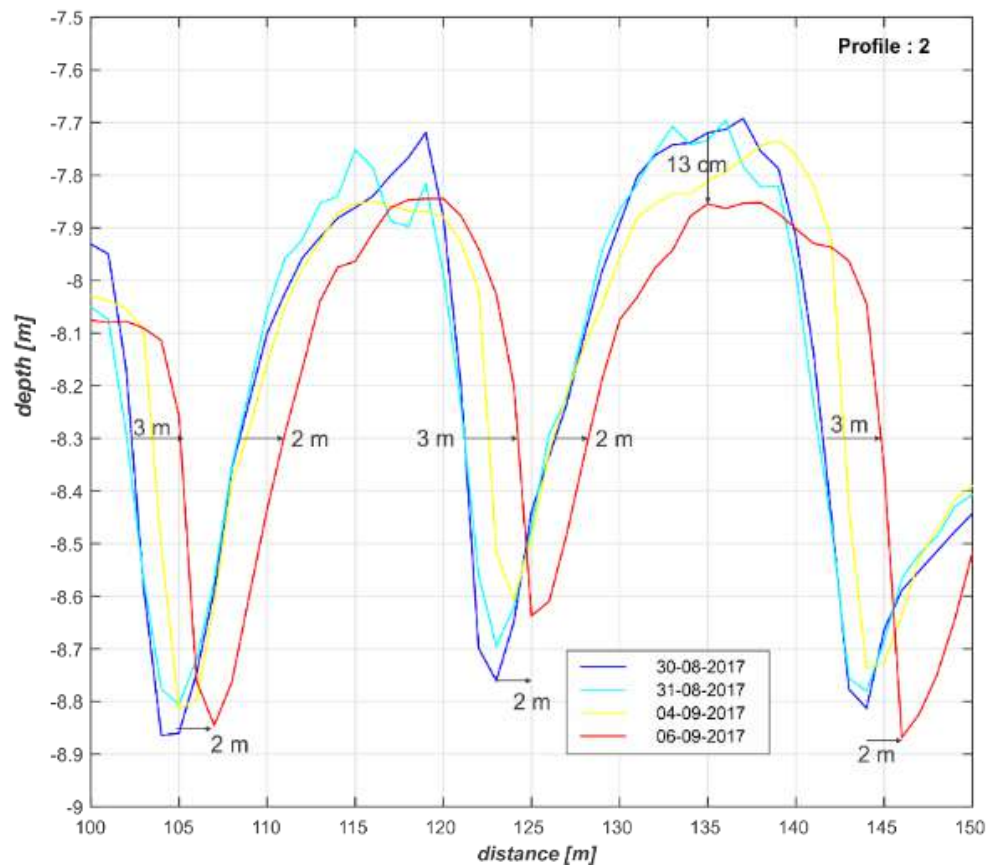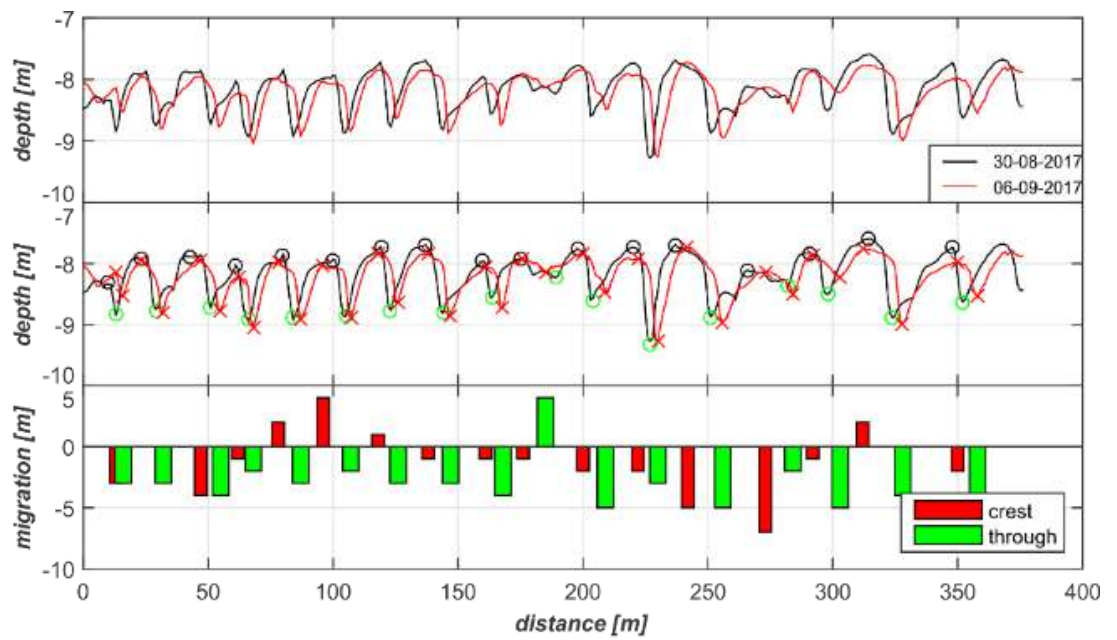
Deltares

Figure 4.31 Example plot of migration rates for transect 2 (see Fig. 4.30a).
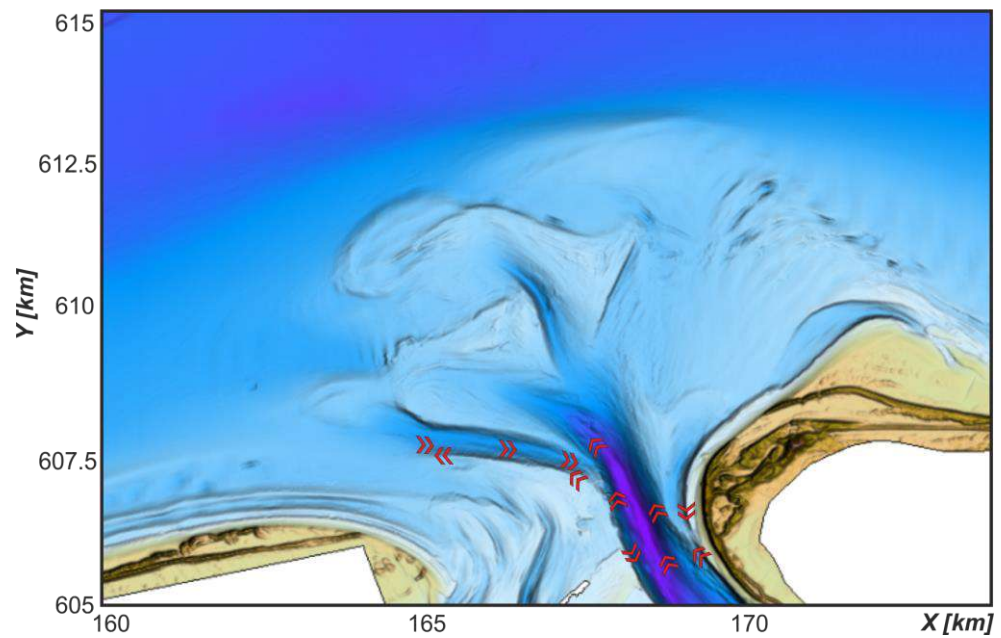
Deltares

Figure 4.32 Summary plot for bedform orientations (based on Elias 2018).

Deltares

4.3.4 X-Band Radar

The marine radar data at the Ameland lighthouse operates in the X-Band range. In addition to vessel tracking, a radar signal reflection is also retrieved from the capillary waves. This additional signal can be processed using specialized software into physical parameters such as waves, currents and water depths. The data provide a snapshot of the sea state for an approximate 7.5 km from the lighthouse which basically covers the entire ebb-tidal delta domain (Figure 4.32). Swinkels et al. (2012) used this data to obtain current estimates. In the Kustgenese 2.0 project focus was on deriving bathymetry (Gawehn et. al. 2020). Gawehn uses a depth inversion method algorithm (XMFit, X-Band Matlab Fitting) to remotely sense the bathymetry from the radar data.
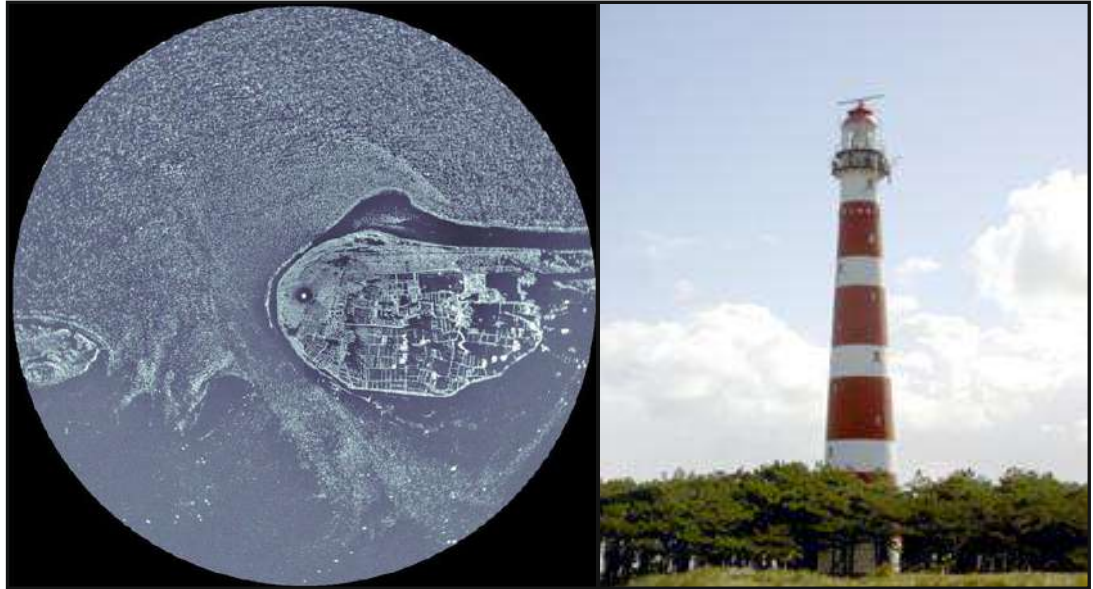
Figure 4.33 An example image of the radar data illustrating its range (left panel). The lighthouse of Ameland with marine radar mounted on its top (right panel).

As part of the Kustgenese 2.0 monitoring program, XMFit software ran operationally on XBand radar data collected at the Ameland lighthouse. The system processes the raw incoming data and approximately once an hour writes out a depth estimate. At present over 15.000 depth estimates of the ebb-tidal delta have been created. Figure 4.33 displays typical XMFit results for daily mean bathymetries produced at the surveys in May 2018, October 2018 and July 2019 (from Gawehn, 2020). From this analysis, Gawehn concludes:

(1) Daily median XMFit results results provide an accurate representation of the major morphological features (such as Borndiep, Westgat, Kofmansbult and Kofmansplaat, and Bornrif).
(2) Estimated depths show a positive bias (small overestimation of depth).
(3) Less accurate results are obtained in areas of intense wave breaking in combination with large bed gradients. These areas remain consistent over time.
(4) The morphological change map between May and July 2019 shows in general good correspondence between observed and estimated patterns and values.

This recent work of Gawehn illustrates that accurate predictions of the morphological changes can now be obtained using the X-Band radar in combination with XMFit. The future use of XMFit derived bathymetry may help us to better understand the responses of the ebb-tidal delta during more energetic conditions (see Secton 4.3.2).

Deltares
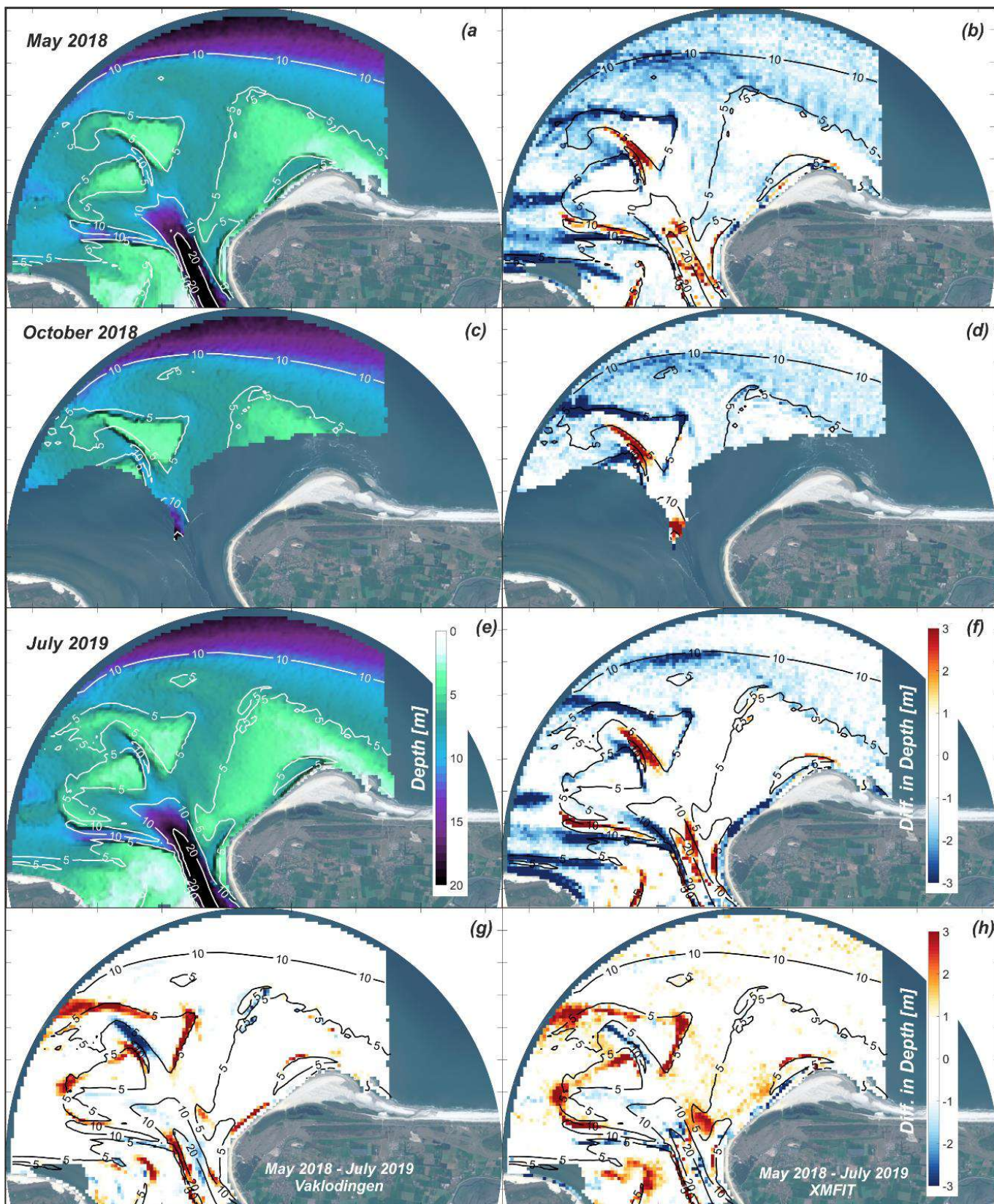
Figuur 4.34 Estimated bathymetries from X-Band Radar compared to Vaklodingen obtained in May 2018 (a,b), Oktober 2018 (c,d), and July 2019 (e,f). Panels (a,c,e): Estimated bathymetry (surf plot) and measured contourlines. Panels (b,d,f): Difference between estimated and measured bathymetry (Blue overestimated depth, red underestimation). Panels (g,h) Sedimentation-erosion maps for Vaklodingen (g) and XMFIT results (h) over the timeframe May 2018 – July 2019

Understanding the morphological processes at Ameland Inlet
1220339-008-ZKS-0008, 4 March 2020

Deltares

4.4   A summary of the Kustgenese 2.0 insights gained from measurements

The sequence of storms and calm conditions that occurred during the Kustgenese 2.0 Amelander Zeegat campaign provides detailed insights in the hydrodynamics and morphodynamic changes of Ameland Inlet.

An analysis of the large-scale flow patterns based on drifter experiment confirms that Westgat forms a transitional area between the areas of influence of Boschgat and Borndiep. Flow along the Terschelling coast, south of Westgat, exchanges with the southern/eastward part of the basin). Flow that enters Borndiep exchanges primarily with the western seaward portion of the ebb-tidal delta.

Tidal flow velocities in Borndiep are considerably larger than the velocities measured on the ebb-tidal delta. During spring tide, velocities exceed 1.35 m/s and reduce to around 0.50 m/s during neap tides. On average, maximum ebb velocities exceed the maximum flood velocities. On the ebb-tidal delta, the tidal velocities are smaller, but the non-tidal (wave- and surge-driven) velocities are significantly higher. These velocities exceed 1.0 m/s during storm events, while during the largest wave event a 1.5 m/s flow velocity was measured. Such velocities can, in combination with breaking waves, pick up and transport vast amounts of sand. Noticeable non-tidal velocity have been recorded at all frame locations. The non-tidal velocity on the ebb-tidal delta of 0.25 m/s exceeds the average of 0.12 m/s measured in Borndiep.

The 13-hour discharge measurements illustrate the relatively large variation in ebb and flood volumes through the inlet gorge. Part of this variation is due to spring-neap variability, but large-scale water level gradients may be important as well. No clear preferential ebb- or flood dominance is observed. This is caused by the small net discharge compared to the gross volumes. Stations placed on the tidal divides measured a large (residual) flow across the tidal divide, especially during strong south-westerly winds. This flow is much larger than was previously assumed.

Wave measurements show the wave sheltering effect of the ebb-tidal delta during higher wave conditions. Wave heights of over 2 m dissipate on the ebb-tidal delta margin. Stations located in the Borndiep/Akkepollegat channel also show a significant tidal modulation of wave heights. Due to wave-current interaction the wave heights almost double on opposing peak ebb currents. During storms the average wave heights increase, which correlates to elevated water levels over the ebb-tidal delta allowing larger waves to propagate over it before breaking in the nearshore area.

The high-resolution, repeated, multi-beam survey data obtained in the Westgat and Borndiep channels shows the sustained presence of multiple bedform fields. Bed-form asymmetry and migration indicate that in Borndiep sediment transport is primarily ebb dominant and in Westgat flood dominant. These transport directions correspond to the sediment transport patterns derived from the morphodynamic features and their changes. Correspondence in repeat surveys on the ebb-tidal delta confirm that (1) bedform asymmetry is an indicator for bedform migration, and (2) coherent, consistent, bedform fields occur through the various surveys.

Through the combined analysis of the processes and the observed morphodynamic changes, it is possible to start to better understand the morphodynamic processes that dominate Ameland Inlet. Figure 4.35 summarizes the lessons learned from this analysis. On the large-scale, the ebb-tidal delta can be subdivided in various zones that are governed by a different balance of tidal versus wave energy (Figure 4.35, zone I – VI). Both processes are important in all regions, but their priority and the morphodynamic response is different.

Zone I – Updrift coastline; The littoral drift along the coastline of Terschelling and the continuous erosion of the island tip Boschplaat form a sediment source for the inlet. Both waves and tides play an important role here. Nearshore waves generate a net eastward driven flow and stir up sediments

Deltares

that can be transported by the flood-dominant tidal flow. These transports feed the sub-tidal platform that is present between Westgat and Boschgat.

Zone II – Sub-tidal platform; The sub-tidal platform, the shallow area between Westgat, Boschplaat and Borndiep, shows a large mobility of the smaller scale channels and shoals, while net change is limited. The platform acts as an exchange area. Sediment is exchanged with the western part of the basin, and is transported net eastward over the platform to Borndiep. Earlier studies (e.g. Elias, 2018) hypothesize that part of the erosion of Boschplaat is related to increased wave exposure as the present-day ebb-tidal delta facing Boschplaat was relatively deep. This allows waves to propagate far onto the ebb-tidal delta, to the coast and into the inlet gorge, introducing an eastward, wave-driven transport along the Terschelling coast and into the inlet (Boschgat area). Part of these sediments deposit in the south-western part of the basin, partly these sediments migrate over the sub-tidal platform and into Borndiep.

Zone III – Ebb- chute and ebb-shield systems; The ebb shields form temporary sand buffers that grow and migrate seaward. Once abandoned they feed the Bornrif shoal. The western, seaward side of the ebb-tidal delta is dominated by tides. At this location two large ebb-chute and ebb-shield systems dominate the morphodynamic changes. Both systems formed along the western side of Borndiep, just north of Westgat. The ebb-chutes and -shields grew and migrated seaward. The main shoal area, the ebb-shield, is asymmetrically shaped with the bulk of the sediments at the downdrift side of the ebb-chute. The steep bed slopes on the seaward side of these features indicate that outbuilding is caused by the tidally driven sediment supply from the ebb-chutes. The detailed measurements obtained at the nourishment site indicate that ebb-chute migration is not a continuous process, but primarily occurs during higher energetic conditions. It can be hypothesized that large wind events generate considerable large-scale setup that can enhance flow velocities through the inlet and onto the ebb-tidal delta. The increased ebb-velocities result in above average ebb-chute and -shield migration. Wave breaking and related sediment transports on the shallow ebb-shields drive sediments landward and eastward. As a result, the ebb-shield shoals not only migrate seaward but also eastward, and the bulk of the sediments is contained on the downdrift side of the ebb-shield. The ebb-shield outbuilding into Akkepollegat constrained its flow (and related transports) even further. As a result, the deep central part of Borndiep now connects directly to the most southern ebb-chute. It is likely that this chute will progressively capture the ebb discharge of Borndiep and thus will take over the role of the Akkepollegat completely. The continued growth of the southern ebb-shield may result in complete closure of the northern ebb-chute channel and merger of the two ebb-shields. This would form a large shoal area in the west-central part of the ebb-tidal delta. A secondary effect of the abandonment of Akkepollegat is the infilling of the (former) channel. Especially along the western margin of the Bornrif platform, a large sedimentation area is observed. This area is fed by the wave driven transports over the Bornrif platform, and by the ebb-tidal currents.

Zone IV – ebb-tidal delta margin. The ebb-tidal delta margin is usually not considered as a separate element of the ebb-tidal delta. However, both the hydrodynamic and the morphodynamic observations indicate that the processes here are slightly different and dominated by storm waves. During most of the year, shoals (such as the ebb-shields and the ebb-delta nourishment) accumulate on the ebb-delta platform. These shoals are in equilibrium with the low-wave energy and tidal energy. During storms, the largest waves break on these shoals and cause large fluxes of sediment towards the east. As a result, episodical large pulses of sediment feed the Bornrif platform and contribute to the sediment accumulation here. The half-yearly volume analysis shows that sediment accumulation in winter significantly exceeds the summer accumulation. After the storm events, this part of the ebb-delta is relatively inactive as it is too deep for waves to break under normal conditions. The dominant transport mechanism is then the alongshore tidal current in both ebb and flood direction that somewhat accelerates as the flow streamlines contract around the ebb-delta.

Understanding the morphological processes at Ameland Inlet
1220339-008-ZKS-0008, 4 March 2020

Deltares

Zone V – Main ebb-delta platform; The main shoal area Bornrif is located downdrift of the main channel. The shoal built out seawards when Akkepollegat was still the main ebb channel, which resulted in sediment accumulation far to the north. This accumulation was the result of the balance between the seaward sand transport by the ebb current and the landward wave-driven transports. After abandonment of Akkepollegat, the landward wave-driven transports now prevail, and net erosion is observed at the delta front. These sediments are transported landward and accumulate in shoal deposits just seaward of the Ameland coast. Large-scale deposition is also observed along the western margin of Bornrif, where Akkepollegat fills in with sediments. It is likely that the wave-driven transports contribute directly and indirectly to these deposits. Indirectly, as sediments are picked up by the tidal flow over the Bornrif platform and along the coast of Ameland. This flow enters Borndiep and sediments are eventually transported seaward by the Borndiep ebb-currents into the abandoned and thus oversized Akkepollegat.

As tidally transported sediments primarily accumulate on the western, updrift margin of the ebb-tidal delta, the distal part of the Bornrif platform becomes sediment-starved. Wave dominance introduces a net landward transport resulting in a lowering of the seaward part of the Bornrif shoal, and sediment accumulation in shoals near the coast. Although this seems contradictory, the landward sediment transport introduces, at least temporary, an increased erosion of the island coastline. This is a commonly observed phenomenon and related to the constriction and contraction of (flood) flow between the coastline and the advancing tidal delta shoals. Typically, the ebb current dominates in the main channel, whereas flood currents dominate the marginal channels along the island coastlines. As the landward migrating shoals increase in height, they increasingly constrict and trap the flow along the coast. As a result, a channel forms directly along the coastline that introduces coastline erosion, and also slows the advance of the shoals (a perfect example of such process is the Noorderlijke uitlopers of the Noorderhaaks versus Molengat channel in Texel Inlet, see Elias and Van der Spek, 2016). The sediments, driven landward by waves, are subsequently transported along the coast by the tidal currents in the channel and accumulate in the shoals that are starting to form on either side. Depending on the sediment supply, these shoals can grow to such dimensions, that they finally overwhelm the channel and episodically attach to the coastline (e.g., Bornrif Strandhaak), or they temporarily grow and finally disappear when sediment supply reduces or stops due to larger-scale changes on the ebb-tidal delta. The bedforms at Ameland Northwest confirm sediment transport that is directed towards Borndiep.

Zone VI – Shoal attachment zone;
The shoal attachment zone is a net accretional area. In the present-day shoreline, the large bulbous form is the remnant of the Bornrif Strandhaak, a former ebb-tidal delta shoal that attached to the coast in 1982. After the Strandhaak attached to the shore, the coastline shifted seaward by 1.5 km, followed by a retreat of over 500 m as the deposits were subsequently eroded and predominantly transported downdrift, feeding the adjacent coast of Ameland. The attachment of the Bornrif Strandhaak is well documented by the yearly shoreline measurements from the JarKus database (see Elias et al., 2019). A new shoal attachment occurred in 2017 as the Bornrif Bankje attached to the coastline at the eastern tip of the Bornrif Strandhaak. In contrast to the previous two attachments that occurred on the north-western tip of Ameland near Borndiep, this recent attachment occurred more downdrift at the ebb-delta margin. The origin of Bornrif Bankje can be traced back to the period 1989-1999. During this interval, the northern ebb-delta front prograded and increased in shoal height at the seaward end of Akkepollegat. This outbuilding continued until 2011. Wave-breaking on this shallow shoal area probably resulted in downdrift sand transport along the ebb-tidal delta margin, and Bornrif Bankje slowly started to emerge on the north-east side of the ebb-tidal delta (2008-2010). The shoal continued to migrate eastward and landward (2011-2014), and by 2014 only a small channel remained separating the Bornrif Strandhaak and Bornrif Bankje. The map of 2017 shows that the tip of Bornrif Bankje finally attached to the Ameland coastline, just downdrift of the Strandhaak.
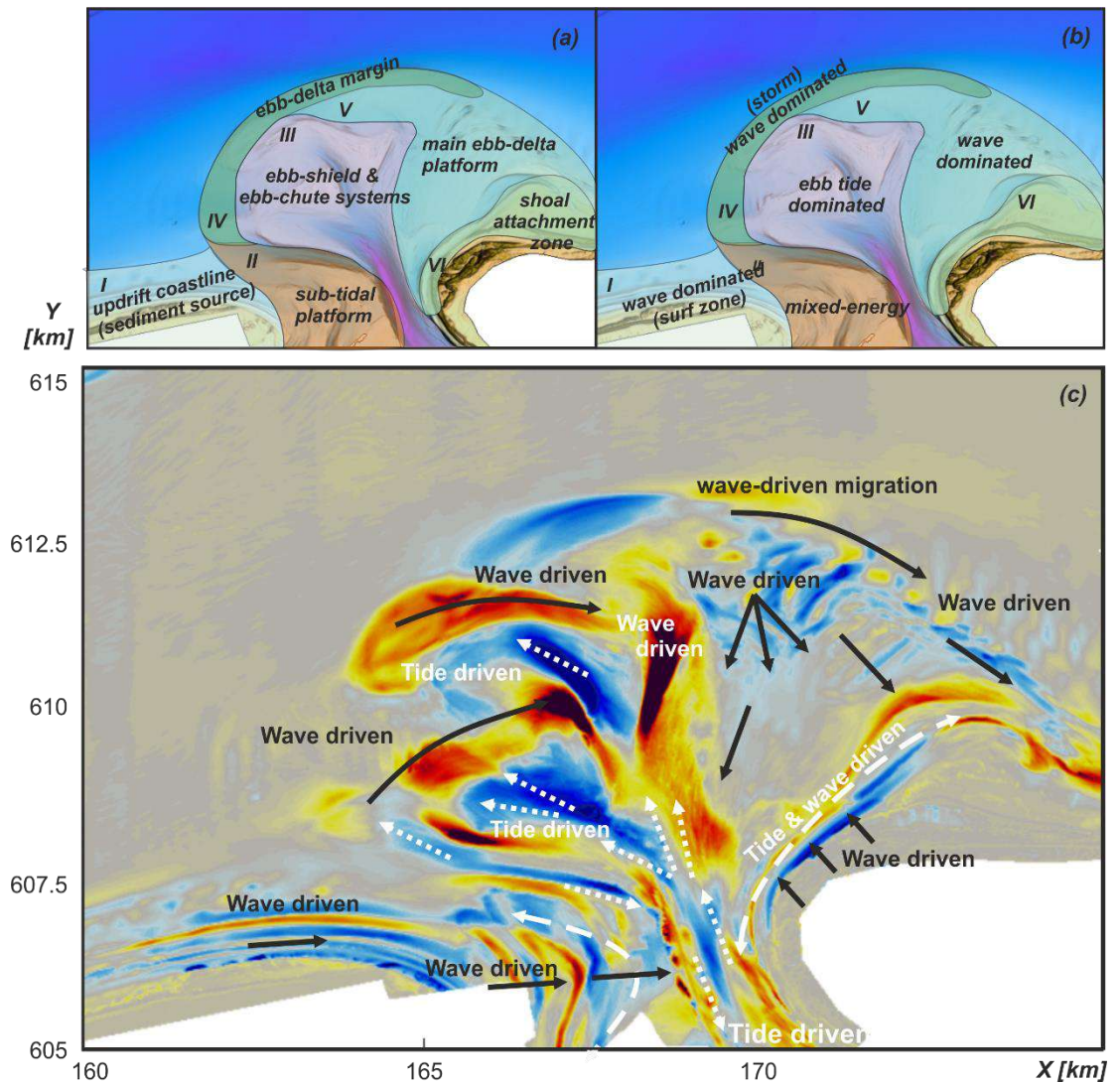
Deltares

Figure 4.35 Conceptual description of the recent morphodynamic behaviour of the ebb-tidal delta at Ameland Inlet. The underlying sedimentation-erosion map is based on the time-frame 2016-2019.

5 Understanding the meso-scale processes at Ameland Inlet; a synthesis

5.1 Sediment-bypassing processes

5.1.1 General principles

Past studies have resulted in various conceptual models to explain the variability in the configuration of inlet shorelines and the distribution of the associated ebb and flood-tidal delta shoals (e.g. Hayes, 1975; 1979; Oertel, 1975; Walton and Adams, 1976; Hubbard et al., 1979; FitzGerald, 1988; 1996; Hayes and FitzGerald, 2013). The configuration of these shoals influences the distribution of wave energy along the adjacent shorelines and controls the sediment-bypassing (Luck, 1976; Oertel, 1977; FitzGerald et al., 1984; FitzGerald, 1996). These studies generally agree on some basic fundamentals. Firstly, the geometry of the back-barrier basin, in combination with tidal range, determines the tidal prism (e.g. Davis and Hayes, 1984) which, in turn, determines the size of the inlet (O'Brien, 1931, 1969; Jarrett, 1976). The ebb-currents accelerate in the narrow constriction of the inlet gorge, and a sediment-laden ebb current enters the open sea. In the open sea, the tidal flow disperses, current velocities drop below the sediment transport threshold value and the sand is deposited. This sand forms a shallow shoal called the ebb-tidal delta in which large volumes of littoral sand can be stored (Dean and Walton, 1975; Walton and Adams, 1976). Ebb-tidal deltas not only form large reservoirs of sand but also participate dynamically in exchanges of sand in and around tidal inlets. Wave shoaling and breaking on these shoals tends to move these sediments landwards. The balance between the wave and tidal processes, determines the morphology of an ebb-tidal delta. Wave-dominated ebb-tidal deltas are comparatively small and pushed close to the inlet throat, whereas tide-dominated ebb-tidal deltas extend offshore (Oertel, 1975). This principle holds for the large-scale of the ebb-tidal delta system, but also for the individual elements that exist on the ebb-tidal delta (such as ebb and flood channels, channel-margin linear bars, terminal lobes and swash-bar patterns).

Based on the pioneering work of Bruun and Gerritsen (1959), various other researchers have further elaborated on conceptual models for sediment-bypassing (FitzGerald, 1982; FitzGerald et al., 1978, 2000; FitzGerald, 1988), while others question the general applicability of the sediment-bypassing concept (Son et al., 2011). The sediment-bypassing process and related bar attachments are often described as periodic or cyclic events (Oertel, 1977; FitzGerald et al., 1984; Israel and Dunsbergen, 1999; Cheung et al. 2007; Robin et al., 2009, Hein et al., 2016). Based on an analysis of the shoaling behaviour on the Wadden Sea ebb-tidal deltas, Ridderinkhof et. al. (2016) concludes that the average period between successive shoal attachments correlates to the tidal prism, and has values ranging between 4 and 130 years.

A conceptual model for cyclic morphodynamic evolution of Ameland Inlet was presented by Van der Spek and Noorbergen (1992), and further refined by Israël (1998), and Israël and Dunsbergen (1999). These authors concluded that a cyclic morphodynamic channel-shoal evolution occurs in Ameland Inlet. The observed cycle spans between 50 and 60 years and consists of four distinct stages in evolution in which the inlet configuration changes between one and two main inlet channels.

5.1.2 Lessons learned from the Ameland sediment-bypassing cycle

As part of the Kustgenese 2 project, a reanalysis of the long-term bathymetric data was made by Elias et al. (2019). These authors conclude that cyclic development and related predictability may not exist at Ameland inlet. Distinct differences in location, shape and volume of the attachment shoals result from differences in sediment-bypassing, which can be driven by morphodynamic

Deltares

interactions at the large scale of the inlet system, *O(10 km)*, and through interactions that originate at the smallest scale of individual shoal instabilities; *O(0.1 km)*. Such shoal instabilities would not be considered to affect the ebb-tidal delta and inlet dynamics as a whole, but can trigger a new sediment-bypassing cycles and result in complete relocation of channels and shoals. These subtle dynamics are difficult, if not impossible, to capture in existing general conceptual models and empirical relationships. These differences are, however, essential for understanding tidal inlet and channel morphodynamics and hence coastal management along the adjacent island coastlines.
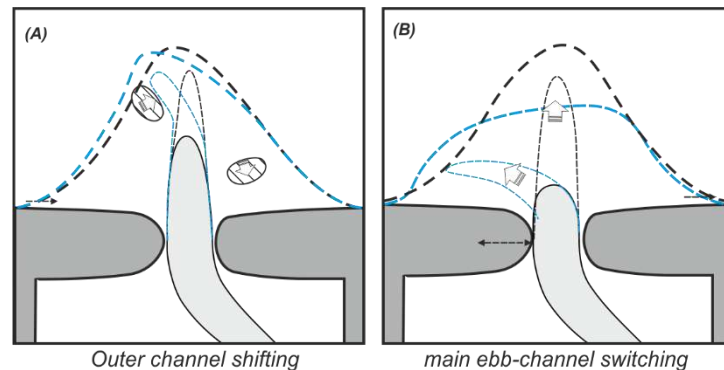

Figure 5.1   Conceptual description of the sediment-bypassing models at Ameland Inlet (a) outer channel shifting and (b) main ebb channel switching (based on concepts of FitzGerald, 1988; FitzGerald et al. 2000).

Elias et al. (2019) further conclude that the present-day ebb-tidal delta dynamics can be explained through 2 modes of sediment-bypassing; (a) outer channel shifting and (b) main ebb-channel switching. See Figure 5.1

(a) Outer channel shifting. In this mode the ebb-tidal delta retains similar features (as was observed between 1854-1926*). The main shoal area is located downdrift of the main ebb-channel. The main ebb-channel remains centrally located with a northwestward orientation in the vicinity of the inlet (Borndiep), but its distal part (Akkepollegat) migrates eastward and periodically switches orientation. Persistent, secondary flood channels occur along the coastlines of Terschelling (Westgat) and along the coast of Ameland. The migration of the Akkepollegat results from sediment accumulation on its updrift side. Under the influence of the prevailing easterly directed wave-driven transport, the shoal migrates eastward, constricting and deflecting flow in the channel until it is finally abandoned. A new, hydraulically more efficient channel with a westerly outflow forms south of the main shoal area, and the cycle restarts. Each cycle results in sediment delivery to the downdrift shoal platform (Bornrif). As sediment accumulates on the downdrift platform, shallow bars start to form, which are then pushed towards the coast by waves breaking on the platform. As these shoals approach the coast of Ameland, flow is constricted, and a narrow channel is formed between the advancing shoal and the barrier island. This channel temporarily causes coastal erosion but also stalls the migration of the shoal. The initial landward migration of the shoals over the platform is rapid, but the final attachment may take several additional years to complete.

(b) Main ebb-channel switching (1926-present). The two main channels in the ebb-tidal delta, Borndiep/Akkepollegat and Westgat, remain in place, but they alternately grow and decay as their ebb discharge increases and subsequently decreases. A dominance of the Borndiep/Akkepollegat channels results in sediment delivery towards the northern part of the ebb-tidal delta and Bornrif. Sediment-bypassing towards Bornrif remains similar. Dominance of the Westgat results in sediment deposition towards the western side of the ebb-tidal delta, building out the ebb-tidal delta close to the coast of Terschelling. As a result, the adjacent Terschelling coast is sheltered from wave energy during storm events, which promotes the spit growth of Boschplaat.

Deltares

5.1.3 New insights from Kustgenese 2.0

Understanding which mode of ebb-tidal dynamics prevails is essential to predict the future evolution of the ebb-tidal delta and especially the adjacent coastlines. The Kustgenese 2.0 measurements have enabled us to study the initiation of a new sediment-bypassing event in high detail. These recent surveys show that (changes in) sediment-bypassing can also be initiated through interactions originating from the smallest-scale level. High-resolution observations taken between 2005 and 2019 illustrate the initiation of a new sediment-bypassing cycle originating from an initial small-scale distortion or shoal instability in the central part of the ebb-tidal delta. This sediment-bypassing cycle consists of five stages of development:
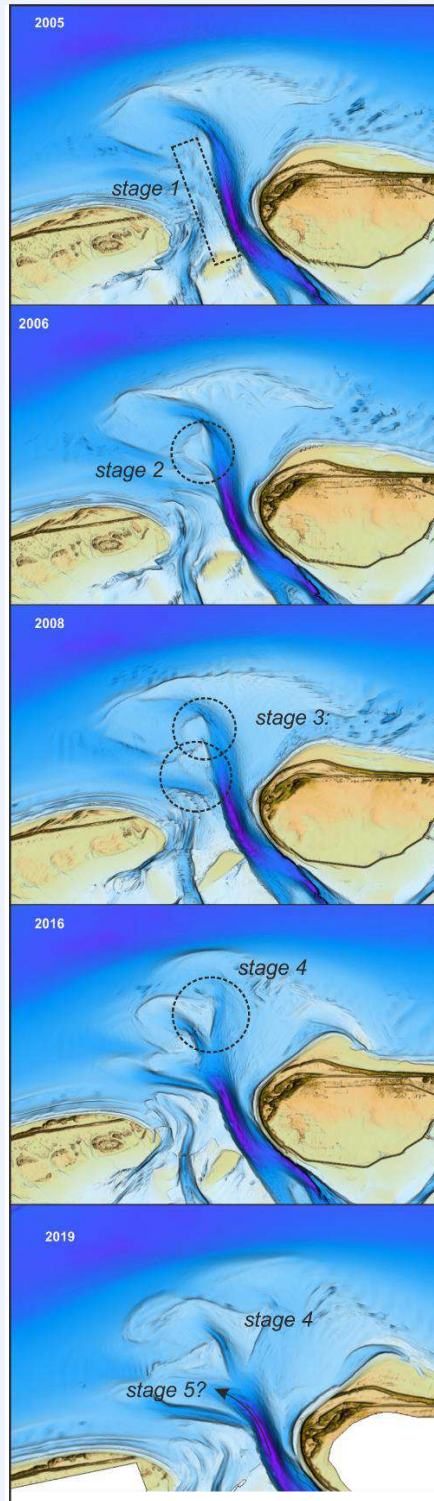
Stage 1; Sediment accumulation along the (central) main channel: Abundant sediment supplied by the updrift coast and through erosion of the western margin of the ebb-tidal delta, is transported into the inlet, and eventually accumulates in an elongate bar flanking the main ebb-delta channel (see 2005).

Stage 2; Morphodynamic instabilities form on this elongate bar: These instabilities result in small spill-overs or ebb-chutes (2005-2006).

Stage 3; Ebb-chute and shield formation of the shoal instabilities: The instabilities rapidly grow and expand seawards into ebb-chute and shield systems (2006-2014), which start to dictate the ebb-shoal morphology.

Stage 4; Channel – shoal interactions: As the ebb-shield grows in height and size, wave-dominant transports become increasingly important. As a result, the ebb-chute and shield systems migrate downdrift (to the east) and thereby constrain the flow in the former main channel Akkepollegat, (2014-2019). The recent 2019 bathymetries show a near-abandoned main ebb channel (Akkepollegat) and initial growth of a new channel to the south. The deeper part of Borndiep connects to the ebb-chute channel. This suggests that another channel switch is imminent (step 5). The flood-channel Westgat remains in place.

Understanding the morphological processes at Ameland Inlet
1220339-008-ZKS-0008, 4 March 2020

Deltares

A fifth step has not happened yet, but it can be hypothesized that the next step in development is: **Stage 5**; Main channel relocation and downdrift shoal attachment: As the main channel becomes hydraulically inefficient, a new channel will form updrift (to the south) of the main shoals (the former ebb-shields now called Kofmansplaat). Downdrift and landward sediment transport contributes to sediment accumulation on the Bornrif shoal, eventually leading to shoal formation and attachment. Thereby the sediment-bypassing cycle would be complete.

The relocation of the main ebb-channel to a more westward position would also affect the flood-dominant channel (Westgat) that is located here. It will be interesting to see how the Westgat channel will react. An option is that a new flood-dominant channel may form to the west, connecting Boschgat and its drainage area directly to the open sea. Such changes would restore the two-channel system, that was also observed to exist in the period 1985-1990.

5.2 An outlook to further change

5.2.1 An outlook to future coastline change; Boschplaat

The formation of a new westward oriented main ebb-channel may also affect the adjacent coastline of Terschelling. While shoal attachments built out the coastline of Ameland, the opposite was observed along the coastline of Terschelling. The eastern most tip of this island, Boschplaat, has receded over 1.5 km since 1975.
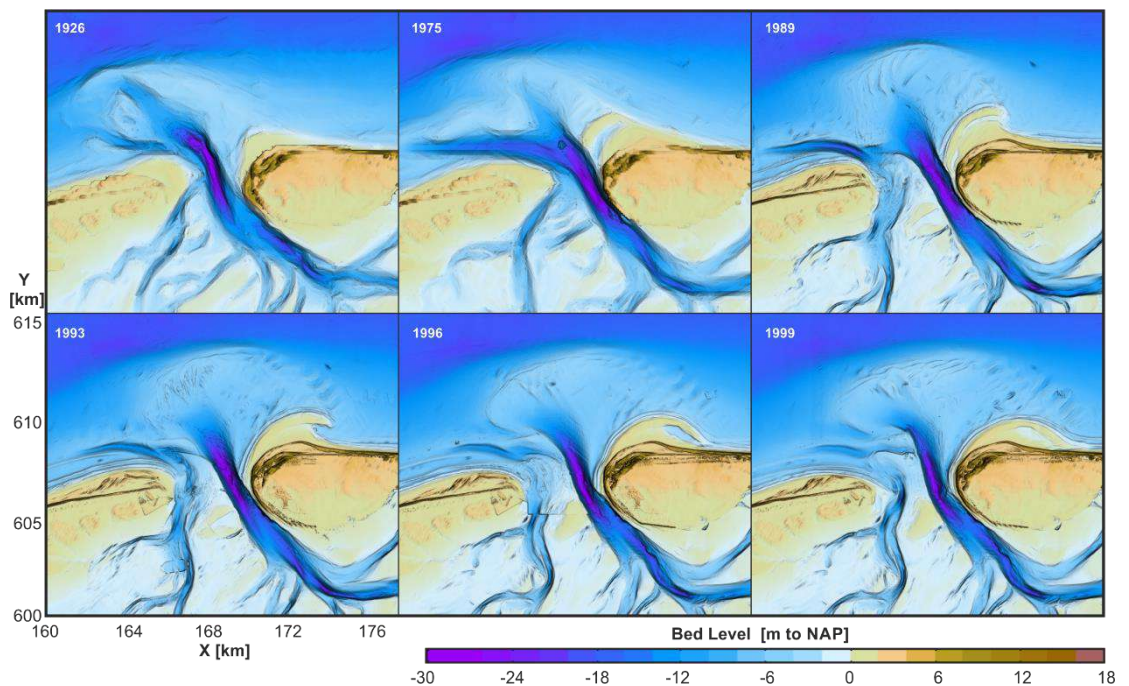
Figure 5.2   An overview of the channels and shoals in the years 1926, 1975, 1989, 1992, 1996 and 1999.

Historically, Boschplaat showed periods of growth and retreat (Elias et al., 2019). Between 1940 and 1974 there was a period of prolonged growth of the Boschplaat (Figure 5.2). This growth was at least partly related to the construction of a sand dike (between 1932 and 1936) to stimulate sand accretion. Besides promoting accretion by capturing wind-blown sediments, this dike has impacted the inlet dynamics because storm surges could no longer flood and easily breach the shoal. The sand dike redirects all flow towards the inlet, increasing the scouring of the inlet during storm events. Since 1934, a continuous deepening of Borndiep can be observed. By 1974, Boschplaat had formed a long narrow spit which protruded well into the inlet (Figure 5.2, 1975). However, structural erosion of Boschplaat has occurred ever since.

Deltares

The formation of a connection between Boschgat and Westgat was one of the main factors of erosion of the island tip between 1989 and 1999 (Figure 5.2). Since 1999, there is no longer a continuous channel, but a shallow platform (around 5 m deep) dissected by several smaller, dynamic channels had formed. Elias (2018) concludes that the continuous erosion of Boschplaat, despite the reduction in channel depth, is mostly related to the changes on the adjacent ebb-tidal delta. As the Westgat channel lost importance, the extensive shoals along its northern, seaward margin could no longer be maintained. These shoals quickly reduced in height and size (1999-2005), and the area between the Kofmansbult and Boschplaat deepened (2005-2016). As a result, waves could propagate far into the inlet. The increase in wave activity and energy resulted in net eastward sediment transport from the tip of Boschplaat, over the shallow platform and into Borndiep. This sediment transport is probably a major contributor to the continued structural erosion of the Boschplaat.

With the formation of a new main ebb-channel in westward direction, this process may be reversed. If this is the case, a main channel configuration as it existed around 1975 would reform, allowing the western margin of the ebb-tidal delta to rebuild. These shoals will provide wave sheltering for the Boschplaat region. A reduction in wave-energy would decrease the sediment transports at Boschplaat and the sediment losses from Boschplaat to Borndiep. A reduction of sediment losses from the island tip may just trigger a transition in coastline behavior from erosion to spit growth.

Potentially, in this scenario, a renewed connection between Boschgat and the open sea could form as well. As the ebb-chute channel grows in size, it pushes the Westgat basin-ward. This may form larger channels towards Boschgat thereby increasing the likelihood that a connection will form here. As a result further erosion of Boschplaat may occur.

5.2.2 An outlook to future coastline change; Ameland north-west

Despite the present-day erosion of Ameland Northwest, shoal attachments and coastal accretion have historically dominated the western island tip of Ameland. Two shoal attachments were observed here since 1985. The attachment of the Bornrif Strandhaak is well documented by the yearly shoreline measurements from the JarKus database (see Figure 5.3). The JarKus profiles indicate the presence of a nearshore shoal around 1970. Between 1970-1986 this shoal grows in height and finally attaches to the Ameland coast, towards Borndiep. A large recurved spit developed. This shoal is known as the Bornrif Strandhaak (the translation of the Dutch name Strandhaak is 'beach hook'). After the tip of the Strandhaak attached to the shore, the coastline migrated seaward by 1.5 km, followed by a retreat of over 500 m as the deposits were subsequently eroded and predominantly transported downdrift, feeding the adjacent coast of Ameland. Behind the spit, an enclosed lagoon formed. Large-scale erosion was observed at the tip of the spit, as the filling and draining of the lagoon developed a small-scale inlet channel, which eroded into the beaches and dunes.

Recently, in 2017, a new shoal attachment occurred as the Bornrif Bankje attached to the coastline at the tip of the Bornrif Strandhaak (Figure 3.2). In contrast to the attachments of the Bornrif Strandhaak, that occurred on the north-western tip of Ameland near Borndiep, this recent attachment occurred more downdrift at the ebb-delta margin. The origin of Bornrif Bankje can be traced back to the 1989-1999 timeframe. During this interval, the northern ebb-delta front showed a large outbuilding and increase in shoal height at the seaward end of Akkepollegat. This outbuilding continued until 2011. Wave-breaking on this shallow shoal area probably resulted in downdrift sand transport along the ebb-tidal delta margin, and Bornrif Bankje slowly started to emerge on the north-east side of the ebb-tidal delta (see Figure 3.2, 2008-2010). The shoal continued to migrate eastward and landward (Figure 3.2, 2011-2014), and by 2014 only a small channel remained separating the Bornrif Strandhaak and Bornrif Bankje. The map of 2017 shows that the tip of Bornrif Bankje finally attached to the Ameland coastline, just downdrift of the Strandhaak.
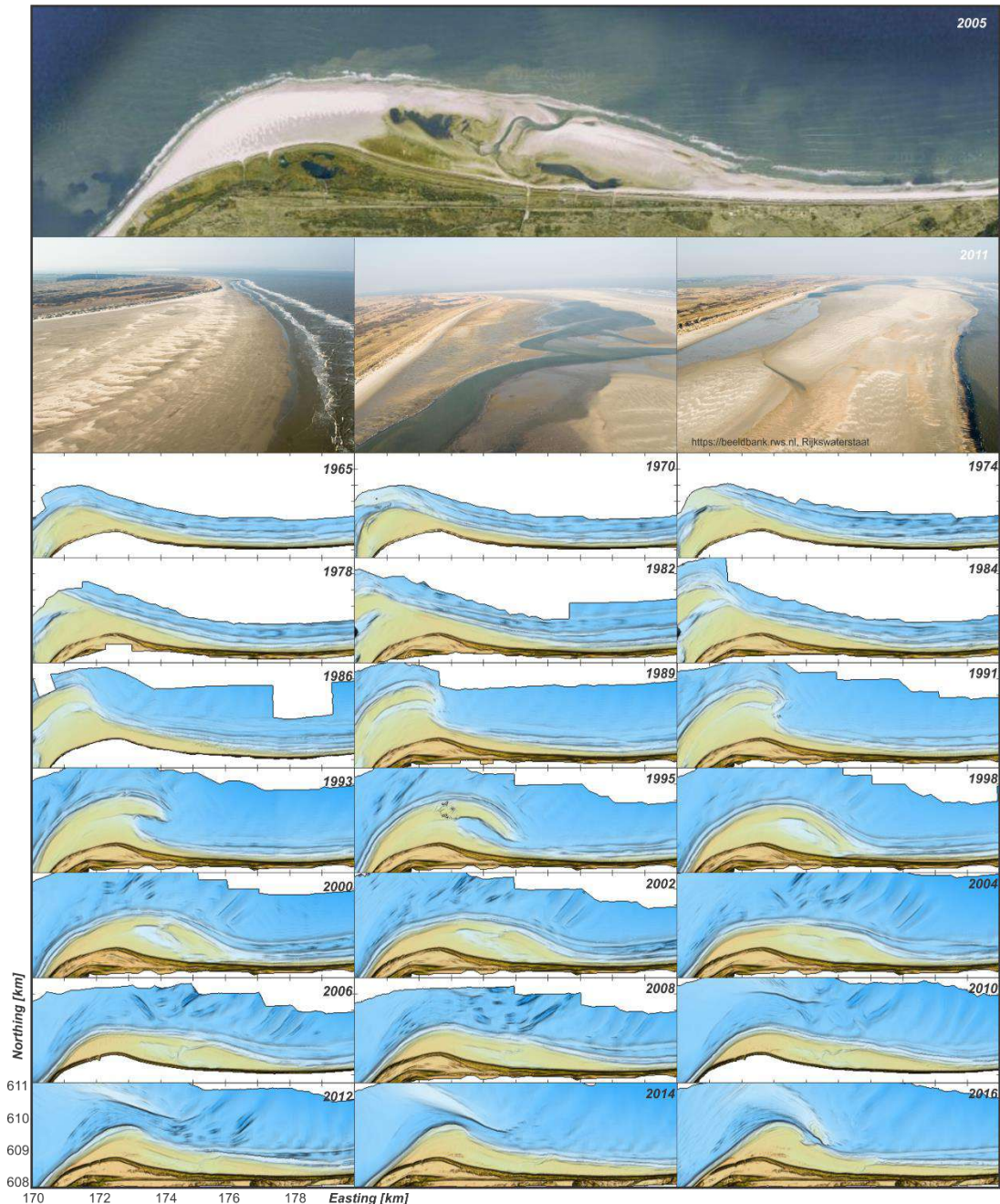
Deltares

Figure 5.3   Formation, attachment and merger of the Bornrif Strandhaak between 1965 and 2016. Top pictures provide an impression of the shoal area in 2011 (from beeldbank.rws.nl. Rijkswaterstaat).

These two very different shoal attachments, both have a different effect on the coastline accretion. Bornrif Bankje is not likely to relief the present-day coastal erosion of Ameland Northwest. It is therefore important for coastal management to better understand how these shoals form, migrate and finally attach to the coast. The Kustgenese 2.0 measurements illustrate the formation of new bypassing shoals on the ebb-tidal delta. The large ebb-shields that were formed around the ebb-chutes will eventually migrate or transition to the Bornrif platform and the Ameland coastline. The net eastward migration of the ebb-shoals due to wave-driven transports is one of the reasons for the reduced efficiency of Akkepollegat, that will likely lead to abandonment of the channel and main ebb-channel switching. As the ebb-channel switches, the seaward ebb-chute and shield will be abandoned and the ebb shield transforms in a normal wave-driven shoal. These shoals may be maintained as an entity and propagate as a shallow shoal over the Bornrif platform, a process very

Understanding the morphological processes at Ameland Inlet
1220339-008-ZKS-0008, 4 March 2020

Deltares

similar to the shoal Onrust in Texel inlet (see Elias 2006, p. 40), or such shoals could dissipate and become part of the Bornrif platform. On the Bornrif platform sediments primarily move landward and temporarily accumulate in shoal deposits in front of island. As tidal currents are trapped between the shoal and the coast, increased coastal erosion is to be expected until a critically small cross-section is reached, the channel is abandoned and these shoals finally attach to the coastline. This process may lead to the formation of a new Bornrif Strandhaak relieving the erosion at Ameland Northwest.

5.2.3 An outlook to future change of the ebb-delta nourishment.

The ebb-delta nourishment was successfully placed on Kofmansbult, which shows that it is technically feasible to place these large volumes of sand on the ebb-tidal delta platform. The nourishment did not alter the morphodynamic behaviour of Kofmansbult and the area south of it. The ebb-chute and shield systems continued to build seawards while ebb-shield deposits were moved eastward. Erosion of the nourishment, especially during major storm events, must have added sediment to the observed accretion in the former Akkepollegat channel. The bulk of the sediment however stayed at the nourishment location. One of the remaining questions is the nature of the wave-driven transports on the ebb-tidal delta. Are these large wave-driven transports a recurring response to storm events, or are these just incidental and a response to a nourishment whose shape and/or height was not yet in equilibrium with the remainder of the ebb-tidal delta? The initial strong response to storm events may just be a response to a non-equilibrium morphology. The storm events following the placement may have reshaped the nourishment to a more-or-less equilibrium depth. If this is the case, the response to future storm events may be less dramatic and the nourishment will remain at a similar location. Continued mapping will be needed to assess the future behaviour of the nourishment.

5.3 Future morphodynamic modelling of tidal inlets and ebb-tidal deltas.

Shoal instabilities are initially small morphodynamic changes and would not be considered to affect the ebb-tidal delta and inlet dynamics as a whole. The analysis presented in this report shows that complete relocation channels and shoals at delta scale can be initiated through interactions that originate on the smallest scale of individual shoals. The resulting morphodynamic changes can fundamentally change the configuration of the ebb-tidal delta, they can trigger a new sediment-bypassing cycle, and fundamentally alter the state of parts of the ebb-tidal delta from tide- to wave-dominated. Similarly, Harrison et al. (2017) suggest that non-seasonal transitions observed in ebb-tidal delta bathymetry may be the result of morphodynamic "tipping points" being reached: system-wide behavior that emerges from processes and interactions at smaller scales. Such small-scale changes would generally not be considered to affect the ebb-tidal delta and inlet dynamics as a whole, and their subtle dynamics are difficult, if not impossible, to capture in the general conceptual models and empirical relationships. The notion that initial small-scale distortions can trigger complete ebb-tidal delta relocation also has important consequences in the way process-based numerical modelling of these systems must be approached. Over the last decade, good progress has been made with process-based modelling of tidal inlets and ebb-tidal deltas (e.g. Hibma, 2004; De Fockert, 2008; Lesser, 2009; Dastgheib, 2012). For a major part, this progress is related to techniques to efficiently accelerate the morphological predictions (Lesser 2009; Roelvink, 2006). Separation of scales is a critical aspect underlying these acceleration techniques. The observed changes at Ameland inlet illustrate that it is essential to critically rethink which processes are noise, an extrinsic condition, or an essential component to include. Subgrid approaches to morphodynamic modelling may provide a solution for bridging the gap in spatial scales (e.g. Volp et al., 2016).

Deltares

6 Conclusions & Recommendations

6.1 Conclusions

The data collected at Ameland inlet during the Kustgenese 2.0 campaign, in combination with older datasets has created an extensive, globally unique, dataset. These datasets allow for an in-depth analysis of the meso-scale morphodynamic changes of the ebb-tidal delta and its adjacent coastlines.

The main conclusions based on the analysis of the hydrodynamics are:
- The 13-hour discharge measurements illustrate the relatively large variation in ebb and flood volumes through the inlet gorge. Part of this variation is due to spring-neap variability, but partly large-scale water level gradients may be important as well. No clear preferential ebb- or flood dominance is observed. Depending on the stage in the spring-neap cycle the net discharges can be eb or flood dominant.
- Stations placed on the tidal divides measured large (residual) flows, especially during strong south-westerly winds. These flows are much larger than was previously assumed.
- Wave measurements show the wave sheltering effect of the ebb-tidal delta during higher wave conditions. Wave heights of over 2 m dissipate on the ebb-tidal delta margin. Landward stations show a significant tidal modulation in wave heights (wave-current interaction). During storms the average wave heights increases due to surge.

The analysis of bedforms and bathymetric change reveal that:

- Bed-form asymmetry and migration indicate that in Borndiep sediment transport is primarily ebb dominant and in Westgat flood dominant.
- The net volumetric change (+4 million m3) between 2016-2019 is relatively small compared to the gross sedimentation and erosion values (respectively 30 million m3 and -26 million m3). Note that during this time frame over 7 million m3 of sand was added to the system in the form of the beach nourishment at Ameland Northwest and the ebb-delta nourishment.
- Both erosion and sedimentation at the seaward margin of the ebb-tidal delta occurs mainly during the more energetic winter months. The higher wave conditions can stir up and transport larger amounts of sand, that are subsequently deposited further landward. Outbuilding of the ebb-shield front and increased erosion of the ebb-chute channel during winter may be related to surge. As the basin drains the ebb-velocities may be considerably increased resulting in strong velocities over the ebb-tidal delta and increased migration of the ebb-chute and shield systems. These findings raise questions of our general conceptual models describing tidal inlet systems.
- The higher temporal resolution of the bathymetric measurements reveals the growth of small-scale perturbations to scales that affect the entire ebb-tidal delta. The ebb-tidal delta is much more dynamic than expected based on literature and existing conceptual models.
- Accurate predictions of the morphological changes can now be obtained using the X-Band radar in combination with XMFit. The future use of XMFit derived bathymetry may be essential to better understand the ebb-tidal delta response during high energetic conditions.

Analysis of the ebb-delta nourishment shows that:
- The ebb-delta nourishment was successfully placed on the Kofmansbult, which shows that it is technically feasible to place such large volumes of sand on the ebb-tidal delta platform.
- The nourishment did not visibly alter the morphodynamic behaviour of the Kofmansbult.
- After placement the bulk of the sediment was retained at the nourishment location.
- Erosion of the nourishment occurred during major storm events.

The large influence of the ebb-tidal delta dynamics on the shoreline response of the updrift and downdrift sides of the inlet is clearly identified (Elias et al. 2019). Periodic growth and decay (net erosion) of the island tip of the updrift island –Terschelling- occurs, while sequences of sediment-bypassing result in shoal attachment to the downdrift coastline of Ameland. No clear evidence exists

Deltares

that a long-term morphodynamic cycle occurs on the scale of Ameland Inlet. Instead, morphodynamic changes start with the accumulation of sediment in various places until tipping points are reached. The mechanisms pushing the ebb-tidal delta towards these tipping points are repetitive. These accumulations tend to repeat in similar areas but are never the same, so a true cycle is never reached. The recent sediment-bypassing cycle (2005-2019) can be described through 5 stages of development.

Near yearly coverage of the ebb-tidal delta between 2005-2019, displays how initial small-scale perturbations in the central part of the ebb-tidal delta (the ebb-chute and shield systems) develop, grow, migrate and start to dominate the developments of the entire ebb-tidal delta. Only through the continuation of these frequent measurements by the Kustgenese 2.0 campaign, it is possible to fully start to understand the potential impacts on the coastal system. Shoal instabilities are initially small morphodynamic changes and would not be considered to affect the ebb-tidal delta and inlet dynamics as a whole but the analysis presented in this report show that complete relocation of ebb-tidal delta scale channels and shoals can be initiated through interactions that originate on the smallest scale of individual shoals.

6.2 Recommendations for future research

The Kustgenese 2.0 monitoring campaign has compiled a wealth of data. Analysis of this data has resulted in new insights in ebb-tidal delta behaviour and underlying processes. In the SEAWAD programme, analyses are still ongoing, and four PhD theses are expected to be published in 2021. It is recommended to integrate these new studies in this synthesis.

Continued monitoring and analysis of the ebb-delta nourishment is recommended. So far, only initial change of the nourishment has occurred. To fully understand how the ebb-tidal delta and nourishment interact, continued monitoring and analysis over the coming years is advised. Since the entire ebb-tidal delta presently shows large yearly changes with possible complete relocation of the main channel, it is highly recommended to continue the yearly measurements of the entire ebb-tidal delta for the coming years.

Yearly monitoring of the ebb-tidal delta has revealed completely new insights in ebb-tidal delta behaviour. This knowledge allows to understand the sediment-bypassing process in detail. Such knowledge is essential if one aims to use the ebb-tidal delta to place nourishments. If the sediment-bypassing process is understood, it may be used to strategically place sediment nourishments in the system. The process of sediment-bypassing basically occurs at all ebb-tidal deltas, but the exact effect on the meso-scale is different for each tidal inlet. Detailed knowledge and prediction of the dynamics of channels and shoals is needed to fit the ebb-tidal delta nourishments into a sediment-bypassing cycle. It is therefore recommended to perform yearly measurements of the other ebb-tidal deltas.

It is recommended to continue both morphostatic and morphodynamic modelling of Ameland inlet. Through morphostatic modelling, the processes underlying the observed morphodynamic changes can be better understood. The role of surge on flow and sediment transports in the inlet need to be better understood. In addition, application of newly developed sediment-tracer functionality allows us to investigate the sediment pathways (and thereby the sediment-bypassing processes) on the ebb-tidal delta and the exchange between ebb-tidal delta and inlet.

The newly obtained insights in morphodynamic behaviour (the importance of small-scale distortions) allows us to improve model schematisations and assumptions, that are essential for medium-term and long-term morphodynamic model simulations. Incorporation of these insights is a next logical step to obtain more realistic morphodynamic models.

Understanding the morphological processes at Ameland Inlet
1220339-008-ZKS-0008, 4 March 2020

Deltares

7 References

Briek, J., Huizinga, M.A., Hut, J., 2003. Stroommeting Zeegat van Ameland 2001. RIKZ-report 2003-169 (in Dutch), Rijkswaterstaat, Directie Noord-Nederland, Delftzijl.

Bruun, P., Gerritsen, F., 1959. Natural bypassing of sand at coastal inlets. Journal of the Waterways and Harbors, Harbor Division, 85 (4), 75-107.

Cheung, K.F., Gerritsen, F., Cleveringa, J., 2007. Morphodynamics and sand bypassing at Ameland Inlet, The Netherlands. Journal of Coastal Research 23 (1), 106-118.

Cleveringa, J., Oost, A.P., 1999. The fractal geometry of tidal-channel systems in the Dutch Wadden Sea. Geologie en Mijnbouw 78, 21-30.

Dastgheib, A., 2012. Long-term process-based morphological modeling of large tidal basins, Ph.D. Thesis, UNESCO-IHE, Delft, The Netherlands.

Davis, R.A., Hayes, M.O., 1984. What is a wave-dominated coast? Marine Geology 60, 313-329.

De Boer, M., Kool, G., Lieshout, M.F., 1991a. Erosie en Sedimentatie in de Binnendelta van het Zeegat van Ameland 1926-1984. Report ANVX-91.H202 (in Dutch), Rijkswaterstaat, Directie Noord-Holland, Haarlem.

De Boer, M., Kool, G., Lieshout, M.F., Ulm, D.L., 1991b. Erosie en Sedimentatie in de Buitendelta van het Zeegat van Ameland 1926-1982. Report ANVX-91.H205 (in Dutch), Rijkswaterstaat, Directie Noord-Holland, Haarlem.

De Fockert, A., 2008. Impact of relative sea level rise on the Amelander inlet morphology. Master thesis, Delft University, Delft, The Netherlands.

De Kruif, A.C., 2001. Bodemdieptegegevens van het Nederlandse Kustsysteem; Beschikbare Digitale Data en een Overzicht van Aanvullende Analoge Data. Report RIKZ/2001.041 (in Dutch), Rijkswaterstaat, National Institute for Coastal and Marine Management RIKZ, The Hague.

De Vriend, 1991. Mathematical modelling and large-scale coastal behaviour, Part 1: physical processes. Journal of Hydraulic Research, 29, 727-740.

De Wit, F.P., Tissier, M.F.S., Pearson, S.G., Radermacher, M., van de Ven, M.J.P., van Langevelde, A.P., Vos, T.A., Reniers, A.J.H.M., 2018. Measuring the spatial and temporal variability of currents on Ameland Ebb-Tidal Delta [Poster]. NCK Days Conference, March 23 2018, Haarlem, the Netherlands.

Dean, R.G., 1988. Sediment interaction at modified coastal inlets: processes and policies. In: Aubrey, D., Weishar, L. (Eds.), Hydrodynamics and Sediment Dynamics of Tidal Inlets. Lecture Notes on Coastal and Estuarine Studies 29. Springer, New York, 412-439.

Dean R.G., Walton, T.L., 1975. Sediment transport processes in the vicinity of inlets with special reference to sand trapping. In: Cronin, L.E. (Ed.), Estuarine Research, Volume 2. Academic Press, New York, 129-150.

Deltares

Dillingh, D., 1990. Frequentie en Dichtheid van Kust- en VakLodingen. Report GWIO-90.003 (in Dutch), Rijkswaterstaat, Tidal Waters Division, Middelburg.

Duran-Matute M., Gerkema T., de Boer G.J., Nauw J.J., Gräwe U., 2014. Residual circulation and freshwater transport in the Dutch Wadden Sea: a numerical modelling study. Ocean Sciences 10 (4), 611–632.

Elias, E.P.L., 2006. Morphodynamics of Texel Inlet. Ph.D. Thesis, Delft University of Technology, Faculty of Civil Engineering and Geosciences (Delft): 261 pp.

Elias E.P.L., Gelfenbaum G., Van der Westhuysen A.J., 2012. Validation of a coupled wave-flow model in a high-energy setting: the mouth of the Columbia River. J. Geophys Res., Vol 117, C09011. doi:10.1029/2012JC008105.

Elias, E.P.L., Van der Spek, A.J.F, Wang, Z.B., De Ronde, J., 2012. Morphodynamic development and sediment budget of the Dutch Wadden Sea over the last century. Netherlands Journal of Geosciences 91 (3), 293-310.

Elias, E.P.L., Van der Spek, A.J.F., 2017. Dynamic preservation of Texel Inlet, the Netherlands: understanding the interaction of an ebb-tidal delta with its adjacent coast. Netherlands Journal of Geosciences 96 (4), 293–317.

Elias, E.P.L., 2018. Understanding the present day morphodynamics of Ameland inlet Kustgenese 2.0, product ZG-A02. Report 1220339-006, Deltares, Delft: 58 p.

Elias, E.P.L., 2019. Een actuele sedimentbalans van de Waddenzee. Deltares rapport 11203683-001, Deltares Delft, 119 p.

Elias, E.P.L., Van der Spek, A.J.F., Pearson, S., Cleveringa, J., 2019. Understanding sediment-bypassing processes through analysis of high-frequency observations of Ameland Inlet, the Netherlands. Marine Geology 415.

Eysink, W. D., 1993. Impact of Sea Level Rise on the Morphology of the Wadden Sea in the Scope of its Ecological Function. General Considerations on Hydraulic Conditions, Sediment transports, Sand Balance, Bed Composition and Impact of Sea Level Rise on Tidal Flats. Report ISOS*2, Project Phase 4. Rijkswaterstaat, National Institute for Coastal and Marine Management RIKZ, The Hague.

FitzGerald, D.M., 1982. Sediment-bypassing at mixed energy tidal inlets. Proceedings of 18th International Conference on Coastal Engineering, Cape Town, 1094-1118.

FitzGerald, D.M., 1988. Shoreline erosional-depositional processes associated with tidal inlets. In: Aubrey, D., Weishar, L. (Eds.), Hydrodynamics and Sediment Dynamics of Tidal Inlets. Lecture Notes on Coastal and Estuarine Studies 29. Springer, New York, 186-225.

FitzGerald, D.M., 1996. Geomorphic variability and morphologic and sedimentologic controls on tidal inlets. In: Mehta, A.J. (Ed.). Understanding Physical Processes at Tidal Inlets Based on Contributions by Panel on Scoping Field and Laboratory Investigations in Coastal Inlet Research. Journal of Coastal Research SI 23, 47-71.

FitzGerald, D.M., Hubbard, D.K., Nummedal, D., 1978. Shoreline changes associated with tidal inlets along the South Carolina coast. Proceedings Coastal Zone 1978, American Society of Civil Engineers, New York, 1973-1994.

Deltares

FitzGerald, D.M., Kraus, N.C., Hands, E.B., 2000. Natural Mechanisms of Sediment-bypassing at Tidal Inlets. Report ERDC/CHL CHETN-IV-30, US Army Corps of Engineers, Vicksburg.

FitzGerald, D.M., Penland, S., Nummedal, D., 1984. Control of barrier island shape by inlet sediment-bypassing: East Frisian Islands, West Germany. Marine Geology 60, 355-376.

Flemming, B.W. & Davis, R.A., 1994. Holocene evolution, morphodynamics and sedimentology of the Spiekeroog barrier island system (Southern North Sea). Senckenbergiana Maritima 24 (1/6), 117-155.

Gawehn, M., 2020. Ontwikkeling en toepassing X-Band radar voor morfologische analyse van het Amelander Zeegat. Eindrapportage ten behoeve van Kustgenese 2.0. Deltares report 1220339-007-ZKS-005, Deltares, Delft.

Gawehn, M., Swinkels, C., van Dongeren, A., Hoekstra, R., de Vries, S., Aarninkhof, S., 2020. A radar-based depth inversion method to monitor near-shore nourishments on an open sandy coast and an ebb-tidal delta, submitted for 2nd review at Coastal Engineering.

Harrison, S. R., Bryan, K. R., Mullarney, J. C., 2017. Observations of morphological change at an ebb-tidal delta, Marine Geology 385, 131-145.

Hayes, M.O., 1975. Morphology of sand accumulation in estuaries: an introduction to the symposium. In: Cronin, L.E. (Ed.), Estuarine Research, Vol. 2. Academic Press, New York, 3-22.

Hayes, M.O., 1979. Barrier Island morphology as a function of tidal and wave regime. In: Leatherman, S.P. (Ed.), Barrier Islands: from the Gulf of St Lawrence to the Gulf of Mexico. Academic Press, New York, 1-27.

Hayes, M.O., FitzGerald, D.M., 2013. Origin, evolution, and classification of tidal inlets. In: Kana, T., Michel, J., Voulgaris, G. (Eds.), Symposium in Applied Coastal Geomorphology to Honor Miles O. Hayes. Journal of Coastal Research SI 69, 14-33.

Hayes, M.O., Kana, T.W., 1976. Terrigenous Clastic Depositional Environments. Technical Report 11-CRD, Geology Department, University of South Carolina, Columbia, South Carolina.

Hein, C.J., Fitzsimons, G.G., FitzGerald, D.M., Fallon, A.R., 2016. Records of migration and ebb-delta breaching at historic and ancient tidal inlets along a river-fed paraglacial barrier island. Journal of Coastal Research SI 75, 228-232.

Hibma, A., 2004. Morphodynamic modelling of channel-shoal systems, Communications on Hydraulic and Geotechnical Engineering, vol. 04-3, Delft University of Technology, Delft, 122 pp.

Hubbard, D.K., Oertel, G., Nummedal, D., 1979. The role of waves and tidal currents in the development of tidal-inlet sedimentary structures and sand body geometry: examples from North Carolina, South Carolina and Georgia. Journal of Sedimentary Petrology 49, 1073-1092.

Israël, C.G., 1998, Morfologische Ontwikkeling Amelander Zeegat. Report RIKZ/OS-98.147x (in Dutch), Rijkswaterstaat, National Institute for Coastal and Marine Management RIKZ, The Hague.

Understanding the morphological processes at Ameland Inlet
1220339-008-ZKS-0008, 4 March 2020

Deltares

Israël, C.G., Dunsbergen, D.W., 1999. Cyclic morphological development of the Ameland Inlet, The Netherlands. Proceedings of Symposium on River, Coastal and Estuarine Morphodynamics, Genova, Italy, Volume 2, 705-714.

Jarrett, J.T., 1976. Tidal Prism – Inlet Area Relationships. General Investigation of Tidal Inlets, Report no. 3. Coastal Engineering Research Center, US Army Corps of Engineers, Washington D.C.

Lesser, G.R., 2009. An approach to medium-term coastal morphological modeling. Ph.D. Thesis, UNESCO-IHE, Delft, The Netherlands.

Luck, G., 1976. Inlet changes of the East Friesian Islands. Proceedings 15th Coastal Engineering Conference, Honolulu, Hawaii. American Society of Civil Engineers, New York, pp. 1938-1957.

Nederhoff, K., Elias, E.P.L., Vermaas, T., 2016. Erosie op Ameland Noordwest. Rapport 1503-0080, Deltares, Delft, 85 pp

O'Brien, M.P., 1931. Estuary tidal prisms related to entrance areas. Civil Engineering 1, 738-739.

O'Brien, M.P., 1969. Equilibrium flow areas of inlets and sandy coasts. Journal of Waterways, and Harbors, Harbor Division, 95 (1), 43-55.

Oertel, G.F., 1975. Ebb-tidal deltas of Georgia Estuaries. In: Cronin, L.E. (ed.): Estuarine Research, vol. 2. Academic Press, New York, 267-276.

Oertel, G.F., 1977. Geomorphic cycles in ebb deltas and related patterns of shore erosion and accretion. Journal of Sedimentary Petrology 47, 1121-1131.

Oost, A.P., 1995. Dynamics and Sedimentary Development of the Dutch Wadden Sea with Emphasis on the Frisian Inlet. A Study of Barrier Islands, Ebb-Tidal Deltas, Inlets and Drainage Basins. Geologica Ultraiectina 126, 454 pp.

Pawlowicz, R., B. Breardsley, and S. Lentz (2002), Classical tidal harmonic analysis including error estimates in MATLAB using T_TIDE, Comput. Geosci., 28(8), 929–937, doi:10.1016/S0098-3004(02)00013-4.

Perluka, R., Wiegmann, E.B., Jordans, R.W.L.. Swart, L.M.T., 2006. Opnametechnieken Waddenzee. Report AGI-2006-GPMP-004 (in Dutch), Rijkswaterstaat, Adviesdienst Geo Informatie en ICT, Delft.

Pugh, D. T., 2004. Changing Sea Levels: Effects of Tides, Weather, and Climate. Cambridge University Press (Cambridge, UK): 267 pp.

Rakhorst, H.D., Kool, G., Lieshout, M.F., 1993. Erosie en Sedimentatie in de Buitendelta van het Zeegat van Ameland en Aangrenzende Kuststroken 1926-1989. Report ANV-92.201 (in Dutch), Rijkswaterstaat, Directie Noord-Holland, Haarlem.

Ridderinkhof, W., Hoekstra, P., Van der Vegt, M., De Swart, H.E., 2016. Cyclic behaviour of sandy shoals on the ebb-tidal deltas of the Wadden Sea. Continental Shelf Research 115, 14-26.

Roelvink, J.A., 2006. Coastal morphodynamic evolution techniques. Coastal Engineering 53, 277 – 287.

Understanding the morphological processes at Ameland Inlet
1220339-008-ZKS-0008, 4 March 2020

Deltares

Robin N. Levoy, F., Monfort, O., Anthony, E., 2009. Short-term to decadal-scale onshore bar migration and shoreline changes in the vicinity of a mega-tidal ebb delta. Journal of Geophysical Research: Earth Surface 114, F04024.

Sha, L.P., 1989. Variation in ebb-tidal delta morphologies along the west and East Frisian Islands, the Netherlands and Germany. Marine Geology 89, 11-28.

Son, C.S., Flemming, B.W., Bartholomä, A., 2011. Evidence for sediment recirculation on an ebb-tidal delta of the East Frisian barrier-island system, southern North Sea. Geo Marine Letters 31, 87-100.

Van der Spek, A.J.F., 1994. Large-Scale Evolution of Holocene Tidal Basins in The Netherlands. Ph.D. Thesis, Utrecht University (Utrecht).

Van der Spek, A.J.F., 1995. Reconstruction of tidal inlet and channel dimensions in the Frisian Middelzee, a former tidal basin in the Dutch Wadden Sea. In: Flemming, B.W., Bartholomä, A. (Eds.), Tidal Signatures in Modern and Ancient Sediments. International Association of Sedimentologists, Special Publication 24. Blackwell Science, Oxford, 239-258.

Spanhoff, R., Biegel, E.J., Van de Graaff, J., Hoekstra, P., 1997. Shoreface nourishment at Terschelling, the Netherlands: feeder berm or breaker berm? In: Thornton, E.B. (Ed.), Proceedings 3rd International Conference on Coastal Dynamics '97. American Society of Civil Engineers, New York, pp. 863- 872.

Stive, M.J.F., Wang, Z.B., 2003. Morphodynamic modeling of tidal basins and coastal inlets. In: Lakhan, C. (Ed.), Advances in Coastal Modelling. Elsevier Oceanography Series 67, 367-392.

Stive, M.J.F., De Schipper, M.A., Luijendijk, A.P., Aarninkhof, S.G.J., Van Gelder-Maas, C., Van Thiel de Vries, J.S.M., De Vries, S., Henriquez, M., Marx, S., Ranasinghe, R., 2013. A new alternative to saving our beaches from sea-level rise: the sand engine. Journal of Coastal Research 29, 1001-1008.

Swinkels,C. Peters, H. and J. van Heesen. 2012. Analysis of current patterns in coastal areas using x-band radar images. Coastal Engineering, 1–10.

Tanczos, I.C., Aarninkhof, S.G.J., Van der Weck, A.W., 2000. Ruimte voor de Zandrivier (in Dutch). Report Z3200, WL|Delft Hydraulics, Delft.

Van Rhijn, M.W., 2019. Sediment transport during the execution of the pilot nourishment Ameland Inlet. MSc. Thesis, Delft University of Technology, Delft,197 pp.

Van der Spek, A.J.F., 1995. Reconstruction of tidal inlet and channel dimensions in the Frisian Middelzee, a former tidal basin in the Dutch Wadden Sea. In: Flemming, B.W., Bartholomä, A. (Eds.), Tidal Signatures in Modern and Ancient Sediments. International Association of Sedimentologists, Special Publication 24. Blackwell Science, Oxford, 239-258.

Van der Spek, A.J.F., Noorbergen, H.H.S., 1992. Morfodynamica van Intergetijdegebieden. Report 92-03, Beleidscommissie Remote Sensing BCRS, The Hague.

Van Sijp, D., 1989. Correcties op Gemeten Eb- en Vloedvolume bij Omrekening naar Gemiddeld Getij in het Friesche Zeegat. Report ANW 89-02 (in Dutch), Rijkswaterstaat, Directie Friesland, Leeuwarden.

Understanding the morphological processes at Ameland Inlet
1220339-008-ZKS-0008, 4 March 2020

Deltares

Van Straaten, L.M.J.U., 1975. De sedimenthuishouding van de Waddenzee. In: Swennen, C., De Wilde, P.A.W.J. & Haeck, J. (Eds): Symposium Waddenonderzoek, April 7, 1973 (in Dutch, with English summary). Mededeling Werkgroep Waddenzee 1 (Amsterdam), 5-20.

Van Veen, J. (1950). "Eb en vloedschaar systemen in de Nederlandse getijwateren (in Dutch)" Tijdschrift Koninklijk Nederlands Aardrijkskundig Genootschap, 303-325.

Van Veen, J, Van der Spek, A. J. F., Stive, M. J. F., and Zitman, T. J. (2005). "Ebb and Flood channel systems in the Netherlands tidal waters" *Journal of Coastal Research*, 21(6), 1107-1120.

Van Weerdenburg, R.J.A. (2019). Exploring the importance of wind for exchange processes around a tidal inlet system: the case of Ameland Inlet. MSc. Thesis Delft University of Technology, Delft, 78 pp.

Van der Werf, J. et al. (2019). Data report Kustgenese 2.0 measurements. Project 1220339-015. Deltares, Delft, 124.

Volp, N.D., van Prooijen, B.C., Pietrzak, J.D., Stelling, G.S., 2016. A subgrid based approach for morphodynamic modelling. Advances in Water Resources, 93, 105–117

Walton, T.L., Adams, W.D. 1976. Capacity of inlet outer bars to store sand. Proceedings 15th Coastal Engineering Conference, Honolulu, Hawaii. American Society of Civil Engineers, New York, 19-37.

Wang, Z.B., Vroom, J., Van Prooijen, B.C., Labeur, R.J., Stive, M.J.F., 2013. Movement of tidal watersheds in the Wadden Sea and its consequences on the morphological development. International Journal of Sediment Research 28 (2), 162-171.

Wang, Y, Yu Q, Jiao, J, Tonnon, P.K., Wang, Z.B, Gao, S., 2016. Coupling bedform roughness and sediment grain-size sorting in modelling of tidal inlet incision. Marine Geology, 381

Wang, Z.B., Elias, E.P.L., Van der Spek, A.J.F., Lodder, Q.L., 2018. Sediment budget and morphological development of the Dutch Wadden Sea - impact of accelerated sea-level rise and subsidence until 2100. Netherlands Journal of Geosciences 97-3, p. 183-214. Van der Spek, A.J.F., 1994. Large-Scale Evolution of Holocene Tidal Basins in The Netherlands. Ph.D. Thesis, Utrecht University (Utrecht).

Zijderveld, A., Peters H., 2006. Measurement program Dutch Wadden Sea. Proceedings 30th International Conference on Coastal Engineering, San Diego, USA. American Society of Civil Engineers, New York, p. 404-410.